CHEMOTAXIS OF *ESCHERICHIA COLI* STUDIED USING IONTOPHORETIC STIMULATION

Thesis by

Jeffrey E. Segall

In Partial Fulfillment of the Requirements

for the Degree of

Doctor of Philosophy

California Institute of Technology

Pasadena, California

1985

(Submitted July 27, 1984)

"The essence lies...in a sort of intoxicated joy and amazement at the beauty and grandeur of this world, of which man can just form a faint notion. It is the feeling from which true scientific research draws its spiritual sustenance, but which also seems to find expression in the song of birds."

A. Einstein

"Seh ich die Werke der Meister an,
So seh ich das, was sie getan;
Betracht ich meine Siebensachen,
Seh ich, was ich hätt' sollen machen."

J. Goethe

ACKNOWLEDGEMENTS

My greatest thanks go to my advisor, Howard Berg. He has scientific insight, technical ability, and a warm personality--an all too rare combination. My partners in abusing bacteria, Mike Manson, Akira Ishihara, and, most of all, Steve Block, provided invaluable aid and ideas. The other members of the lab, especially Markus Meister and Pat Conley, also have made important contributions. I appreciate the comments and help provided by the members of my thesis committee: H. Lester (in whose lab I have always been welcome), C. Brokaw, D. Fender, J. Hopfield and M. Simon. Nancy Gill and Kathy O'Loughlin were always there to guide me cheerfully through the maze of details that is the bane of inhabitants of all ivory towers. Caren Oto willingly typed this thesis on amazingly short notice. All in all, I have found Caltech to be a beautiful campus filled with people who are interested in helping each other, which is a refreshing change from the bureaucracy of Harvard University.

Theresa Beyer, my fiancée and best friend, made life after lab in the Los Angeles area a lot of fun, and drew my attention to the Goethe poem. The past and present members of J. Alfred Prufrock House and the J.A.P. eating group formed my Los Angeles family.

Finally, I owe it all to my parents, Edwin and Jo Ann Segall, for giving me their love and support from the start. Ed showed me the Einstein quotation.

I gratefully acknowledge funding by an NSF predoctoral fellowship, an NIH training grant, and the Weigle Memorial Fund.

ABSTRACT

Chemotactic responses of the bacterium *Escherichia coli* were elicited by iontophoretic ejection of charged compounds from micropipettes. Responses were measured using cells tethered by a single flagellum and following the direction of rotation of the cell body (with cells viewed from above the surface to which the flagellum is attached) . Mean response latencies to addition of attractant or repellent were 0.1 to 0.2 seconds. Brief pulses of attractants and repellents were used to determine the impulse response for chemotaxis. In response to a brief pulse of attractant the counterclockwise (CCW) bias (fraction of time that the flagellar motor spent rotating CCW) increased rapidly to a peak, then fell below the prestimulus value, returning to baseline within 5 seconds--the response was biphasic. Repellent impulse responses were similar but inverted. The attractant impulse response accurately predicted responses to step changes, linear ramp changes and sine wave changes in receptor occupancy. Mutants defective in the enzymes responsible for methylation (*che*R) and demethylation (*che*B), which do not adapt to attractant stimuli, gave monophasic impulse responses--only the initial peak was evident. Mutants defective in the *cheZ* gene product had responses that were slower than the wild-type by a factor of about 10. The responses of flagellar motors on filamentous cells also were studied. The reversals of two motors on the same cell were not correlated, but fluctuations in bias were correlated for motors less than 10 microns apart. Responses of motors of filamentous cells to iontophoretic application of aspartate indicated that the internal chemotaxis signal travels about 2 microns in cells lacking the *che*R and *che*B gene products and about 6 microns in cells with a defective *cheZ* gene product. These data are consistent with a simple model involving destruction of a cellular chemotaxis signal by the *cheZ* gene product.

TABLE OF CONTENTS

Page

Quotations ii

Acknowledgements iii

Abstract iv

Table of Contents v

General Introduction. 1

Chapter I — The Latency of the Chemotactic Response 20

Signal Processing Times in Bacterial Chemotaxis 27
(reprinted from Nature 296:855-857.
copyright 1982, Macmillan Journals Ltd.).

Additional Data. 30

Chapter II — Impulse Responses in Bacterial Chemotaxis 36
(reprinted from Cell 31:215-226
copyright 1982, MIT)

Chapter III — Further Impulse and Step Response Studies 50

Chapter IV — Coordination of Flagella on Filamentous 81
Cells of *Escherichia coli*
(reprinted from J. Bacteriol. 155:228-237
copyright 1983, Am. Soc. Microbiol.)

Chapter V — Iontophoretic Studies of Chemotactic Signalling 93
in Filamentous Cells of *Escherichia coli*
(submitted to J. Bacteriol.)

Chapter VI — Summary and Speculations 138

References 156

INTRODUCTION

Bacteria are the simplest free-living organisms that exhibit behavior. Through a sophisticated motility system involving about 50 gene products, *Escherichia coli* cells can accumulate in regions containing attractants, and avoid repellents (Parkinson, 1981). Taxis is the movement of an organism toward or away from a source of stimulation (Weibull, 1960). Although in a strict sense bacterial responses are not tactic responses (Diehn et al., 1977) because they do not orient themselves in a particular direction (see below), the responses to light, oxygen, temperature, and chemicals are usually described as phototaxis, aerotaxis, thermotaxis, and chemotaxis. I will follow the majority and use these terms to describe bacterial behavior.

Many species of bacteria can have tactic responses. The utility of such behavior for bacteria is easy to understand, but its ecological significance has not been directly determined (Chet and Mitchell, 1976; Doetsch and Sjoblad, 1980). It is likely that tactic behavior is important for two reasons: 1) it enables cells to move towards sources of nutrients or towards sites which they can infect; and 2) tactic cells can leave overpopulated or poisonous regions (Seymour and Doetsch, 1973). Theoretical studies suggest that in an inhomogeneous environment chemotactic bacteria should be able to compete effectively with nonchemotactic strains that would outgrow them in a homogeneous environment (Lauffenburger et al., 1982). Indeed, it has been demonstrated that aerotactic cells can outgrow nonmotile strains in unstirred cultures, presumably by remaining in regions where oxygen levels can support growth (Old and Duguid, 1970; Smith and Deutsch, 1969). A dramatic example of the ability of chemotactic bacteria to follow the nutrient supply is a swarm plate (Hazelbauer et al., 1969). This is an agar medium containing nutrients into which a localized inoculum of bacteria is made. The bacteria use up the nutrients near them, resulting in local gradients of nutrients. The cells then migrate up the gradients,

and are seen as outward moving rings. Nonchemotactic cells remain in the center, near the original inoculation site. Such a difference in the spread of chemotactic and nonchemotactic strains may occur in the wild, since similar results have been reported for inoculations of chemotactic and nonchemotactic strains of *Rhizobium meliloti* into soil (Soby and Bergman, 1983). Chemotaxis may be important in the infection of the intestine by *Vibrio cholerae* (Freter et al., 1981), and in the infection of the urinary tract by *E. coli* (Herrmann and Burman, 1983). Studies of the ecological significance of tactic behavior by bacteria are needed.

Brief History of Studies of Bacterial Taxis

Antoni van Leeuwenhoek is credited with the discovery of bacteria (Bardell, 1982). His earliest recorded observation of bacteria is a report written in 1676 describing an attempt to determine why pepper had such a potent taste. He had placed pepper in water for several weeks and upon looking at the solution with his microscope, he saw creatures that were "incredibly small." However, the main purpose of that report was to explain that the hot taste of peppers was due to sharp-pointed microscopic particles that irritated the tongue! A more complete description of the types of bacteria found in dental plaque was given in 1683.

Later workers, as well as Leeuwenhoek, noted that bacteria would collect around food particles or air/water surfaces. More detailed analyses of the tactic responses exhibited by a variety of species of bacteria did not start until the 1880's (for reviews, see Berg, 1975; Weibull, 1960). Engelmann described the responses of bacteria to oxygen and light, termed respectively aerotaxis and phototaxis. Pfeffer studied the chemotaxis to such items as meat extract, salts, sugars, acids, bases, and morphine, using an assay that he developed. Today's

version of that assay is called the Pfeffer assay (Adler, 1969; 1973), in which the tip of a capillary tube containing a solution of the compound to be tested is placed in a bacterial suspension. If the bacteria are attracted to the compound in the capillary, they accumulate inside the tube, while if they are repelled, fewer bacteria are found inside than enter by random motion. The final type of taxis clearly demonstrated was thermotaxis, in which bacteria respond to changes in temperature.

The mechanism that led to accumulation of bacteria in a region containing a higher concentration of attractant (or lower concentration of repellent) was thought to be a shock reaction. Upon leaving the region containing the attractant, bacteria often stopped swimming and backed up. Thus, cells were thought to swim into a region containing attractant, and then not be able to leave, leading to a local increase in cell number. Although attractants tended to be nutrients and repellents tended to be harmful, there was not a tight correlation between the nutritional value of a compound and the tactic response to it. It was thought that high salt concentrations might be repellents through an osmotic effect. Phototactic responses in *Rhodospirillum rubrum* were found to have a close correlation with photosynthesis and the conclusion drawn was that sudden changes in photosynthetic rate produced a tactic response. Quite recently it has been learned that the major light-transducing pigments are not involved in phototactic responses of *Halobacterium halobium*. There is a special pigment which seems to be responsible only for phototactic responses (Bogolmoni and Spudich, 1982) in this species.

Although staining techniques could demonstrate that dead bacteria had flagella (long, helical appendages), Reichert perfected dark field techniques that allowed the motion of the flagella of most species to be seen while the bacteria were moving. Metzner also carried out comprehensive analyses of the movement

of flagella and the correlation with bacterial movement. While it could not be determined whether the flagella were rotating or bending (as do eukaryotic flagella), most workers believed that movement of the flagella generated the propulsive force that produced bacterial motion. With the advent of the electron microscope, bacterial flagella were found to be much smaller than eukaryotic flagella (10-20 nm compared to 200nm; Lowy and Hanson, 1965). The structure of the filament is much simpler--it contains only one type of protein and appears to be a simple tube, shaped as a three-dimensional helix.

In 1966, Julius Adler initiated the modern era of studies of bacterial chemotaxis (Adler, 1966). Although earlier workers had worked on many different species, he selected *E. coli* as the bacterium to study because of the large amount of biochemical and genetic information that was available for this organism. This proved to be a wise choice. Today over 10 groups are studying in detail the physiology, genetics, and biochemistry of tactic responses of *E. coli* and *Salmonella typhimurium* (which has very similar physiology and behavior). In addition, other groups are studying bacteria such as *Bacillus subtilis*, *H. halobium*, *Caulobacter cresentia*, and *Spirochaetia aurantia*, and comparing their responses to those exhibited by *E. coli* and *S. typhimurium*. My work has concentrated exclusively on *E. coli* and unless otherwise stated I will be discussing results from studies on *E. coli* or *S. typhimurium*.

Swimming Behavior of *E. coli*

E. coli is a single-celled bacterium with a diameter of 0.5-1 μm and length of 1.5-3 μm, depending on growth rate (Trueba and Woldringh, 1980). It is a gram negative bacterium, having (from the outside in) an outer membrane, a cell wall (also called the peptidoglycan layer) with periplasmic space, and finally a cytoplasmic membrane. It is peritrichously flagellated, with 5-8 flagella arising

at random points on the cytoplasmic membrane and passing through the wall and outer membrane (Iino, 1977). Flagella are about 15 microns long (Silverman, 1980). The average *E. coli* spends about half its lifetime in the colon, and the other half in the soil (Savageau, 1983). Although most isolates of *E.coli* from the intestine are motile (Koch, 1971), it is not known whether taxis is important in both habitats or not. Cells swimming in a simple buffer and salts solution exhibit two alternating modes of motion. These consist of a period of forward motion lasting about one second, called a run, followed by a period of uncoordinated motion lasting about 0.1 sec, called a tumble or twiddle (Berg and Brown, 1972; Berg and Brown, 1974). The tumble randomly reorients the direction of the next run. During a run the flagellar filaments come together to form a bundle which drives the cell forward. The bundle then flies apart and the filaments are isolated during a tumble (Macnab and Koshland, 1974). This continuous series of runs alternating with tumbles generates a three-dimensional random walk. The distributions of run and tumble lengths are exponential.

When a cell swims in a spatial concentration gradient of attractant, runs that carry it up the gradient are lengthened, while runs that carry it down the gradient are not. This imposes a bias upon the random walk (Berg and Brown, 1972; Berg and Brown, 1974) and the net motion is up the gradient. Note that this is a different response from the shock reaction described in earlier studies - in them one might say that runs down the gradient were seen to be shortened.

The mechanism that a cell uses to determine if it is swimming up an attractant gradient involves a temporal comparison (Macnab and Koshland, 1972; Brown and Berg, 1974). Rapid mixing of cells with a high concentration of attractant causes the cells to swim in one uninterrupted run lasting as long as 300 seconds, depending on the concentration change (Spudich and Koshland, 1975). Removal of attractant or addition of repellent causes a short period of

tumbling. Cells respond to changes in concentration by increasing the length of runs or tumbles, but with time they also adapt, returning to the run and tumble lengths that occurred before the addition of attractant or repellent.

The response of a single flagellar motor to stimuli can also be studied. The flagellar motor is a true rotary motor (Berg and Anderson, 1973; Silverman and Simon, 1974), powered by the protonmotive force (Larsen et al., 1974a; Manson et al., 1977). Using antibody to the flagellar filament, a single filament can be attached to a glass coverslip, and the rotation of the flagellar motor then results in rotation of the cell body instead (Silverman and Simon, 1974)! Cells tethered in this fashion rotate alternately clockwise (CW) and counterclockwise (CCW) with mean intervals of about 1 sec for either direction of rotation (Berg and Tedesco, 1975). Addition of attractant or removal of repellent produces continuous CCW rotation (Larsen et al., 1974b), when viewed such that the cell body is between the observer and the coverslip to which the filament is attached. Removal of attractant or addition of repellent produces CW rotation. Rotation returns to the prestimulated mode with a time course similar to that seen with adaptation of swimming cells. Adaptation to addition of large concentrations of attractant takes as long as five to ten minutes, and adaptation to removal of attractant occurs in under 20 seconds. Therefore CCW rotation of the flagella generates a run, while CW rotation generates tumbles. This is consistent with the left-handed helicity of the flagellar filament. CCW rotation of the flagella forces liquid away from the cell body. This enhances the formation of a bundle (Anderson, 1975; Macnab, 1977). CW rotation causes jamming of the bundle and even changes the waveform of the filament, resulting in the erratic movement characteristic of a tumble (Macnab and Ornston, 1977).

The responses of swimming cells in competition experiments, their ability to respond to nonmetabolizable analogues of attractants, and the isolation of

mutants defective in responses to classes of compounds all suggest that the measurement of external attractant concentration utilizes binding to a receptor (Adler, 1969). Motion of swimming cells up a preformed attractant gradient (Dahlquist et al., 1976) and sensitivity measurements using Pfeffer assays (Mesibov et al., 1973) show a hyperbolic dependence on changes in concentration. The effects on mean run length of enzymatically generated increases in attractant concentration were best fit by the rate of change of receptor occupancy (Brown and Berg, 1974). Finally, the adaptation times of swimming and tethered cells could be interpreted as being proportional to the change in fraction of receptor binding attractant (Berg and Tedesco, 1975; Spudich and Koshland, 1975).

Genetics

The study of mutants has been an important method for analyzing the mechanisms of bacterial chemotaxis. The types of defects that occur give clues as to the function of proteins in generating chemotactic responses. The loss of a biochemical activity such as binding or enzymatic reaction in a particular mutant suggests that the activity is necessary for proper chemotactic behavior. There are three categories of mutations based on the extent of the defect in chemotactic ability.

First, there are mutants defective in the response to a particular compound (usually a sugar) and its analogues (Hazelbauer et al., 1969). Such mutants often have a defect in the periplasmic binding protein involved in transport of the sugar (Hazelbauer and Adler, 1971; Adler et al., 1973). Thus the binding proteins are involved in two systems--the transport system and chemotactic responses. In the case of sugars transported by the phosphotransferase (PTS) system (such as glucose, mannitol, and D-glucosamine), the binding proteins have specific

proteins to which they, in turn, must bind for both transport and chemotaxis to occur (Adler and Epstein, 1974). Therefore, transport may be required for the chemotactic response to these sugars (Pecher et al., 1982). The responses to the non-PTS sugars maltose, ribose and galactose do not require other components of their respective transport systems. Responses to oxygen and other electron receptors require electron transport and are mediated by cytochrome oxidases (Laszlo and Taylor, 1981).

The second type of mutant is defective in responses to a group of structurally unrelated compounds. Such pleiotropic taxis mutants (Reader et al., 1979) have a defect in one of three cytoplasmic membrane proteins of molecular weight (MW) about 60,000 daltons. These proteins represent a stage at which the processing of responses to different compounds converges. One protein mediates responses to ribose and galactose via their binding proteins and is called the *trg* protein (*t*axis to *r*ibose and *g*alactose) (Ordal and Adler, 1974; Kondoh, Ball and Adler, 1979). A second protein is the aspartate receptor, binds the maltose binding protein, and also mediates the response to the repellents Co and Ni; it is called the *tar* protein (*t*axis to *a*spartate and *r*epellents) (Reader et al., 1979). The final protein binds serine and also mediates the responses to the repellents leucine and indole; it is called the *tsr* protein (*t*axis to *s*erine and *r*epellents) (Parkinson, 1975). These proteins can bind amino acid attractants directly, might bind the repellents, and interact with sugar binding proteins to mediate the responses to particular sugars not transported by the PTS system.

The *tar* and *tsr* proteins are also sensitive to several other types of stimuli. They produce responses to changes in temperature (Mizuno and Imae, 1984; Maeda and Imae, 1977). Weak acids and bases generate chemotactic responses by altering the internal pH, which is sensed by these proteins (Repaske and Adler, 1981; Kihara and Macnab, 1981; Slonczewski et al., 1982). Glycerol is

a repellent that may interact with the cytoplasmic membrane in such a way that the *trg*, *tsr* and *tar* proteins all are involved in generating the response (Oosawa and Imae, 1983).

Finally, there are mutants that are not chemotactic to any compounds. Such generally nonchemotactic mutants are designated *che* mutants (Armstrong and Adler, 1969), with a letter specifying a particular gene. There are about eight *che* genes--A,B,C,R,V,W,Y, and Z (for a review see Parkinson, 1981). These mutants have an altered direction of rotation of the flagellar motor--*che* A,R,W,Y have excessive CCW rotation, B and Z are CW biased. *Che*C and V can have altered bias in either direction and are also important in the construction of the flagellar motor. Some *che* mutants can still respond to attractants and repellents, but often with increased thresholds. The alteration in direction of rotation alone will seriously affect the running and tumbling behavior and thus reduce the ability of swimming cells to migrate up an attractant gradient. The *che*A gene codes for two proteins, which are identical except that the smaller product is missing the N-terminal portion of the larger protein.

The localization and physical interactions of some of the *che* gene products have been studied. Localization was done by fractionating cells and measuring the amount of each protein in the various fractions (Ridgway et al., 1977). The *che*Y and W proteins and the smaller *che*A protein were found only in the cytoplasmic fraction. The *che*B, R, and Z proteins, and the larger *che*A protein were found in both inner membrane and cytoplasmic fractions. The *tsr* and *tar* proteins were found only in the inner membrane fraction. Crosslinking studies with a cleavable crosslinker (Chelsky and Dahlquist, 1980a) suggest that the *che*W, B, and Z proteins form complexes with other proteins, possibly with each other. An alternative method for studying interactions is to look for suppression of mutations in one gene by mutations in a second gene. *Che*Z and Y mutations

can be suppressed by mutations in *che*C or V (Parkinson and Parker, 1979; Parkinson et al., 1983). Complementation studies suggest that *che*Z may also interact with *che*B, and *che*Y with *che*R (Parkinson, 1978; DeFranco et al., 1979). From these data it has been suggested that the *che*C and V proteins form a switch complex on the flagellum that determines the direction of rotation, and that the *che*Y and Z proteins can bind to this switch to produce CW and CCW rotation, respectively (Parkinson et al., 1981).

Biochemistry

The major biochemical reaction known to be important in bacterial chemotaxis is methylation (Kort et al., 1975). The *tar*, *trg* and *tsr* proteins are specifically methylated by the cheR gene product (Springer and Koshland, 1977) at glutamic acid residues (Kleene et al., 1977; van der Werf and Koshland, 1977) with S-adenosylmethionine as the methyl donor (Armstrong, 1972; Aswad and Koshland, 1975). The *che*B gene product catalyzes the demethylation of these residues (Stock and Koshland, 1978; Snyder and Koshland, 1981), releasing methanol (Toews and Adler, 1979). The *tar*, *trg* and *tsr* proteins are also termed MCP's (*m*ethyl-accepting *c*hemotaxis *p*roteins, Kort et al., 1975). Methylation of a particular MCP is strongly correlated with adaptation to the responses mediated by that protein (Goy et al., 1977). Thus addition of aspartate causes methylation of the *tar* protein with a time course similar to the time course of adaptation (Springer et al., 1977). The net result is that tar has increased methylation while methylation of the other MCP's does not change. Addition of Ni or Co produces specific demethylation of *tar*. The same holds true for methylation of *tsr* and *trg* (Kondoh et al., 1979) and adaptation to the compounds whose responses require those proteins.

The MCP's are multiply methylated (Boyd and Simon, 1980; Chelsky and Dahlquist, 1980b; DeFranco and Koshland, 1980; Engstrom and Hazelbauer, 1980). Methylation occurs on two tryptic peptides (Chelsky and Dahlquist, 1981; Kehry and Dahlquist, 1982a). In cells adapted to buffer there is a basal level of 1-2 methyl groups per molecule. Repellents can reduce this level by 50% while cells adapted to attractants can have 3 to 4 times as many (Stock and Koshland, 1981).

A second reaction catalyzed by the *che*B gene product (Hazelbauer and Engstrom, 1981; Sherris and Parkinson, 1981) is deamidation of glutamines on newly synthesized MCP's, which converts those residues to glutamic acids which then can be methylated (Kehry et al., 1983). Indeed, this modification appears to be required in order for some residues that are originally glutamic acid residues to be methylated (Kehry and Dahlquist, 1982b). *Che*B modification is stimulated by repellents and may allow some adaptation to repellent stimuli in *che*R mutants (Rollins and Dahlquist, 1981; Stock et al., 1981).

Strains carrying a mutation in the *che*R gene have motors with a strong CCW bias and reduced levels of methylation of their MCP's (Rollins and Dahlquist, 1980; Silverman and Simon, 1977). Addition of repellent can produce CW rotation (Parkinson and Revello, 1978; Goy, Springer and Adler, 1978). Motors of strains carrying a mutation in the *che*B gene have a strong CW bias, and addition of high levels of attractant will produce CCW rotation (Yonekawa et al., 1983). This information combined with the correlation of methylation with adaptation implies that a comparison of the concentration of a particular compound with the level of methylation of the MCP's determines the direction of rotation of the flagellar motor (Boyd and Simon, 1982). This comparison is most likely done by each MCP molecule--binding of attractant could cause the MCP to

send a signal to the flagellar motors to rotate CCW while methylation would block the sending of that signal.

Simultaneous addition of attractant and repellent stimuli to wild-type cells produces a motor response consistent with summation of the individual responses, even if the attractant and repellent are processed by different MCP's (Berg and Tedesco, 1975; Tsang et al., 1973; Adler and Tso, 1974). This suggests that the signal sent to the motor is the sum of the states of all the MCP's. The signal does not depend on methylation because *che*R*che*B double mutants still respond to attractants (Sherris and Parkinson, 1981).

This signal also controls to some extent the rates of methylation and demethylation catalyzed by the *che*R and *che*B gene products. Under steady state conditions the methyl groups on the MCP's turn over and this turnover is reflected in the release of methanol. Addition of an attractant whose response is mediated by a single MCP such as aspartate will block the demethylation of all MCP's until the cells have adapted (Toews et al., 1979). This suggests that there is an effect on *che*B methylesterase activity by the signal. However, turnover rates have returned to normal in an adapted cell when the signal has returned to its original level (Springer et al., 1982), while the methylation level of the appropriate MCP remains increased (Goy et al., 1977). This means that there must also be a structural change in the MCP when it binds attractant that makes the MCP more susceptible to methylation (Hayashi et al., 1982; Kleene et al., 1979).

The DNA sequences of the MCP's have been determined, and there are strong homologies among them (Boyd et al., 1983; Krikos et al., 1983; Russo and Koshland, 1983). All have an N-terminal hydrophobic amino acid sequence which may be an uncleaved signal sequence, followed by a long hydrophilic region which is different for each molecule. Then there is a stretch of hydrophobic amino

acids which is long enough to span the membrane once as an alpha helix. Past this putative membrane spanning sequence is a very long region whose amino acid sequence is highly conserved among the MCP's. It includes the two methylated regions and a sequence between them 40 amino acids long that is 98% identical in all three MCP's. Each methylated glutamic acid residue is next to a second unmethylated glutamic acid residue. There is a fourth MCP of unknown function whose gene was found next to that coding for *tar*; it is called *tap* for *t*axis *a*ssociated *p*rotein (Boyd et al., 1981; Wang et al., 1982). This gene does not appear to be necessary for chemotaxis and it has not been implicated in any known response.

It is generally believed that the MCP's are oriented with the N-terminal hydrophilic region in the periplasmic space, where the binding to attractants, binding proteins, and repellents that is specific to each MCP type can occur. The C-terminal end, which is highly conserved and methylated by the cytoplasmic enzymes *che*R and *che*B probably lies in the cytoplasm (Boyd et al., 1982; Wang and Koshland, 1980) and is very likely involved in the control of the direction of rotation of the flagellar motors.

Coupling of Receptors to Flagella

The nature of the signal sent to the flagella in *E. coli* when receptor binds attractant is a complete mystery. It is clear that metabolism is only involved in the responses to electron acceptors such as oxygen (Taylor, 1983). The responses to attractants such as sugars, aspartate and serine do not require their metabolism (Adler, 1969). As noted above, it appears that summation of signals sent by different MCP's occurs. But it is not even clear that the responses to PTS sugars utilize the same signals as the responses mediated by the MCP's. It could be that several different compounds can affect the motor and its direction

of rotation is determined by the relative concentrations of all of these compounds.

Some proposed messengers include membrane potential (Szmelcman and Adler, 1976), divalent cations (Ordal, 1977), cGMP (Black et al., 1980), cAMP (Black et al., 1983) and ion fluxes across the cytoplasmic membrane (Kosowar, 1983; Eisenbach et al., 1983; Szmelcman and Adler, 1976). It is unlikely that membrane potential per se mediates the chemotactic response although changes in the membrane potential can affect the direction of rotation of the motor (Miller and Koshland, 1977; Snyder et al., 1981; Margolin and Eisenbach, submitted) . The responses to oxygen and blue light may be due to changes in protonmotive force (Taylor, 1983; Khan and Macnab, 1980). In *S. aurantia* membrane potential may be involved in chemotactic signalling, because clamping the membrane potential does affect chemotactic responses (Goulbourne and Greenberg, 1981; 1983). In *B. subtilis* there is evidence that Ca or Mg concentrations may affect the direction of rotation of the motor (Ordal, 1977), but this is unlikely to be true for *E. coli* (Snyder et al., 1981). Initial results suggesting that cGMP levels change in response to chemotactic stimuli could not be reproduced (Black et al., 1983). There is some evidence that adenyl cyclase may be involved in the response to PTS sugars, but is definitely not involved in the response to aspartate (Black et al., 1983). There is evidence that arsenate blocks the ability of the motor to generate tumbles, due to lowering the levels of ATP or a metabolite of ATP (Shioi et al., 1982; Arai, 1981; Kondoh, 1980).

A Brief Summary

Text-figure 1 summarizes the information presented in this introduction. There are several types of receptor systems--those involving PTS sugars, electron acceptors, and MCP's. The MCP system is the best characterized. In

that system binding of attractant to an MCP or to a receptor which then binds to an MCP initiates a change in direction of flagellar rotation, probably through a change in the concentration of an intracellular compound. At the same time there is a slow increase in the level of methylation of the appropriate MCP. There are interactions of the *cheY* and *cheZ* proteins that could be involved in either sending the signal to the flagellar motor and/or controlling the rate of methylation. Methylation probably is involved in returning the bias of the flagellar motor to the unstimulated level by returning the level of the intracellular compound to the unstimulated level. Methylation is not involved in adaptation to PTS sugars or oxygen (Niwano and Taylor, 1982).

My Work

At the time when calcium and membrane potential had been suggested as possible intracellular signals, Howard conceived of making a very long *E. coli* cell, stimulating one end, and seeing if the other end of the cell received the signal. Any membrane potential or action potential type of signal should rapidly reach the other end. His belief was that some type of long range signalling system did exist and would be revealed by this experiment. Observations of *Spirillum volutans*, which has tufts of flagella at both ends, showed that the reversals of direction of rotation of the two ends were coordinated to within 60 msec (Krieg et al., 1967). Since *S. volutans* cells are 20-50 microns long, a chemical messenger diffusing from one end to the other would take 0.2 sec or longer--possibly too slow. Thus if *E. coli* had a similar signalling system, long filamentous cells of *E. coli* could have long-range coupling.

Two technologies had to be developed for this experiment: 1) growing long filamentous cells and attaching markers to the flagellar motors so that the directions of rotation could be followed, and 2) a stimulation system that would

Text-figure 1. Summary of bacterial chemotaxis system.

This is a simplified summary of the information given in the Introduction. The outer membrane and cell wall are drawn as a thick outer shell with pores for diffusion of compounds of small molecular weight (e.g., aspartate and serine). The cytoplasmic membrane is drawn as a thin line with methyl-accepting chemotaxis proteins (MCP's: tar, tsr, and trg), flagellar motor, the sugar phosphotransferase system (PTS), and protonmotive force (PMF) system embedded in it. Binding proteins for maltose (MBP), ribose (RBP), and galactose (GBP) are drawn in the periplasmic space. Details of the PTS and PMF systems are not included. The MCP's are drawn with some methyl (CH_3) groups attached. Addition of methyl groups is catalyzed by the *che*R gene product (R) from S-adenosylmethionine (SAM). Removal of methyl groups from the MCP's is catalyzed by the *che*B gene product (B). Signalling to the flagellar motor is indicated by the thin black lines, with the *che* gene products that have unknown function included (Y,A,W,Z). Possible interactions between the *che*Z and *che*B and between the *che*Y and *che*R proteins are indicated by the double arrows. The *che*V and *che*C gene products are shown interacting with the motor and with the signal pathway. Figure adapted from Niwano et al., 1982.

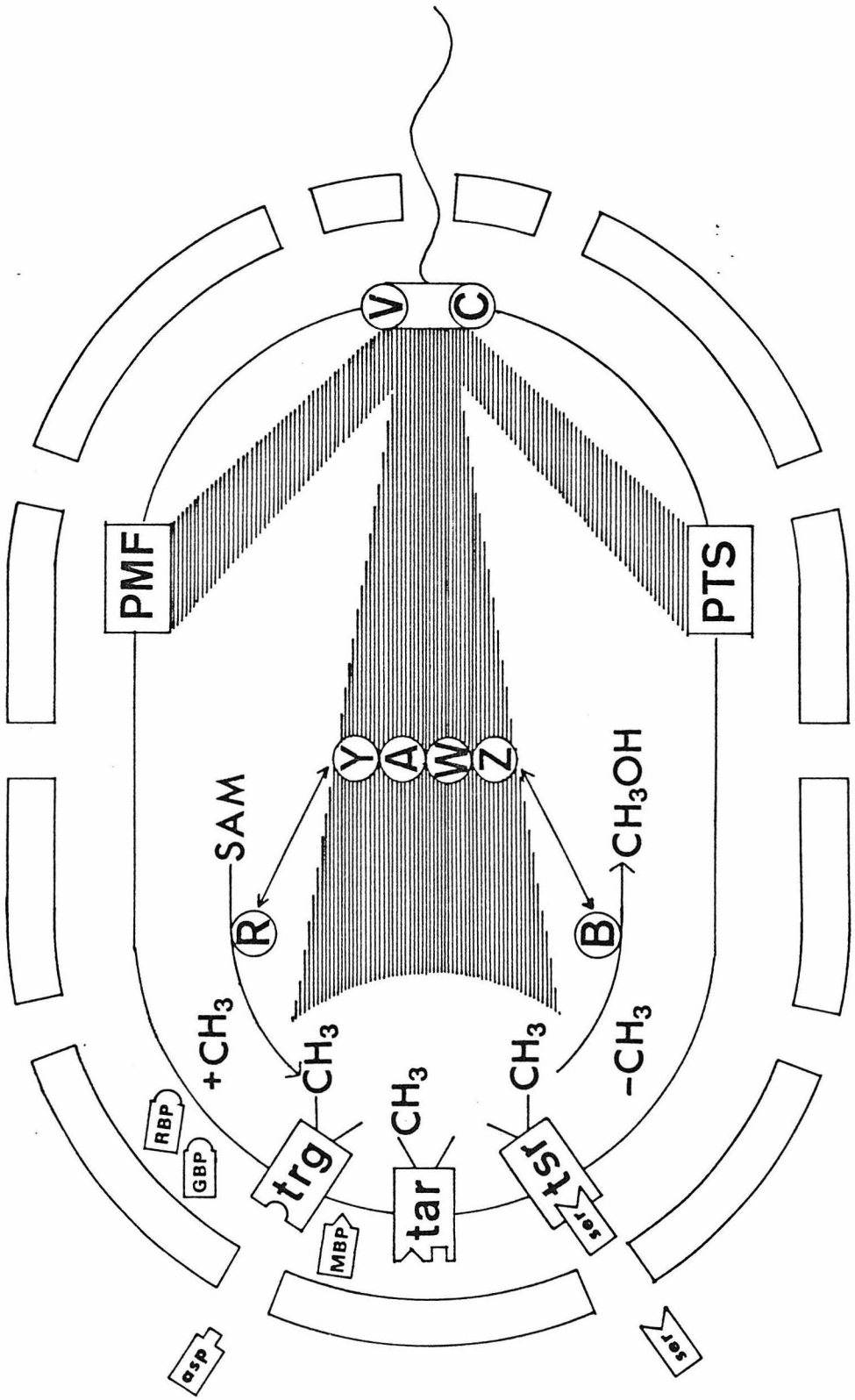
V
C
PMF
PTS
Y
A
W
Z
R
SAM
B
CH3OH
+CH3
CH3
CH3
CH3
-CH3
RBP
GBP
trg
MBP
tar
tsr
tsr
GSP
tsr

stimulate rapidly in a confined volume so that one end of the filamentous cell could be stimulated independently of the other end. Mike Manson and Howard were developing these techniques when I joined the lab. Iontophoretic stimulation using a micropipette filled with a charged attractant had been chosen as the method for producing a local change in attractant concentration. As a control Mike had started testing normal length tethered cells to determine their responses under this stimulation. I joined him on this and finished developing the application of iontophoresis to the stimulation of *E. coli*. The first three chapters cover my studies of the responses of tethered cells of normal length to iontophoretic application of attractants and repellents in collaboration with Mike Manson and Steve Block.

Although Mike had also worked out the basic strategy for how to attach markers to long filamentous cells, I did not work further on this immediately for two reasons. First, a great deal could be learned studying normal tethered cells using the rapid stimulation method of iontophoresis, and second, I did not believe that *E. coli* had a long distance signalling system. Akira Ishihara joined the lab a few years after I came and worked out the details of the filamentous cell technology. It was a monumental feat for which he deserves much credit. The fourth and fifth chapters cover my collaboration with him, including the test of long range coupling. The final chapter contains some concluding speculations and thoughts on bacterial chemotaxis.

Chapter I

THE LATENCY OF THE CHEMOTACTIC RESPONSE

The purpose of this experiment was to develop the procedures for stimulating *E. coli* iontophoretically, and to measure some of the characteristics of responses to iontophoretic stimulation. The experimental apparatus had to: 1) follow the direction of rotation of a tethered cell with good time resolution, 2) allow the placement of a micropipette near the cell, and 3) pass a current through the pipette, ejecting charged molecules.

Cells were tethered to the upper surface of a glass coverslip which was then attached to the bottom of a stainless steel flow cell (Berg and Block, in press). The flow cell sat on an aluminium, temperature-controlled stage that could be positioned accurately with two micrometer screws. Tethered cells were observed with a Nikon S-Ke microscope equipped with a Zeiss 40X water-immersion phase-contrast objective which was electrically and thermally insulated from the microscope and whose temperature also could be controlled. The direction of rotation of a tethered cell was followed using a linear graded filter apparatus, a device originally used in an attempt to detect steps in the rotation of the flagellar motor, adapted from Kobayasi et al., 1977, by Howard (Berg et al., 1982). The output provides the x- and y-coordinates of the center of brightness of the cell image. These signals were filtered to remove noise, ac-coupled, and recorded on a strip-chart recorder (Brush Mark 220, 25 mm/sec) together with an event marker indicating the direction of rotation of the tethered cell (determined from the relative phase of the two signals by a circuit that checked the sign of the x-coordinate whenever the y-coordinate crossed zero). The amount of filtering normally used introduced about a 0.06 sec time lag in the x- and y- signals.

The micropipette was positioned using a micromanipulator (Narishige MO-103). The current injection circuit was built by Howard, following the design of Dreyer and Peper, 1974). Pulses of predetermined amplitude (0.01-1000 nA)

and outside, the only difference being the addition of charged attractant to the solution inside the micropipette. We felt that an important control for these experiments was that pipettes containing only buffer should not stimulate cells. Given this control, any responses observed would be due to whatever compound had been added to the buffer. Unfortunately, there were still some problems, which Mike and I tackled together.

The original buffer tested was a standard chemotaxis buffer, containing phosphate pH 7, NaCl and/or KCl, and EDTA (to chelate divalent cations that inhibit motility). Although negative currents (up to -100 nA) from pipettes containing only this buffer did not normally stimulate cells, we found that positive currents (+10 to +100 nA) did. This was not an electrical effect because positive currents could be attractant or repellent stimuli. Even currents from the same pipette could suddenly switch from being attractant to repellent! Cells responded to pipettes containing Tris buffer, less strongly if the salt was choline chloride. It was not due to compounds leaching out of the micropipette surface (the glass normally used for pipettes is a borosilicate), because micropipettes made from aluminosilicate glass or even fused quartz still stimulated cells. (Mike noted that aluminosilicate pipettes were more fragile than quartz or borosilicate pipettes.) Micropipettes pulled by F. Haer (a commercial supplier) or by ourselves had similar effects. The response was not due to temperature or any stimuli mediated specifically by *tsr* or *tar*, because mutants in both those proteins still responded. Also, the temperature change due to resistive heating should be independent of the sign of the current (although usually the resistance to positive currents was about twice the resistance to negative currents). Quite often it appeared that strong fluid flows accompanied the current. We thought that this might be due to a surface charge effect--glass surfaces are negatively charged. Mike tried adding BSA to the buffer in hopes of coating the surface but

that had no effect. I tried silanizing the micropipettes, but that also had no effect; the tips of such pipettes tended to clog and they were difficult to fill.

Finally, Jim Hudspeth suggested that we add thorium to the buffer. I initially thought he was joking, but he was not. Thorium cations are tetravalent, which causes them to bind quite tightly to negatively charged surfaces. This then reduces electroosmotic flows and other problems due to surface potentials (Schanne et al., 1968). Because phosphate and EDTA bind thorium, I used Tris and tetren (Reilley and Vavoulis, 1959) as buffer and divalent chelating agent, respectively. I found that 10^{-5} molar thorium chloride dramatically reduced the responses to positive currents. Thus we concluded that a surface charge effect, possibly resulting in the release of an excess of cations for positive currents, was producing the response.

The buffer that we now use is Tris buffer containing NaCl and KCl salts to stabilize the antibodies used for tethering, tetren, thorium chloride, lactate as an energy supply for the cells, and methionine to insure that methylation processes are not limiting. This buffer is not ideal--the Tris is near the edge of its buffering range and the pH of the solution changes drops 0.05 units per week at room temperature. The thorium chloride cannot be kept as a more concentrated stock solution but must be made fresh for each new buffer solution. It is added only to buffers put in the micropipettes. Fortunately, the buffers containing 10^{-5}M thorium can be stored for several months at 4^{o}C. The resistance behavior of a pipette filled with a solution without adequate thorium has a characteristic time course. During pulses several seconds long the resistance slowly declines. For pipettes filled with "good" solutions the resistance remains fairly constant during the pulse (less than 10 % change). The resistance change in pipettes filled with "bad" solutions may reflect changing ionic conditions at the tip during current flow.

This technique works quite well for ejection of charged compounds such as aspartate, α-methylaspartate, benzoate, nickel, and D-glucosamine. A test of the speed of release was made by filling pipettes with buffer containing fluorescein(which is negatively charged) and following the release in darkfield with a pinhole and a photomultiplier (Berg, 1976; Text-figure 2). This was only a crude test because of contributions from out of focus regions, but it gave us confidence that release of fluorescein was beginning within 10 msec of the start of current flow and ending soon after the end of current flow. As it turns out, this is sufficiently rapid for studies of bacterial chemotactic responses.

The amount of α-methylaspartate released is roughly what would be estimated from the relative mobilities of the ions in the buffer. I estimated that the steady state concentration of α-methylaspartate 4 microns from the tip of the pipette containing 10 mM α-methylaspartate should be 0.5 mM for a -100 nA current, and should decrease linearly for smaller concentrations in the pipette. This is roughly what is observed (see table in Segall et al., 1982, below).

The limitations of this technique are that 1) only a fraction of the current is carried by the compound of interest because of the buffer solution, requiring a concentration inside the pipette of as much as 20 times the dissociation constant of the receptor to be studied; and 2) the efficiency of ejecting uncharged compounds such as serine and sugars has not been determined. It is possible that one might be able to use flows out of the tip driven by current to eject uncharged compounds. Also, serine is charged at a higher pH, and thus it may be possible to use a higher pH inside the pipette to produce movement of serine. At higher pH's the surface charge of the glass will be different, possibly producing greater flows.

Text-figure 2. Iontophoretic release of fluorescein

Fluorescence changes 4 μm away from a micropipette containing fluorescein. The thin line is the average of three records of the light coming through a pinhole placed in the image plane of the microscope following current injection beginning at time 0.168 sec (arrow) and ending 0.596 sec later (arrow). The effective diameter of the pinhole in the object plane was about 1 micron. A micropipette containing 5 mM fluorescein was placed 4 microns away from the point at which the pinhole was centered. Darkfield optics were used so that most of the light coming through the pinhole was due to fluorescence of the dye. (The output of the photomultiplier was put through an RC filter with a 12 msec time constant and recorded on a Brush 220 strip chart recorder running at 125 mm/sec. The records were digitized on an HP7470 plotter interfaced to an Apple II/e and shifted by 12 msec to compensate for the RC filter). A -100 nA current was used. The time axis is divided into 0.2 sec intervals. The heavy line is a theoretical estimate of the total fluorescein in a vertical column centered four microns from the micropipette. I modeled the pipette tip as a point source and used the diffusion equation to predict the change in concentration with time in the column. The diffusion constant used for fluorescein was 2.5×10^{-6} cm^2/sec (Lanni et al., 1981).

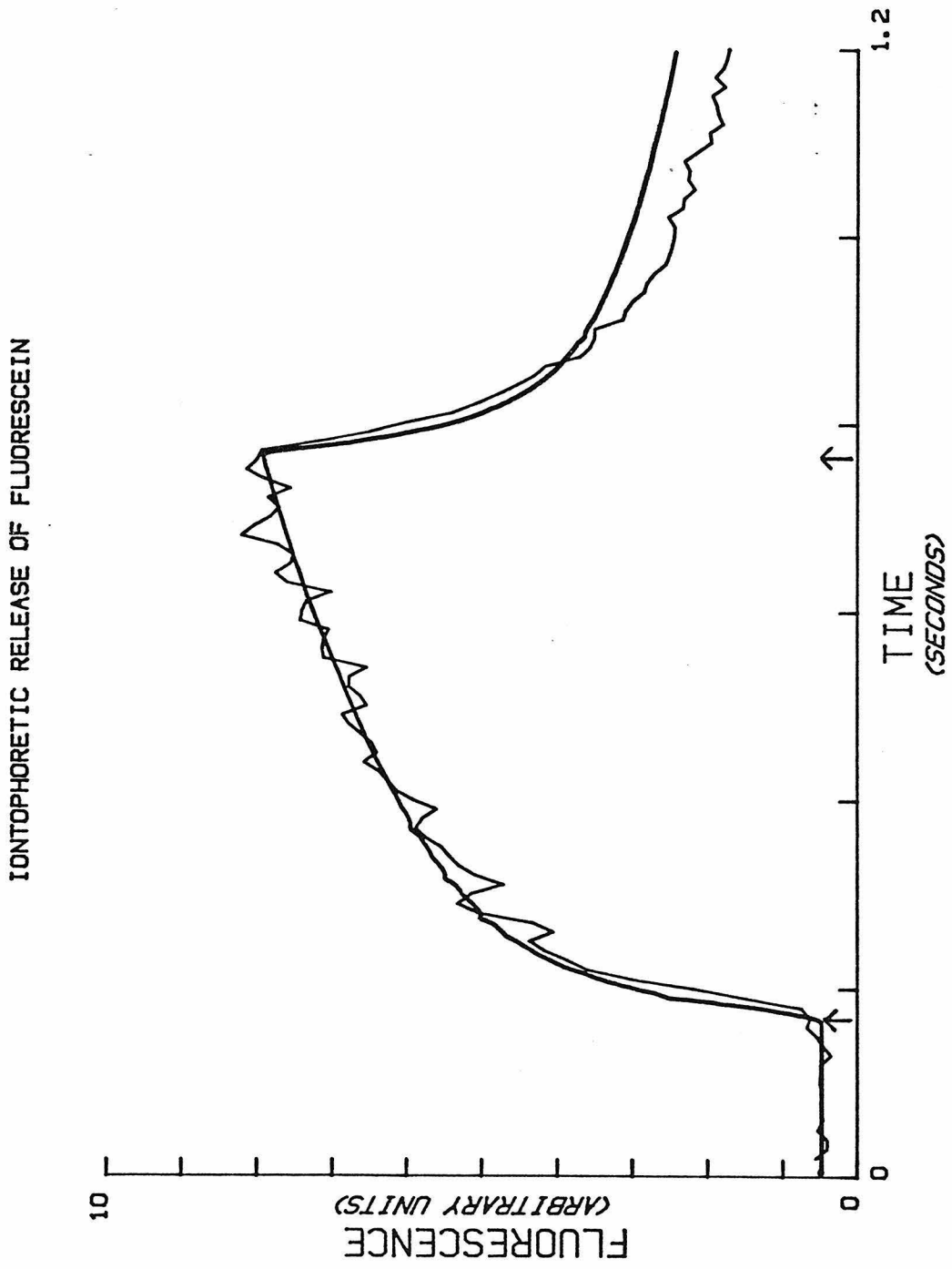
IONTOPHORETIC RELEASE OF FLUORESCEIN
FLUORESCENCE
(ARBITRARY UNITS)
10
0
0
1.2
TIME
(SECONDS)

Reprinted from Nature, Vol. 296, No. 5860, pp. 855-857, 29 April 1982

Signal processing times in bacterial chemotaxis

Jeffrey E. Segall, Michael D. Manson* & Howard C. Berg

Division of Biology 216-76, California Institute of Technology, Pasadena, California 91125, USA

The bacterium *Escherichia coli* responds to changes in the concentrations of various chemicals in its environment[1]. A cell swims along a smooth trajectory (runs), moves erratically for a brief time (tumbles) and then runs again, choosing a new direction at random[2]. If a run happens to carry the cell up a gradient of an attractant (such as aspartate, serine and certain sugars), the occupancy of the appropriate chemoreceptor increases with time[3,4] and a signal is sent to the flagellar motors that increases their counterclockwise bias[5]. On the average, this extends favourable runs and the cell moves up the gradient. The receptors for aspartate and serine[6-8] are proteins found in the cytoplasmic membrane, known as methyl-accepting chemotaxis proteins[9,10], and are the products of the *tar* and *tsr* genes[11]. A cell can adapt to sustained changes of receptor occupancy by carboxymethylating these proteins[12]; it is not known, however, how these proteins signal the flagellar motors or how the signal controls the direction of flagellar rotation. Products of several *che* genes involved in signalling and adaptation have been identified[13,14], but with the exception of a methyltransferase[15] (the *cheR* product) and a demethylase[16] (the *cheB* product), their functions are largely unknown. In an attempt to learn more about the events that trigger a chemotactic response, we have now exposed cells to rapid changes in the concentration of attractants and repellents and measured the time required for flagellar reversal. In wild-type cells and in cells containing a *cheR–cheB* deletion, the response latency is ~0.2 s. In *cheZ* mutants, it is much longer.

Cells were tethered to glass with antibodies directed against flagellar filaments, so that rotation of a cell body could be used to monitor the rotation of a flagellar motor[17]. Individual cells were observed with a microscope equipped with an opto-electronic device that provided a continuous readout of the cell's angular position[18,19]. A micropipette containing sodium α-methyl-DL-aspartate (α-MeAsp, a non-metabolizable analogue of the attractant aspartate) was positioned with its tip a few micrometres away from the cell, and the cell was stimulated iontophoretically by the passage of current. As the addition of α-MeAsp causes a cell to spin counterclockwise[5], the current was switched on when the cell changed its direction of rotation from counterclockwise (CCW) to clockwise (CW). We measured the interval of time from the beginning of this stimulus to the next reversal (the response latency), with a resolution of ~0.03 s. A typical response is shown in Fig. 1. Stimuli were given about every 30 s, and distributions of interval lengths were constructed (see Fig. 2). The experiments were repeated with different concentrations of α-MeAsp in the pipette and the results are summarized in Table 1. When the concentration in the pipette was ≤0.01 mM, the distributions of interval lengths did not differ significantly from those observed in the absence of a stimulus (Fig. 2*a*). When the concentration was ≥0.1 mM, responses occurred in ~0.2 s (Fig. 2*b*; Table 1). When the concentration was increased by a factor of 100, the mean latency decreased by less than a factor of 2 (Table 1).

To interpret these results, one needs to know the initial concentration of α-MeAsp near a cell and the time course of the change generated by the stimulus. A cell exposed to a step change in concentration of α-MeAsp spins CCW for a time (the transition time) proportional to the change in receptor occupancy. This time is ~180 s for a shift from 0 to 0.16 mM, the apparent dissociation constant of the receptor[20,21]. The initial concentration of α-MeAsp near a cell was estimated by suddenly bringing the pipette from far away to its final position. No response was detected with ≤1 mM α-MeAsp in the pipette. With 10 mM α-MeAsp in the pipette, a transition time of ~20 s was observed, corresponding to a jump in concentration at the cell from 0 to ~0.008 mM. The maximum concentration change that could be generated by the stimulus was estimated by measuring the transition time after the pipette was in position and the current was switched on and left on. Steady-state concentrations determined in this way are given in the last column of Table 1. Negative ions carried out of the pipette by the current ultimately reach the cell by diffusion. For diffusion from a point source switched on at time $t = 0$ (ref. 22), the concentration at the cell increases as $C = C_\infty \mathrm{ERFC}\,[r/(4Dt)^{1/2}]$, where C_∞ is the steady-state concentration, ERFC is the error function complement, r is the distance between the cell and the tip of the pipette ($\sim 4 \times 10^{-4}$ cm) and D is the diffusion constant of α-MeAsp (8.9×10^{-6} cm^2 s^{-1}). The concentration rises rapidly, reaching one-third, one-half and two-thirds of its steady-state value in 0.01, 0.02 and 0.05 s respectively. With 0.1 mM α-MeAsp in the pipette, the cells responded on the average in 0.32 s (Table 1), at which time the receptor occupancy was 2.3%. With 1 mM or 10 mM α-MeAsp in the pipette, this change in receptor occupancy should have occurred in 0.002 s or 0.004 s, respectively. The

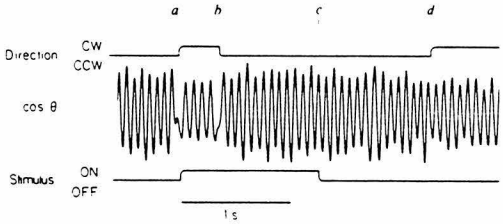

Fig. 1 A strip-chart record of iontophoretic stimulation of tethered *E. coli* strain AW405. The middle trace shows the cosine of the angle of orientation of the cell, cos θ; sin θ also was recorded (not shown). These two signals were used to generate the event marker shown in the upper trace, which indicates the direction of rotation of the cell. The event marker was updated every time sin θ = 0, that is, twice per cycle, and was used to trigger the stimulus. A second event marker, shown in the lower trace, was turned on when current was injected into the pipette[32]. The latency was determined by measuring the interval between the onset of the stimulus and the next reversal, as indicated by sin θ or cos θ. The measurement was corrected for the lag in the electronics used to smooth these signals (0.06 ± 0.02 s). A spontaneous reversal occurred at *a*. The cell was stimulated 0.03 s after this event was flagged by the upper event marker. Another reversal (the response) occurred at *b*, 0.34 s later (0.28 s when corrected for lag in the electronics). The stimulus ended at *c*, and the cell changed direction again at *d*. Cells were grown as described previously[20] on glycerol rather than glucose, washed twice with a tethering medium containing 90 mM NaCl, 10 mM KCl, 10 mM Tris *p*H 7.0 and 0.1 mM tetraethylenepentamine (tetren[33]), resuspended in this medium at one-tenth the original volume, sheared by passage between two syringes equipped with 26-gauge needles and washed once more. Then they were tethered, as described previously[20]. The micropipette (F. Haer 30-31-1 Pyrex 7740 tubing pulled on a D. Kopf 700C puller) was filled with tethering medium containing, in addition, 10 mM sodium α-MeAsp (Sigma) and 0.01 mM $ThCl_4$ (see below). Its resistance was about 50 MΩ. Connection to the current-injection circuit was made with AgCl-coated Ag wires. The tip of the pipette was positioned 2 μm above a point 4 μm away from the point of attachment of the cell. The stimulus current was −100 nA (negative ions ejected). No positive back current was used. The bath was perfused slowly with tethering medium to prevent any long-term buildup of attractant. The cell was observed with a ×40 water-immersion phase-contrast objective (Zeiss) electrically insulated from the microscope. The experiment was done at room temperature (22 ± 1 °C). $ThCl_4$ was added to the medium in the pipette to neutralize negative charges on the surface of the glass[34] which we think were responsible for stimulus artefacts (responses that occurred without any α-MeAsp in the pipette, particularly to the passage of positive currents). As thorium is precipitated by phosphate and chelated by EDTA, these components of the standard tethering medium[20] were replaced by Tris and tetren respectively.

* Present address: Fakultät für Biologie, Universität Konstanz, D-7750 Konstanz 1, FRG.

cells responded on the average 0.25 or 0.23 s later, when the changes in receptor occupancy were 10 or 69%, respectively. We conclude that the cells respond with a latency of ~0.2 s when the change in receptor occupancy is as small as 2% and that larger changes in receptor occupancy do not change the latency much. The latency is well within the upper limit for a chemotactic response time (~0.7 s) set by the rapid-mixing experiments of Macnab and Koshland[3].

The proper functioning of the pipettes (see ref. 23) was checked by replacing the α-MeAsp with 10 mM fluorescein and measuring the fluorescence near the tip of the pipette with a photomultiplier mounted on a dark-field microscope. Changes in fluorescence occurred during the passage of a pulse of negative current on a time scale consistent with that predicted by the diffusion theory to within ~0.01 s.

We looked for correlations between the mean latency of a cell and the pre-stimulus directional bias of its flagellar motor. In the 34 cells examined, the ranges of mean CW intervals, mean CCW intervals and fractions of time spent CW were 0.34–1.89 s, 0.66–3.12 s and 0.11–0.71, respectively. The mean latencies were not correlated with any of these parameters.

The following controls demonstrated that we were dealing with *bona fide* chemotactic responses. Wild-type cells (strain AW405) did not respond when the pipette contained only tethering medium (Table 1); they responded to benzoate (100 mM in the pipette) as a repellent, that is, by spinning CW in response to a pulse of negative current. A *tar* mutant (strain AW539) failed to respond to α-MeAsp but did respond to benzoate as a repellent. A *tsr* mutant (strain AW518) responded to both α-MeAsp and benzoate as attractants, as expected[24]. Whenever a response occurred, the latency was ~0.2 s.

What steps in the signal-processing pathway cause the latency? Recall that the latency changes very little when the concentration of α-MeAsp is increased by a factor of 100 (Table 1). With large stimuli, more attractant can diffuse to the cell, enter the periplasm and bind to the receptor in a given time, so none of these processes can be limiting. Reactions whose rates are proportional to the amount of bound receptor cannot limit the latency either, because the limit is reached with changes in receptor occupancy as small as 2%. The times required for a small molecule to diffuse from the receptor to the flagellar motor or for an electrogenic impulse to travel along the cytoplasmic membrane are a few milli- or microseconds respectively, so signal transmission *per se* is not likely to be limiting. Finally, the time required for the flagellar motor to change the direction of rotation of a tethered cell once a reversal is initiated is 0.01 s or less[25], so this factor is not important. Either the *tar* protein activates a sequence of one or more reactions that signal the motor with a delay averaging 0.2 s, or the motor, having received the signal, is not able to initiate a reversal in a shorter time.

The latency of a strain containing a *cheR–cheB* deletion is normal (strain RP1273)[26]. Therefore, excitation does not involve methylation[12], demethylation[26] or other processes catalysed by the *cheR* or *cheB* gene products. The latencies of strains containing *cheZ* mutations are very long, ~2 s (strains RP5006 = *cheZ* 292, an amber mutant, and RP5007 = *cheZ* 293, ref. 27). It is known from reversion analysis and interspecies complementation tests that the *cheZ* gene product interacts with both the demethylase (the *cheB* gene product) and with components of the flagellar motor involved in controlling the direction of rotation (the *cheC* = *flaA* and *cheV* = *flaB* gene products)[28]. Our results suggest that the *cheZ* product lies on the excitation pathway. Alternatively, its binding to the flagellar motor is required for rapid initiation of CCW rotation.

The lack of correlation between latency and the directional bias of the motor observed in wild-type cells also seems to be the case for cells containing *cheR–cheB* or *cheZ* mutations. The time required for a cell to adapt to a step change in the concentration of α-MeAsp, however, is strongly correlated with the directional bias of the motor (with the mean CCW interval)[29]. This implies that the signals involved in excitation and adaptation reach the motor by separate pathways or that the latency is due to a step that occurs after these pathways merge.

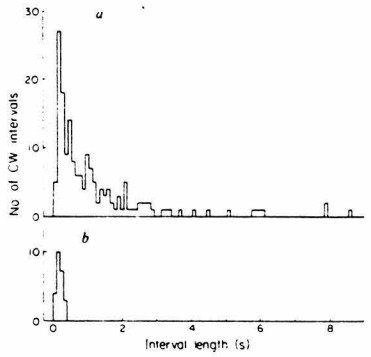

Fig. 2 Distributions of rotation intervals observed before (*a*) and after (*b*) iontophoretic stimulation of *E. coli* strain AW405 (as indicated in Fig. 1). Distribution *a* includes CW intervals observed immediately preceding each stimulus (3–5 intervals per stimulus, 171 in all, mean ± s.d. 1.32 ± 1.93 s). Distribution *b* includes CW intervals observed during each stimulus (1 interval per stimulus, 24 in all, mean ± s.d. 0.18 ± 0.10 s, corrected for the lag in the electronics). Distribution *a* is exponential, except for a paucity of intervals of length ≤0.1 s; distribution *b* is bell-shaped. The distribution of CCW intervals observed immediately preceding each stimulus (not shown, 179 intervals in all, mean ± s.d. 1.36 ± 1.40 s) was similar to the corresponding distribution of CW intervals (*a*).

Table 1 Response of the wild-type strain to different concentrations of α-MeAsp

Concentration in pipette (mM)	CW interval (s)		No. of cells	Total no. of stimuli	Steady-state concentration at the cell (mM)*
	Before stimulus	During stimulus			
10	0.89 ± 0.31	0.23 ± 0.07	8	100	0.52
1	0.89 ± 0.50	0.25 ± 0.05	9	173	0.022
0.1	0.90 ± 0.47	0.32 ± 0.09	10	164	0.0044
0.01	1.18 ± 0.34	0.92 ± 0.23	3	26	<0.0005
0	1.04 ± 0.10	1.00 ± 0.49	3	31	0

Measurements were made as described in Figs 1 and 2 legends, with −100 nA pulses of length 0.3–5 s. Each cell was tested at only one concentration of α-MeAsp in the pipette. Values for the CW interval are the mean and s.d. of the mean intervals for each cell, each cell weighted equally.

* Estimated from the transition time, t, for adaptation to a continuous −100 nA pulse, using the formula $C = 0.16\, t/(360 - t)$, where C is in mM, t in s (see Fig. 2 of ref. 20). The fractional change in receptor occupancy is $C/(K_d + C)$, where K_d is the apparent dissociation constant of the receptor.

Although *cheZ* mutants generally have abnormally high tumbling rates, *cheZ–cheC* double mutants exist that fail to move up gradients even though their tumbling rates are normal[30]. Mutants of this sort may represent a new kind of *che* phenotype, in which the defect lies in the rates at which cells respond to time-varying stimuli. If the latency of a cell is longer than its mean run length, it will choose a new direction at random before it has had a chance to make the appropriate response.

Why is the latency of wild-type cells as long as 0.2 s? There is no reason, *a priori*, that the response to a large stimulus could not occur within a few milliseconds. However, a cell must time-average its measurement of receptor occupancy if it is to sense small changes in concentration in the presence of statistical fluctuations. For most of the stimuli encountered in nature, averaging times of hundreds of milliseconds are required[31]. There may never have been any selective pressure for the development of more rapid signal-processing machinery.

We thank Steve Block, Jim Hudspeth, Victor Neher and Bob Smyth for valuable suggestions and Sandy Parkinson for bacterial strains. This work was supported by grant AI16478 from the US NIH.

Received 14 December 1981; accepted 15 March 1982.

1. Adler, J. *Science* **166**, 1588–1597 (1969).
2. Berg, H. C. & Brown, D. A. *Nature* **239**, 500–504 (1972).
3. Macnab, R. & Koshland, D. E. Jr *Proc. natn. Acad. Sci. U.S.A.* **69**, 2509–2512 (1972).
4. Brown, D. A. & Berg, H. C. *Proc. natn. Acad. Sci. U.S.A.* **71**, 1388–1392 (1974).
5. Larsen, S. H., Reader, R. W., Kort, E. N., Tso, W.-W. & Adler, J. *Nature* **249**, 74–77 (1974).
6. Clarke, S. & Koshland, D. E. Jr *J. biol. Chem.* **254**, 9695–9702 (1979).
7. Hedblom, M. L. & Adler, J. *J. Bact.* **144**, 1048–1060 (1980).
8. Wang, E. A. & Koshland, D. E. Jr *Proc. natn. Acad. Sci. U.S.A.* **77**, 7157–7161 (1980).
9. Kort, E. N., Goy, M. F., Larsen, S. H. & Adler, J. *Proc. natn. Acad. Sci. U.S.A* **72**, 3939–3943 (1975).
10. Springer, M. S., Goy, M. F. & Adler, J. *Proc. natn. Acad. Sci. U.S.A.* **74**, 3312–3316 (1977).
11. Silverman, M. & Simon, M. *Proc. natn. Acad. Sci. U.S.A.* **74**, 3317–3321 (1977).
12. Springer, M. S., Goy, M. F. & Adler, J. *Nature* **280**, 279–284 (1979).
13. Parkinson, J. S. *A. Rev. Genet.* **11**, 397–414 (1977).
14. Silverman, M. & Simon, M. I. *A. Rev. Microbiol.* **31**, 397–419 (1977).
15. Springer, W. R. & Koshland, D. E. Jr *Proc. natn. Acad. Sci. U.S.A.* **74**, 533–537 (1977).
16. Stock, J. B. & Koshland, D. E. Jr *Proc. natn. Acad. Sci. U.S.A.* **75**, 3659–3663 (1978).
17. Silverman, M. & Simon, M. *Nature* **249**, 73–74 (1974).
18. Kobayasi, S., Maeda, K. & Imae, Y. *Rev. scient. Instrum.* **48**, 407–410 (1977).
19. Berg, H. C., Manson, M. D. & Conley, M. P. *Symp. Soc. exp. Biol.* **35**, 1–31 (1981).
20. Berg, H. C. & Tedesco, P. M. *Proc. natn. Acad. Sci. U.S.A.* **72**, 3235–3239 (1975).
21. Spudich, J. L. & Koshland, D. E. Jr *Proc. natn. Acad. Sci. U.S.A.* **72**, 710–713 (1975).
22. Crank, J. *The Mathematics of Diffusion*, 2nd edn (Clarendon, Oxford, 1975).
23. Purves, R. D. *J. Neurosci. Meth.* **1**, 165–178 (1979).
24. Muskavitch, M. A., Kort, E. N., Springer, M. S., Goy, M. F. & Adler, J. *Science* **201**, 63–65 (1978).
25. Berg, H. C. *Cold Spring Harb. Conf. Cell Proliferation* **3**, A47–A56 (1976).
26. Sherris, D. & Parkinson, J. S. *Proc. natn. Acad. Sci. U.S.A.* **78**, 6051–6055 (1981).
27. Parkinson, J. S. *J. Bact.* **135**, 45–53 (1978).
28. Parkinson, J. S. *Symp. Soc. gen. Microbiol.* **31**, 265–290 (1981).
29. Spudich, J. L. & Koshland, D. E. Jr *Nature* **262**, 467–471 (1976).
30. Parkinson, J. S. & Parker, S. R. *Proc. natn. Acad. Sci. U.S.A.* **76**, 2390–2394 (1979).
31. Berg, H. C. & Purcell, E. M. *Biophys. J.* **20**, 193–219 (1977).
32. Dreyer, F. & Peper, K. *Pflügers Arch. ges. Physiol.* **348**, 263–272 (1974).
33. Reilley, C. N. & Vavoulis, A. *Analyt. Chem.* **31**, 243–248 (1959).
34. Schanne, O. F., Lavalée, M., Laprade, R. & Gagné, S. *Proc. IEEE* **56**, 1072–1082 (1968).

Additional Data

The space constraints of Nature did not allow a complete presentation of the latency data, and some further studies have provided more information. A revised table, showing all the latency data acquired, is given in Table 1. Response latencies to pipettes containing 0.091 M α-methylaspartate were also measured. It is interesting that latencies to pipettes containing higher concentrations of attractant do decrease, but only by around 15% for each order of magnitude increase in concentration from 0.001M to 0.091M. The latencies measured to pipettes containing the repellents nickel or benzoate are also shown in Table 1. I believe that the nickel measurements more accurately represent the latency in response to large repellent stimuli, because the benzoate stimulation appeared to be near threshold. Some cells did not respond to benzoate, and a large concentration (0.2M) was necessary to produce a response. On the other hand, I have seen that 0.001 M nickel chloride in the pipette (1/100th of the concentration used for measuring the latencies in Table 1) is sufficient for stimulating cells. I also believe that the difference in latencies between the addition of nickel (or the removal of α-methylaspartate) and the addition of α-methylaspartate is significant, possibly reflecting generation of a CW signal, as described in Chapter 5. A final note on nickel: I noted that with 0.1M $NiCl_2$ in the pipette, the leakage from the pipette will initially cause a repellent response when the pipette is placed near a tethered cell, but that with time the tethered cell stops reversing and rotates in the CCW direction! This change is not permanent because passing positive current through the pipette will cause a repellent response. Some of the latencies recorded in Table 1 were acquired from such cells.

Text-figure 3 shows an ensemble histogram of the latencies in response to -100 nA from pipettes containing 0.010 M or 0.091 M α-methylaspartate. The

Table 1
Response Latencies

Strain	Compound	Conc. in pip.(mM)	Prestimulus Interval Lengths (sec) CW	CCW	Latency[a]	No. of Cells	No. of Stim.
			Attractant Stimuli				
AW405	α-Me-Asp	91.0	.77±.46	1.86±.67	.19±.06	7	78
		10.0	.89±.31	1.85±.70	.23±.07	8	100
		1.0	.89±.50	1.46±.54	.25±.05	9	173
		0.1	.90±.47	1.56±.80	.32±.09	10	164
		0.01	1.18±.34	1.02±.29	.92±.23	3	26
	Buffer		1.04±.10	1.08±.17	1.00±.49	3	31
cheZ[c]	α-Me-Asp	10-90	nr	nr	3.3±.30	12	164
			Repellent Stimuli				
AW405	α-Me-Asp[c]	91.0	2.05±.07	1.94±.92	.13±.07	4	32
	Benzoate	200.0	.95±.34	1.54±.65	.20±.03	3	57
	Nickel[d]	100.0	nr	nr	.11±.06	9	81

[a]For attractant (repellent) stimuli the stimulus begins during a CW (CCW) interval and the latency is the length of the interval after the start of the stimulus.

[b]Many *cheZ* cells spun continuously CW, so that prestimulus interval lengths were not recorded (nr).

[c]Cells were adapted to a -10 nA current from the pipette, which was then shut off at the start of a CCW interval.

[d]Most cells were continuously CCW, so that no prestimulus intervals were recorded.

Text-figure 3. Comparison of stimulated and unstimulated CW interval distributions

Histograms of unstimulated (light line) and stimulated (heavy line) CW interval lengths for cells stimulated with pipettes containing 0.91 M or 0.010 M α-methylaspartate. Lists of stimulated and unstimulated CW intervals greater than 0.06 sec long were made for each cell and 0.06 sec was subtracted from each interval length. (The average lag between the start of a CW interval and the start of current flow is estimated to be 0.06 sec.) The mean interval length for each cell was calculated and then the mean of the means (the ensemble mean) was calculated. Histograms for each cell were constructed by binning intervals into fractions of each cell mean, as described in Block et al., 1983. Then the histograms were combined to produce an ensemble histogram. The bin size was chosen so that the bin size for the ensemble histogram was 0.03 sec for both stimulated and unstimulated intervals. The maximum bin size was 65 for the unstimulated and 23 for the stimulated intervals. Intervals longer than 3 sec are not shown. The unstimulated ensemble mean was 0.79 ± 0.1 sec (mean and s.e.m. for 15 cells, 1,290 intervals) and the stimulated ensemble mean was 0.21 ± 0.02 sec (mean and s.e.m. for 15 cells, 180 intervals).

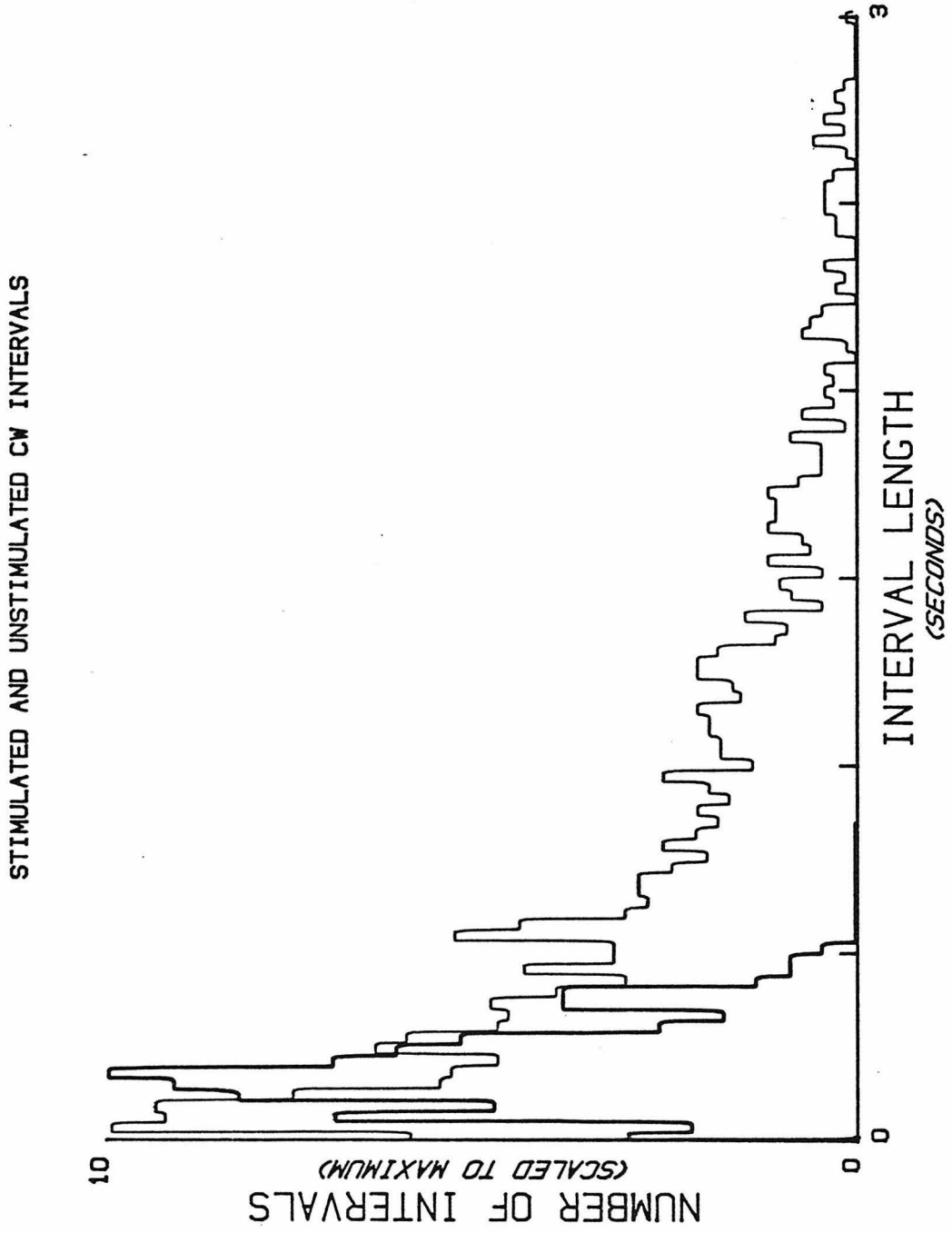
STIMULATED AND UNSTIMULATED CW INTERVALS
NUMBER OF INTERVALS
(SCALED TO MAXIMUM)
10
0
0
3
INTERVAL LENGTH
(SECONDS)

latency distribution for each cell is scaled to the ensemble mean and all the latencies compiled into a grand ensemble histogram. Although this technique is not foolproof, the net result gives some idea of the average latency distribution. It is clear that latencies vary quite a bit, and that the distribution is not sharply peaked about the mean value. On the other hand, the distribution is not exponential, as are the distributions of unstimulated CW and CCW intervals. If the CW interval length of the motor were instantaneously switched to a new mean value, one might expect the latency distribution to be more exponential. Note that there is a paucity of events less than 30 msec long in the unstimulated distribution in Text-figure 3, while in the stimulated distribution there is a paucity of events less than about 200 msec long. This suggests that either the motor cannot reverse immediately upon reception of a signal to reverse, or the generation of the signal to reverse is partially rate limiting and is reflected in the initial rise of the latency distribution.

The final information in Table 1 concerns the latencies of cells containing a mutation in the *cheZ* gene to α-methylaspartate. I have tested 5 different mutants, and all show greatly increased response latencies. Since strongly CCW or CW biased motors can respond rapidly(nickel results reported above and data in Chapter 2), the long latency of *cheZ* cells is probably not due to the extreme CW bias of the motor but reflects a defect in the signal processing pathway. More information on *cheZ* and other mutants will be given in Chapters 2 and 3. Interpretation of the long *cheZ* latency will be discussed in Chapter 5.

Chapter II

IMPULSE RESPONSES IN BACTERIAL CHEMOTAXIS

This paper was the culmination of a collaboration between Steve Block and myself. The iontophoresis technique was combined with the data digitization and analysis programs that Steve had developed for the experiments involving programmed flow (Block et al., 1983). The result was an extremely powerful method for studying chemotactic responses of bacterial cells.

Because of the amount of data that has been collected since the submission of this paper, I have put unpublished data on step and impulse responses in a separate chapter--Chapter III.

Cell, Vol. 31, 215–226, November 1982, Copyright © 1982 by MIT 38

Impulse Responses in Bacterial Chemotaxis

Steven M. Block, Jeffrey E. Segall and Howard C. Berg
Division of Biology
California Institute of Technology
Pasadena, California 91125

Summary

The chemotactic behavior of Escherichia coli has been studied by exposing cells tethered by a single flagellum to pulses of chemicals delivered iontophoretically. Normally, wild-type cells spin alternately clockwise and counterclockwise, changing their direction on the average approximately once per second. When cells were exposed to a very brief diffusive wave of attractant, the probability of spinning counterclockwise quickly peaked, then fell below the prestimulus value, returning to baseline within a few seconds; repellent responses were similar but inverted. The width of the response indicates that cells integrate sensory inputs over a period of seconds, while the biphasic character implies that they also take time derivatives of these inputs. The sensory system is maximally tuned to concentration changes that occur over a span of approximately 2 sec, an interval over which changes normally occur when cells swim in spatial gradients; it is optimized to extract information from signals subject to statistical fluctuation. Impulse responses of cells defective in methylation were similar to those of wild-type cells, but did not fall as far below the baseline, indicating a partial defect in adaptation. Impulse responses of *cheZ* mutants were aberrant, indicating a serious defect in excitation.

Introduction

Flagellated bacteria swim in a purposeful manner. They move up gradients of some chemicals (attractants) in search of food and down gradients of other chemicals (repellents) to avoid noxious substances. The cells are propelled by thin, helical flagella, each driven at its base by a reversible rotary motor. The behavioral repertoire of Escherichia coli and Salmonella typhimurium consists of runs and tumbles. During a run, the flagellar filaments rotate in concert in a helical bundle, pushing the cell steadily forward. Each run is terminated by a tumble, during which the filaments change their direction of rotation, the bundle flies apart and the cell moves erratically, with little net displacement. At the end of a tumble, the cell runs again, moving off in a new direction. The direction of rotation of a flagellar motor is determined in part by sensory inputs. In a chemically isotropic environment, changes in the direction of rotation occur at random, and a cell executes a three-dimensional random walk. Run and tumble intervals are each distributed exponentially, with time constants on the order of 1 and 0.1 sec, respectively. In a gradient of an attractant (or repellent) the rotational bias is altered in such a way that runs that happen to carry the cell in a favorable direction are extended. This imposes a drift on the random walk that carries the cell up (or down) the gradient. Temporal changes in concentration experienced by the cell as it moves in a gradient lead to variations in the occupancy of chemoreceptors that, in turn, alter the rotational bias of the flagellar motors. (For recent reviews on bacterial chemotaxis see Macnab, 1978; Springer et al., 1979; Koshland, 1981; Parkinson, 1981; Boyd and Simon, 1982.)

What is the pathway linking the receptors to the flagella? How does it function? While many of the components of this pathway have been identified genetically and some of their biochemical interactions are known, most of the events that occur during signal processing remain obscure. The work reported here defines the physiological properties of the sensory-transduction pathway in detail, both in the wild-type and in certain mutant cells. It is based on a method that provides means for systematic analysis of chemotactic behavior at the level of an individual flagellar motor.

The output of a single motor can be monitored by tethering the flagellar filament to a glass surface (Silverman and Simon, 1974). When the filament is held fixed, the motor spins the cell body alternately clockwise (CW) and counterclockwise (CCW). Rotation in the CCW direction (as viewed from a point in the external medium above the cell) corresponds to the run mode, while rotation in the CW direction corresponds to the tumble mode (Larsen et al., 1974). This preparation is particularly useful for the study of behavior: the cell remains at a fixed position for observation, while the chemical milieu may be changed at will. When properly energized, cells remain active for hours. A tethered cell can be stimulated by mixing in an attractant or a repellent (Larsen et al., 1974), by displacing one medium with another containing an attractant or a repellent (Berg and Tedesco, 1975) or by positioning an iontophoretic micropipette containing a charged attractant or repellent near the cell and passing an electric current (Segall et al., 1982).

The first two methods have been used in studies of adaptation, wherein cells exposed to the sudden addition of a large amount of attractant spin CCW for minutes, spin CW for a somewhat shorter time and then gradually relax to their initial mode of behavior (Berg and Tedesco, 1975). Cells exposed to the sudden removal of attractant spin CW for many seconds, spin CCW for a shorter time and then resume their initial mode of behavior. Similar responses are observed when repellents are removed or added, respectively. The biochemical basis for this adaptive behavior appears to be the reversible carboxymethylation of proteins found in the cytoplasmic membrane called methyl-accepting chemotaxis proteins (MCPs;

Kort et al., 1975). Individual polypeptides are multiply methylated in a sequential fashion, the final steady-state level of methylation reflecting the external concentration of attractant or repellent (Boyd and Simon, 1980; Chelsky and Dahlquist, 1980; DeFranco and Koshland, 1980; Engström and Hazelbauer, 1980). The time course for methylation in response to addition of attractant closely parallels that for physiological adaptation (Goy et al., 1977). When the concentration of an attractant increases (or that of a repellent decreases), methyl groups are added gradually; when the concentration of an attractant decreases (or that of a repellent increases), they are removed rapidly. These steps are catalyzed by two cytoplasmic enzymes: a methyltransferase, the product of the *cheR* gene (Springer and Koshland, 1977), and a methylesterase, the product of the *cheB* gene (Stock and Koshland, 1978); *che* refers to generally nonchemotactic. The MCPs also serve to integrate information from different sets of receptors and to relay that information to the flagellar motors. Accordingly, their genes have been designated *tar* (taxis to aspartate and some repellents), *tsr* (taxis to serine and other repellents) and *trg* (taxis to ribose and galactose) (Silverman and Simon, 1977; Springer et al., 1977; Kondoh et al., 1979).

Several other gene products are involved in signal processing. Direct interactions between some of these components have been demonstrated by reversion analysis and interspecies complementation. For example, the *cheY* gene product interacts with the methyltransferase and with components of the flagellar motor involved in controlling the direction of rotation (the *cheC*, or *flaA*, and the *cheV*, or *flaB*, gene products). The *cheZ* gene product interacts with the methylesterase and with these components of the motor as well. The functions of these and other *che* gene products, such as *cheA* and *cheW*, are not known (see Parkinson, 1981).

The iontophoretic method has been used in studies of excitation, in particular, to measure response latencies (Segall et al., 1982). When cells are exposed to rapid step changes in the concentration of attractants or repellents, responses to these stimuli occur in about 0.2 sec. This is true both for wild-type cells and for cells carrying a *cheR–cheB* double deletion. Response latencies of *cheZ* mutants are much longer. These latencies are relatively insensitive to the magnitude of the stimulus, provided that the change in chemoreceptor occupancy is above the threshold level. The response latency is a measure of the time required for signals to be processed by the complete transduction pathway. Given the small size of the organism, the latency of wild-type cells is surprisingly long, suggesting that the excitation pathway is complex.

There are two serious problems with the studies of tethered cells made thus far. The first is that measurements of adaptation times and response latencies provide only a limited amount of information about the transduction machinery. The second is that the stimuli used are so large that this machinery is driven into saturation; the information that is obtained may not be relevant to the behavior of the cell in the real world, where stimuli are much smaller. Cells swimming in spatial gradients do not experience large temporal stimuli, because discontinuities in concentration are smoothed out by diffusion.

We have used the iontophoretic technique to expose cells to impulsive stimuli rather than to large-step stimuli, and we have followed each cell's behavior for many seconds, not just to the next flagellar reversal. In these experiments, a small amount of chemical is ejected from the micropipette over a period of a few milliseconds. The chemical spreads outwards as a diffusive wave, passing over the tethered cell and rapidly dissipating in the external medium. If the time course of the wave is sufficiently short, it can be treated as an idealized impulse. The behavior of the cell toward this stimulus is an impulse response. Impulse responses have two very useful features. The first is that they reflect only the time constants of processes occurring in the system under study, not the time constants of the stimulus itself. A simple analogy is a bell struck by the percussive impulse of a clapper: a characteristic tone is generated that decays with time. The fundamental frequency of the tone and its rate of decay reflect intrinsic properties of the bell itself, not properties peculiar to the clapper. The second feature is that the impulse response contains all the information necessary to predict the behavior of the system when it is exposed to an arbitrary stimulus. One need only decompose the arbitrary stimulus into a series of impulses of appropriate magnitude and timing and compute the sum of the responses that would be observed, were these impulses applied separately. However, for this computation to work, the stimulus must be small enough that there are no nonlinear effects: the response to each impulse must remain independent of whether or not the cell is still responding to previous impulses (see Papoulis, 1977; Marmarelis and Marmarelis, 1978).

The early events in chemotaxis occur on a time scale of tenths of a second, and cannot be resolved by methods previously used to explore bacterial behavior. The iontophoretic technique has allowed us to generate stimuli that are short enough to be impulsive. By monitoring the rotation of tethered cells with an optoelectronic device accurate to a fraction of a cycle, we have achieved the temporal resolution necessary to characterize the response to these stimuli. The response has properties that imply that the sensory system in E. coli is optimally designed to allow cells swimming in spatial gradients to extract information about changes in concentration from signals subject to statistical fluctuations.

Results

Computation of the Impulse Response

Cells were tethered to a glass window and viewed through the water-immersion lens of a phase-contrast microscope. The microscope was equipped with linearly graded optical filters that extract the x and y coordinates of the centroid of the image of a spinning cell; sensors viewing these filters generate signals that contain information about the cell's angular velocity and direction of rotation. A micropipette was positioned within about 4 μm of the cell, and the cell was stimulated by short iontophoretic pulses, repeated at intervals of about 1 min. Time records of the x and y signals were made on a strip-chart recorder, together with event markers indicating the direction of rotation of the cell and the timing of the stimulus current. The size of the stimulus to which the cell was exposed could be varied by adjusting either the magnitude of the current passed through the pipette or its duration. These parameters were adjusted by hand during the experiment to ensure that responses occurred, but under conditions in which the stimuli were impulsive (see below). Records of 20 sec duration bracketing each iontophoretic pulse were digitized and stored in a computer for subsequent analysis.

The rotational behavior of a tethered bacterium is a binary, stochastic process: it is the probability of spinning CW or CCW that is modulated by the sensory apparatus. Therefore, we took as our measure of the response the probability that a cell spins CCW. We obtained an estimate of this probability by taking the average of a series of records, each containing data obtained with a single stimulus. The procedure is outlined in Figure 1. A typical result obtained with 25 records from a single cell is shown in Figure 2. The fluctuation about the baseline before and after the stimulus results from the averaging of binary signals. Its amplitude obeys the binomial distribution; the mean amplitude decreases as the inverse square root of the number of records. To verify this fact and to test our data-reduction procedures, we used a Monte Carlo method to construct records of an "artificial cell" whose CW and CCW rotation intervals were given by exponential distributions. These records were processed in the same way as the real data. The probabilities computed from artificial and real data had similar statistical properties, which agreed with theory.

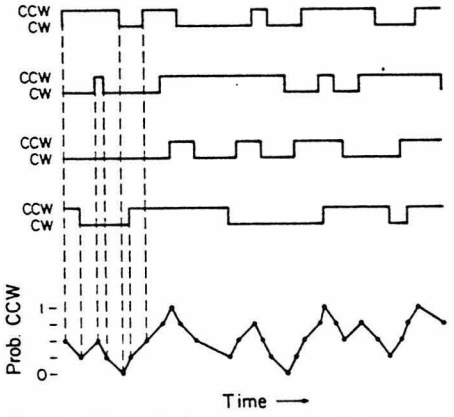

Figure 1. Scheme for Averaging Data Records

Individual binary records of rotational behavior (four are shown) were placed in register at the time of stimulation. A value of +1 was assigned to each record when the direction of rotation was CCW and 0 when it was CW. The average value of these numbers was computed each time a transition (an event) occurred in any one of the individual records. The result (bottom) is a function that can assume any one of $n + 1$ values between 0 and 1 inclusive, where n is the number of records. The value of this function provides an estimate of the probability of CCW rotation, and the density of points along the time axis gives an estimate of the average reversal rate. The algorithm actually used to perform this computation is described in the experimental Procedures.

Impulse Responses of Wild-Type Cells

The impulse response to attractant stimuli is shown in Figure 3A. The same response was observed with aspartate and α-methylaspartate; only the threshold concentrations differed. Prior to stimulation, the directional bias of the cells averaged 64% CCW. After the pulse at time zero (5 sec on the scale shown in the figure), the probability of spinning CCW rose sharply to a maximum value at 0.4 sec, then fell in a smooth manner, crossing the baseline at 1 sec and reaching a minimum value at 1.5 sec, and finally returning to its initial value at approximately 4 sec. The excursion below baseline (the response undershoot) is important, because it implies that the chemosensory system has adaptive properties in the 1 sec time domain (see below). The areas of the two lobes of the response were equal.

The impulse response to repellent stimuli is shown

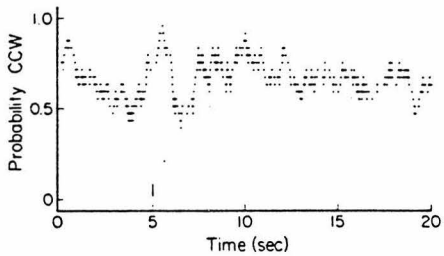

Figure 2. Impulse Response of a Single Cell

A single cell was stimulated 25 times by a pulse given at 5 sec (vertical line). The graph shows the probability of CCW rotation as a function of time, estimated as described in the legend to Figure 1. The pipette contained 100 mM α-methyl-D,L-aspartate, a negatively charged attractant. Pulses were generated by switching the current from 0 to −100 nA for a period of 100 msec. The discrete layer lines that appear in the data are determined by the 26 quantized values obtained when 25 binary records are averaged. Data were not smoothed.

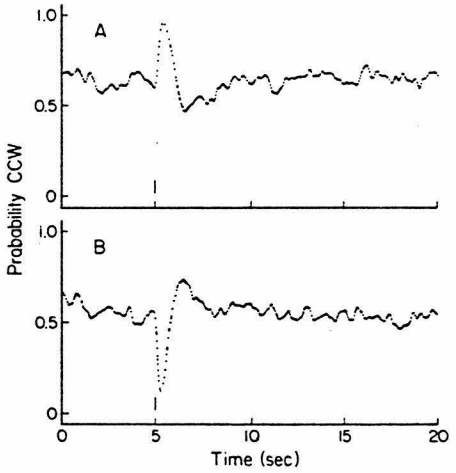

Figure 3. Impulse Responses of Wild-Type Cells

The probability of spinning CCW is shown as a function of time, with stimuli given at 5 sec (vertical line). The data were smoothed, as described in the Experimental Procedures.

(A) Attractant response. The pipettes contained either 1 mM L-aspartate or 7 mM α-methyl-D,L-aspartate. Pulses were generated with currents ranging from −1 to −100 nA switched on for periods of 20–100 msec. The graph was constructed from 172 records containing 3193 events obtained with nine different cells; 399 points are displayed; 115 of the records were from stimulation by L-aspartate, 57 from stimulation by α-methyl-D,L-aspartate.

(B) Repellent response. The experiment was carried out as described in (A), but with pipettes containing 200 mM benzoate or 1 mM L-aspartate. Benzoate was injected at −100 nA for 20–50 msec. L-aspartate was added continuously at −2 to −3 nA, and the addition was interrupted by switching to +3 to +10 nA for 20–40 msec. Addition of repellent or removal of attractant gave the same response. The graph was constructed from 169 records containing 2785 events obtained with seven different cells; 397 points are displayed; 86 of the records were from addition of repellent, 83 from removal of attractant.

in Figure 3B. The responses to the addition of benzoate and to the removal of aspartate were similar. The repellent response resembled an inverted attractant response, with a similar time course and biphasic character. The cells responded to the addition of benzoate and nickel chloride on a slightly shorter time scale than they did to the removal of aspartate (data not shown).

The pulses used represented true impulses, as indicated by the following experimental criteria: pulses were adjusted to be close to, but generally above, threshold for a response; in a trial experiment, stimuli of lower amplitude resulted in a smaller probability of a change in directional bias, but gave an impulse response with the same time course; and cells with different thresholds, exposed to pulses of different amplitude and duration, also gave an impulse response with the same time course. Finally, a theoretical calculation of the diffusive wave (Segall et al., 1982) showed that for the 20–40 msec pulses used with wild-type cells, the change in chemoreceptor occupancy had fallen to less than 3% of its maximum value by 200 msec after the onset of the pulse, long before the end of the response was observed.

As stated above, the impulse response has predictive value when the system operates in a linear domain—that is, when responses to different stimuli add algebraically to give the overall response. In this domain, the response to an arbitrary stimulus is given by the convolution of that stimulus with the impulse response (Papoulis, 1977), a process that decomposes the stimulus into an infinite set of impulses of appropriate magnitude and timing and adds their responses together. For the simple case of the response to a step, the convolution reduces to the integral of the impulse response with time. The extent to which such a convolution predicts the system response is a measure of the linearity. In Figure 4, the measured response of wild-type cells to a small step change in concentration of an attractant is compared with the response predicted by integration of the impulse response; the agreement is satisfactory.

Does the response to an impulse depend on the initial state of the flagellar motor? That is, does it matter in which direction a cell happens to be spinning when it is stimulated? To answer this question, we separated the data into two parts: one containing those records for which the cell was spinning CW at a given instant, and another containing those for which the cell was spinning CCW at that instant. If this is done for an arbitrary time, t_0, the records will be autocorrelated around that time in both directions. For example, if a cell happened to be spinning CCW at time t_0, it is likely that it was also spinning CCW for times close to t_0. For CCW intervals that are distributed as $\exp(-k_r t)$ and CW intervals distributed as $\exp(-k_t t)$, where k_r and k_t are the run and tumble rate constants, respectively, the autocorrelation function decays as $\exp[-(k_r + k_t)|t - t_0|]$. This effect is seen in Figure 5A. Both curves decay symmetrically to the baseline with similar time constants. The small difference in baseline for the two curves is a reflection of the fact that records chosen for cells that happen to be spinning in a given direction at an arbitrary time are more likely to belong to cells that are generally biased in that direction. If, however, the time t_0 is chosen to coincide with the time of the pulse, an intriguing result is obtained, as seen in Figure 5B. The two curves are back-correlated, as in Figure 5A, but now they follow an identical time course once cells that were spinning CW have had time to change their direction of rotation—that is, after an interval equal to the response latency. (The somewhat larger disparity in baselines for Figure 5B relative to Figure 5A also reflects the way in which the records were chosen, and is not statistically significant.) This implies that the response does not depend on the initial state of the

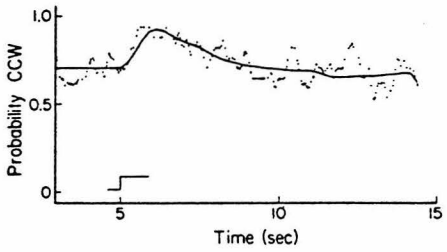

Figure 4. Small-Step Response of Wild-Type Cells

The probability of spinning CCW is shown as a function of time, with stimuli given at 5 sec (step mark). The data were smoothed, as described in the Experimental Procedures. The response to a small step increase in concentration of attractant (dotted line) is compared with the response predicted from integration of the impulse response (solid line). The pipette contained 0.1 mM L-aspartate. Steps were generated by switching the current from 0 to a value of −3 nA and maintaining that value for at least 10 sec. The experimental probability function was constructed from 34 records containing 417 events obtained with a single cell; 209 points are displayed. The impulse response was integrated from the beginning of the step onward in accordance with the convolution theorem (see text). The choices of baseline and amplitude for the predicted curve are arbitrary; they were scaled to match the baseline and amplitude of the experimental data. The impulse response used was similar to that shown in Figure 3A. It was derived from 237 records containing 4585 events obtained with 11 different cells.

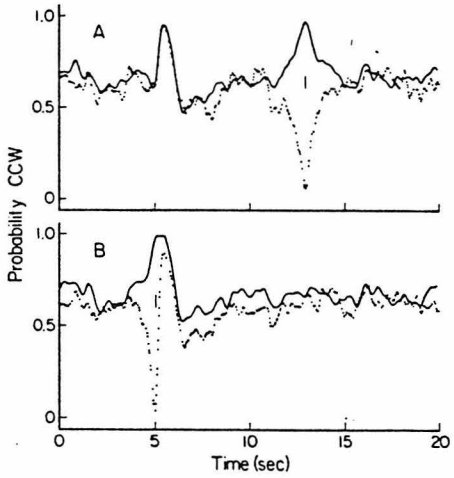

Figure 5. Stimulation during Either a CCW or a CW Interval

(A) The individual records used to compute Figure 3A were separated into two groups: those for cells that were rotating CCW (solid line) 8 sec after the pulse (at 13 sec; vertical line), and those that were rotating CW (dotted line). These groups were averaged separately to yield the graphs shown. The probability of being in the CCW or the CW mode is unity at 13 sec and decays exponentially in either direction to the baseline, as determined by the autocorrelation function (see text).

(B) The same records were separated into two different groups: those for cells that were rotating CCW (solid line) at the time of the stimulus pulse (5 sec; vertical line), and those that were rotating CW (dotted line). Both probabilities decay backwards in time, as in (A), but now the curves are nearly identical for times greater than 5.2 sec—that is, after an interval equal to the response latency.

motor, and that the mechanism responsible for the impulse response overrides the mechanism that generates spontaneous reversals.

Reversal Rate during Impulse Responses

As noted in the legend to Figure 1, the density of points along the time axis of the probability function provides an estimate of the average reversal rate. Such an estimate is shown in Figure 6, together with the repellent response from which it was derived. Once again, fluctuations around the baseline reflect the underlying statistical process; here, the amplitude of the fluctuations obeys a distribution related to the Poisson distribution, with a characteristically large variance. During the initial phase of the response, the reversal rate rose sharply, to a value of greater than 3 reversals/sec/cell, a consequence of the fact that cells that happened to be spinning CCW at the time of the pulse changed their direction of rotation within a narrow time interval. Shortly after the response minimum, the reversal rate fell to its lowest value, of approximately 0.3 reversals/sec/cell: the reversal rate is actively supressed during the response. A subsidiary peak in the reversal rate occurred during the overshoot, whereafter the rate returned to its initial value. Reversal rates for attractant responses were nearly identical, but showed a somewhat less pronounced initial peak (1.5 reversals/sec/cell; data not shown). We will return to these data later when we discuss the two-state system (see Discussion).

Impulse Responses of Mutant Cells

The impulse response was determined for several generally nonchemotactic mutants, provided by J. S. Parkinson. Where possible, mutants with nonpolar deletions were used to ensure the null phenotype. The attractant response of cells carrying *cheR–cheB* double deletions is shown in Figure 7A. These mutants lack genes for both the methyltransferase and the methylesterase; they are defective in adaptation. Nevertheless, they have about the same directional bias as the wild-type and respond to large-step stimuli. Their impulse response was similar to that of the wild-type (Figure 3A); however, the initial peak was longer, and the undershoot was substantially smaller, in the mutant cells. The degree of undershoot varied from cell to cell; when examined individually, the cells whose average response is shown in Figure 7A showed different degrees of undershoot, ranging from none at all to a size comparable with that of the wild-type.

Mutants in *cheZ* have a large CW bias, high response thresholds and abnormally long response latencies (Parkinson, 1978; Parkinson and Parker, 1979; Segall et al., 1982). Very short impulses of L-aspartate failed to produce a response; however,

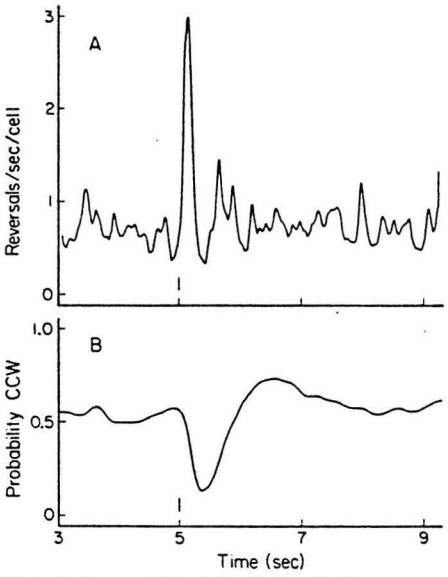

Figure 6. Reversal Rate during the Impulse Response

(A) The instantaneous reversal rate for cells undergoing an impulse response, plotted as a function of time. Note the expanded time scale. The reversal rate was calculated from the density of points along the time axis in the data summarized in Figure 3B.

(B) The curve of Figure 3B, shown on the same expanded time scale for comparison. Data were smoothed.

somewhat longer pulses proved effective, with the result shown in Figure 7B. The response latency was highly variable, ranging from 0.2 sec up to 5 sec or more. Typically, a cell changed its direction of rotation from CW to CCW after a relatively long (but variable) latency, spun CCW for a period of less than a second and then exhibited a few brief CCW intervals over the next 5 sec, before returning to its initial (CW) behavior. In some cases, responses continued over a much longer time period. Note (Figure 7B) that the response failed to return to baseline even 15 sec after the pulse. The low peak probability for CCW rotation apparent in the figure arose for the following reasons: some cells responded to every pulse, but with a variable time course, so that peak responses failed to add together in phase; and some cells responded with a probability less than unity—they continued to respond over the course of the experiment, but not to every pulse.

Mutants with *cheB* deletions are missing the methylesterase; they have a large CW bias and very high response thresholds (Parkinson, 1978; Sherris and Parkinson, 1981). Mutants with *cheR* deletions are missing the methyltransferase; they have a large CCW bias and high response thresholds (Goy et al., 1978; Parkinson and Revello, 1978). The responses of these mutants to attractants and repellents are shown in Figures 7C and 7D, respectively. These responses resembled those observed for the wild-type; in each case, the initial peak had a similar time course. The

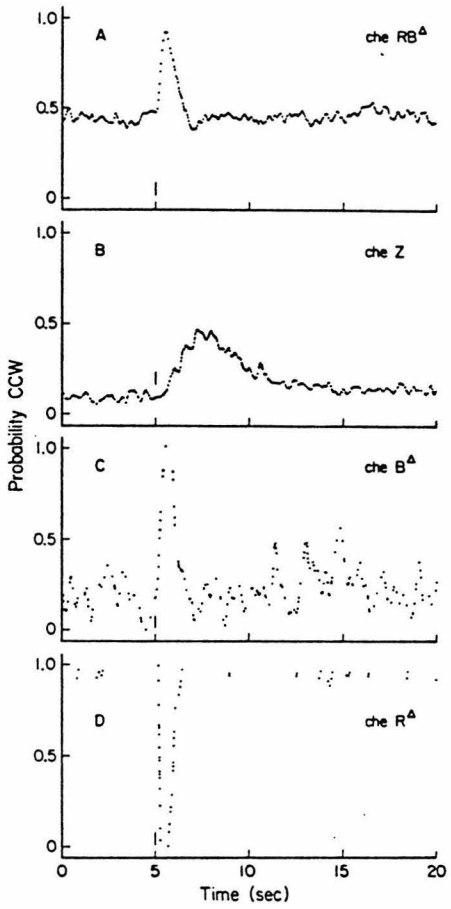

Figure 7. Impulse Responses of the *che* Mutants

The probability of spinning CCW is shown as a function of time, with stimuli given at 5 sec (vertical lines). The data have been smoothed, as described in the Experimental Procedures.

(A) Attractant response of cells carrying *cheR–cheB* double deletions. Pipettes contained 10 mM L-aspartate. Pulses were generated with currents ranging from −20 to −100 nA switched on for periods of 9–225 msec. The graph was constructed from 167 records containing 4260 events obtained with 11 different cells; 335 points are displayed.

(B) Attractant response of the *cheZ* point and amber mutants. Pipettes contained 1 mM L-aspartate. Pulses were generated with currents of −10 to −100 nA switched on just long enough to give a response (0.2–1.8 sec). The graph was constructed from 132 records containing 2034 events obtained with five different cells; 339 points are displayed.

(C) Attractant response of a cell carrying a *cheB* deletion. Pipettes contained 100 mM L-aspartate. Pulses were generated with a current of −100 nA switched on for 200–300 msec. The graph was constructed from 14 records containing 248 events obtained with a single cell. The mutant was CW-biased; noise in the baseline arose from occasional spontaneous reversals.

(D) Repellent response of a cell carrying a *cheR* deletion. Pipettes contained 100 mM nickel chloride. Pulses were generated with currents of +2 nA switched on for 20 msec. The graph was constructed from 19 records containing 63 events obtained with a single cell. The mutant was CCW-biased; points on the baseline represent rare spontaneous reversals.

greater amplitude of this peak and the lack of undershoot (or overshoot) in the mutant cells may simply reflect the altered range available for changes in directional bias. A run-biased *cheR* point mutant (*cheR202*) gave a similar response to the *cheR* deletion mutant (data not shown). Mutants in *cheB* proved extremely hard to excite: only a small fraction of the cells responded reproducibly to stimulation by L-aspartate, even with relatively high concentrations in the pipette.

The records for the *cheR–cheB* and *cheZ* mutants were separated into two groups: those corresponding to cells that were stimulated while spinning CW, and those that were stimulated while spinning CCW. Although the probability functions differed from mutant to mutant (data not shown), it was clear in these mutants, as well as in the wild-type (Figure 5), that the mechanism determining the response to an impulse overrides the mechanism that generates spontaneous reversals.

Discussion

A conceptual distinction has been drawn in bacterial chemotaxis between excitation and adaptation (Goy et al., 1978; Springer et al., 1979). While the addition of an attractant or repellent causes an almost immediate response (excitation), that response gradually disappears with time, even if the attractant or repellent is still present (adaptation). In most cases, adaptation is complete: the behavior of the cell does not depend on the ambient concentration after a sufficiently long period of time (Macnab and Koshland, 1972; Tsang et al., 1973). There are some exceptions: for example, when cells in motility medium are exposed to serine (Berg and Brown, 1972), or when enough weak acid is added to cells in an acidic medium to perturb seriously the cytoplasmic pH (Kihara and Macnab, 1981). For the relatively large stimuli used in previous work, the time required for a cell to respond (the response latency) is about 0.2 sec (Segall et al., 1982). However, the time required for a cell to adapt (the adaptation time) ranges from several seconds to several minutes, depending on the magnitude of the change in receptor occupancy (Spudich and Koshland, 1975; Berg and Tedesco, 1975). These characteristic times are so different as to suggest that the pathways for excitation and adaptation are distinct. This notion is supported by the observation that cells carrying mutations in the *cheR* gene have normal response latencies (Segall et al., 1982) but fail to adapt (Goy et al., 1978; Parkinson and Revello, 1978). Alternatively, the disparity in characteristic times for excitation and adaptation might be an artifact of the step-stimulus paradigm, in which a large change in concentration rapidly drives the system into saturation. Measurements of the impulse response have allowed us to characterize the behavior of cells in the small-signal domain. Our results suggest that the bacterial sensory system is matched to the task that it is required to perform. Both excitation- and adaptation-related phenomena occur on a time scale of seconds. The initial events in signal processing are similar in wild-type cells and in cells unable to methylate or demethylate, or both; however, they are markedly different in cells carrying *cheZ* mutations.

Characteristics of the Wild-Type Response

The impulse response shown in Figure 3A has a substantial width; it persists for about 4 sec. This means that a cell integrates stimuli that have occurred over the past few seconds in determining its present bias: variations in concentration that occur on a time scale much shorter than this average out. This is characteristic of a low-pass filter, a device that passes low frequencies in preference to high frequencies. The impulse response also is biphasic; one lobe is above the baseline and the other is below it. This means that the cell is sensitive to changes in concentration that have occurred over the past few seconds: variations in concentration that occur on a time scale much longer than this also average out. This is characteristic of a differentiator, or high-pass filter, a device that is sensitive to changes in input—that is, that passes high frequencies in preference to low frequencies. If the areas of the two lobes are equal, the output returns to its initial value after a stepwise change in input, as illustrated in Figure 4; the device is fully adaptive. In summary, the impulse response has bandpass properties; the cell is maximally sensitive to frequencies at which the low-pass and high-pass contributions overlap.

We could carry this analysis further by exposing the cell to sinusoidal stimuli and measuring the amplitude of the resultant swings in rotational bias as a function of frequency. But this is not necessary, because an equivalent result is obtained by decomposing the impulse response into its spectral components by means of the Fourier transform (Papoulis, 1977). A Bode (log–log) plot of this spectrum, shown in Figure 8, shows the bandpass properties. The system has a maximum pass frequency at 0.25 Hz, corresponding to a time span of 4 sec. A decomposition of the system into constituent filters is done by matching the slopes on either side of the pass frequency. Positive slopes indicate high-pass characteristics, and negative slopes indicate low-pass characteristics. The steepness of the slope determines the sharpness of the frequency cutoff: an asymptotic slope of $20n$ dB/decade indicates an nth order filter. The wild-type sensory system behaves roughly as a first order high-pass filter in cascade with a third order low-pass filter.

The 4 sec bandpass time implies that the system is maximally sensitive to changes occurring with this periodicity. This bandpass covers the range of frequencies that a cell generates by its motion when

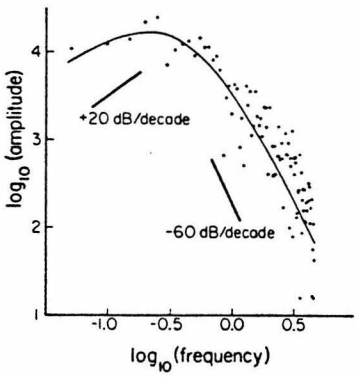

Figure 8. Fourier Transform of the Wild-Type Response

A Bode plot—$\log_{10}$(amplitude) versus $\log_{10}$(frequency)—of the absolute magnitude of the complex Fourier transform of the impulse response shown in Figure 3A. The transform peaks at approximately 0.25 Hz, corresponding to a bandpass centered at 4.0 sec. Slopes of +20 dB and −60 dB are shown for reference. The response system, if linear, is approximated by a first order high-pass filter in cascade with a third order low-pass filter. The response array of 1024 points was digitally filtered prior to transformation to reduce high-frequency contamination. Low-frequency trends were eliminated by subtracting out the baseline determined by a least-squares fit to the data obtained before and well after the response. The solid line is the transform of a nonlinear least-squares fit to the impulse response of a sum of four exponentials.

swimming in a spatial gradient. As we noted earlier, a swimming cell executes a random walk with steps (runs) averaging approximately 1 sec. The concentration rises and falls as the cell moves up and down the gradient; frequencies on the order of 0.25 Hz are prominent.

As noted above, the distributed nature of the impulse response indicates that cells make use of information over a time span extending at least 4 sec into the past. The Fourier analysis shows that they weight spectral components of stimuli with periods around 4 sec most heavily. Thus, while it can be said that a cell has "memory," it does not have a memory characterized by a single decay time. A time span of 2 sec is roughly equal to the persistence time of a cell swimming in a spatial gradient—that is, the mean time during which there is a component of cell motion up the gradient (Macnab and Koshland, 1973; Lovely and Dahlquist, 1975). This is another way of saying that the sensory system is optimized to sense those changes in concentration encountered when the cell swims in a gradient.

The question of memory time in bacterial chemotaxis has been addressed before. The long relaxation times for adaptation to steps in concentration imply a kind of "memory" in the limited sense that prior to adaptation, the cell continues to respond to a change made in the past (Macnab and Koshland, 1972). Adaptation times, however, are a function of the stimulus size (Spudich and Koshland, 1975; Berg and Tedesco, 1975) and do not point to a particular characteristic memory time, t_m. Memory is not "useful" if it extends so far into the past that the information retained is not relevant to the current trajectory of the cell (Macnab and Koshland, 1973). Computer simulations of cells swimming in a spatial gradient show that a long memory is clearly detrimental (Brown and Berg, 1974). For cells with a memory that decayed exponentially with a time constant t_m, the rate of drift up the gradient fell off exponentially with a time constant of the order of $2t_r$, where t_r is the mean run interval. For values of $t_m > 5t_r$, chemotaxis was essentially abolished.

Why should the mean run interval be about 1 sec? On the one hand, runs must be long enough to allow the cell to sense changes in concentration in the presence of random fluctuations (noise); the precision with which such changes can be sensed improves with the square root of the measurement time (Berg and Purcell, 1977). On the other hand, the runs must not be so long that the curvature induced by rotational Brownian movement causes the cell to deviate significantly from its path before the measurement is complete. For a cell the size of E. coli, this is a serious problem for times on the order of 10 sec (Brown and Berg, 1974). The mean run interval must be shorter than this, so that when favorable runs are extended, they still fall within this limit. Hence the optimum run interval is determined by these physical constraints.

Modulation of a Two-State System

Very little is known about the machinery that generates the impulse response, but it is known that the baseline behavior of the cell involves random switching between two rotational modes. The underlying events that terminate CCW and CW intervals have constant probabilities in time. The simplest model that has this property is a two-state system, in which the states dictate either CCW rotation (runs) or CW rotation (tumbles). These states might represent alternate configurations of a protein that determine the direction of rotation, the binding and unbinding of a ligand on such a protein, or the like. Transitions between the two states are governed by first order rate constants k_r and k_t, which are the probabilities per unit time of terminating a run or a tumble, respectively.

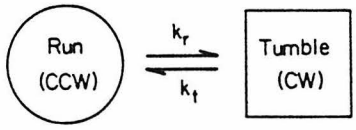

In this system CCW intervals are distributed as $\exp(-k_r t)$ and CW intervals are distributed as $\exp(-k_t t)$. If k_r is greater than k_t, the motor spends most of its time in the tumble mode; if k_t is greater than k_r, the run mode predominates. In general, if both k_r and k_t are large, the reversal rate is high; if both k_r

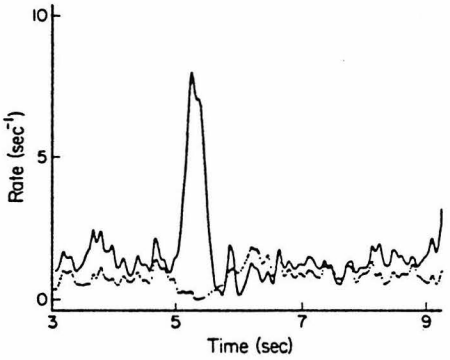

Figure 9. Rate Constants for the Two-State Model

The rate constants k_r (solid line) and k_t (dotted line) computed for the impulse response of Figure 3A and shown as a function of time. Note that k_r and k_t are anticorrelated during the positive phase of the impulse response, which lasts about 1 sec, as well as during the subsequent undershoot. The relatively high noise level reflects the large statistical variance in the reversal rate. This graph was prepared from the impulse response, its time derivative and the instantaneous reversal rate, as described in the text; see equations (3) and (4).

and k_t are small, the reversal rate is low. We suppose that the sensory system modulates k_r and k_t. The changes that occur during the impulse response can be derived from measurements of the probability of spinning CCW and the reversal rate, as outlined in Experimental Procedures. The results are shown in Figure 9. During the initial phase of the response, k_t rises and k_r drops. During the undershoot, k_r exceeds k_t, and tumbles are transiently favored. The response to a repellent gives essentially the same result, but with the roles of k_r and k_t interchanged (data not shown). If the cell actually works in this way, k_r and k_t must be controlled jointly by the sensory system, and they must be modulated in an antagonistic manner. If this modulation is to override the steady state reversal behavior, as implied by the results in Figure 5, the mechanism that controls the rate constants must act quite rapidly. Cells with different unstimulated biases (and different mean CCW and CW rotation intervals) give impulse responses with virtually identical time courses (data not shown). This suggests that the mechanism that controls the rate constants is quite similar from cell to cell, but distinct from the mechanism that sets the prestimulus values of these constants. The latter mechanism has a large biological variability (Berg and Tedesco, 1975; Spudich and Koshland, 1976).

Characteristics of Mutant Responses

It should be possible through the analysis of generally nonchemotactic mutants to work out the functions and interrelationships of different components of the signal-transduction pathway (see Parkinson, 1981; Boyd and Simon, 1982). One needs a combined assault with the use of genetics, biochemistry and physiology. Although a great deal has been learned with slower methods, our results show that important physiological events occur on a relatively short time scale: a time scale not accessible to those methods. Defects in some mutants are so severe that the cells fail to respond to any stimuli; these strains are not amenable to the analysis undertaken here. Fortunately, other *che* mutants do respond, to varying degrees, and we have begun by examining some of these.

The impulse response of cells with a *cheR–cheB* double deletion shown in Figure 7A is similar to that of wild-type cells (Figure 3A). It begins at roughly the same baseline, has essentially the same rise time and follows a similar time course for the first second or so, but it does not have as large an undershoot. As noted in the Results, this feature varied from cell to cell. The lack of a pronounced undershoot, on the average, for the mutant implies that it lacks some of the high-pass (adaptive) properties of the wild-type strain. This was confirmed through measurements of responses to small-step stimuli that unlike those for wild-type cells shown in Figure 4, failed to return to the baseline (in 10 sec, the longest period studied). These responses agreed with those predicted by convolution of a step stimulus with the mutant impulse response (data not shown).

The diminution in the undershoot is correlated with the absence of the enzymes that methylate and demethylate the MCPs. Therefore, it is likely that this aspect of the impulse response is caused by increased levels of methylation that accompany an increase in the concentration of attractant. This suggests that a transient burst of methylation initiated by the impulse feeds back in such a way as to depress the CCW bias.

We would expect these mutants to possess some chemotactic ability. As the cells move up a gradient, however, their CCW bias will become so great that the run intervals will soon exceed the limits of usefulness imposed by rotational Brownian movement (see above). In this limit, the cells will no longer be chemotactic. It is possible, at least in theory, to perform chemotaxis in the complete absence of adaptation. Runs up the gradient of an attractant will still be longer, and runs down will be shorter. In this case, however, chemotaxis will only be effective over a limited range in concentration, a range over which the rotational bias of the cell remains unsaturated and run lengths do not exceed the Brownian limit. Cells carrying *cheR–cheB* double deletions do, in fact, form chemotactic rings on soft agar containing tryptone (data not shown). These rings, although much smaller than those produced by wild-type cells, are substantially larger than swarms formed by completely nonchemotactic strains, such as *cheY* or *cheZ*. The possibility remains that the cells carrying *cheR–cheB* deletions are in fact adaptive, but only over a time span much longer than that probed by our measurements. (For examples of adaptation to other attrac-

tants not involving methylation, see Niwano and Taylor, 1982.)

Cells carrying mutations in either the *cheB* or *cheR* genes also have impulse responses that resemble that of the wild-type, at least for the first second or so (Figures 7C and 7D). The shape and duration of the first lobes are much the same, but any undershoot or overshoot is obscured by the baseline biases, which are almost exclusively CW or CCW, respectively. We conclude that the mechanisms responsible for generating the first lobe of the impulse response do not involve methylation or demethylation.

The *cheZ* mutants appear to be defective in excitation and to have a very long "memory time." The response shows a long rise time and a very slow recovery (Figure 7B). An undershoot, if it exists, did not develop on the time scale of our measurements. Short impulses of the kind used to stimulate wild-type cells had essentially no effect. Longer pulses (still short on the time scale of the response) set in motion a characteristic sequence of brief CCW bursts; some of these sequences lasted for many seconds. The response did not return to baseline, even 15 sec after the onset of a pulse. As noted earlier, a cell that averages temporal information with such a long time base cannot be chemotactic, because the older information is not relevant to the current trajectory. There exist *cheZ–cheC* double mutants that fail to move up gradients, even though their tumbling rates are normal (Parkinson and Parker, 1979). They are likely to be nonchemotactic both because of a slow response and because of an excessive memory time.

Preliminary measurements of responses of *cheZ* mutants to step stimuli did not agree with those predicted by convolution with the impulse response. The discrepancy might be due to long-range behavior occurring outside the time domain that we investigated, to a nonlinearity in the *cheZ* response or to the fact that the limited amount of step-stimulus data available was not representative of the population of *cheZ* cells as a whole. Further work on these mutants is in progress.

Epilogue

In a recent review, Boyd and Simon (1982) discussed the implications of evolution for chemotaxis. They suggested that chemotaxis initially arose as a response to a transient change in the cellular state (such as perturbation of pH or protonmotive force). Cellular mechanisms of homeostasis restored that state, thus providing a primitive form of adaptation within a limited range. Other mechanisms of adaptation, involving methylation, developed later, allowing adaptation to occur over a wider dynamic range. The components of this system then became sensitive to specific sensory inputs. Our data on responses to aspartate are consistent with this view. Even without methylation or demethylation, E. coli has the ability to integrate information over lengths of time comparable with the duration of a run and has a limited capacity to adapt. The imperfections inherent in this process might have been compensated for by the development of a system that restores the rotational bias of the motor, so that a cell that has drifted up a gradient remains able to respond. Reversible carboxymethylation of the MCPs might provide a basis for such a system, with the primary function of range adjustment. In any event, it is clear from our results that E. coli contains sophisticated machinery for chemotaxis. This machinery processes sensory information over a time span of a few seconds, making maximal use of the information available. The iontophoretic technique provides a means of defining the physiological properties of mutants with defects in this machinery, and thus of learning more about how signal transduction works.

Experimental Procedures

Chemicals

α-Methyl-D,L-aspartate and D,L-leucine were obtained from Sigma; other L-amino acids (A grade) were obtained from Calbiochem; nickel chloride was obtained from Fisher; benzoic and lactic acids (reagent grade) were obtained from Mallinckrodt; and thorium chloride was obtained from ICN-K&K Pharmaceuticals. Tetraethylpentamine (tetren; technical grade) was obtained from Aldrich and purified according to the method of Reilley and Vavoulis (1959).

Bacterial Strains

The wild-type strain was AW405, an E. coli K12 derivative auxotrophic for threonine, leucine and histidine, obtained from J. Adler (Armstrong et al., 1967). Mutant strains were: *cheR* deletion, RP4968; *cheB* deletion, RP4972; *cheR–cheB* double deletions, RP1273 (Sherris and Parkinson, 1981), RP4969, RP4970; *cheZ* point mutants, RP5007 (*cheZ293*) and RP5008 (*cheZ278*) (Parkinson, 1978). All *che* mutants were provided by J. S. Parkinson.

Preparation of Tethered Cells

Cells were grown to saturation in a minimal growth medium containing glycerol and essential amino acids (Hazelbauer et al., 1969), diluted 1:100 and grown again in the same medium, and harvested at mid-exponential phase. The cells were grown at 35°C in a rotary incubator; collected by centrifugation; washed once or twice in a motility medium containing 90 mM NaCl, 10 mM KCl, 10 mM Tris–Cl (pH 7.0 at 32°C), 10 mM sodium lactate, 0.1 mM tetren and 0.001 mM methionine; and resuspended in this medium at one-fifth the original volume. The cells were sheared by passage of this suspension 60 times between two syringes equipped with 26-gauge needles connected with an 8 cm length of polyethylene tubing (0.58 mm internal diameter). The cells were washed twice more, and tethered to a coverslip as described by Berg and Tedesco (1975).

Data Acquisition

The coverslip to which the cells were tethered was sealed to the bottom of a stainless-steel chamber mounted on the stage of a phase-contrast microscope. The cells were viewed through a 40× water-immersion objective (Zeiss). Both the stage and the objective were heated to 32.0°C. The objective was thermally and electrically isolated from the microscope body. The preparation was slowly perfused with motility medium during the entire experiment. Iontophoretic pipettes filled with motility medium containing 0.01 mM thorium chloride and either attractants or repellents were prepared as described by Segall et al. (1982). Pipette resistances were 15–50 megohms. A current-injection circuit (Dreyer and Peper, 1974) was used to pass current (1–200 nA) through the pipettes via Ag/AgCl wires. Control experiments, in which no attractant or repellent was added to the

medium in the pipettes, yielded no response (Segall et al., 1982). The microscope was equipped with an optoelectronic device that extracts the x and y coordinates of the centroid of the image of a spinning cell, $x = \sin(\omega t)$ and $y = \sin(\omega t \pm \phi)$, where ω is the angular velocity of the cell and ϕ is a 90° phase shift, the sign of which indicates the handedness of the rotation (apparatus of Kobayasi et al., 1977, as modified by Berg et al., 1982). Cells that were monitored with this device met several criteria: they were tethered around a point near one end; they rotated with a regular, circular motion; their center of rotation did not change appreciably when they underwent reversals; and their angular velocity was between 5 and 12 Hz. Cells were stimulated about once a minute. Records of the x and y coordinates were made on a strip-chart recorder (Gould Brush 220; run at 25 mm/sec), together with event markers indicating the sign of ϕ and the timing of the stimulus current, as illustrated in Figure 1 of Segall et al. (1982). The positions of the phase discontinuities, evident in the x and/or y signals, were digitized with a strip-chart digitizer built for the purpose. The data, a list of numbers representing the times of CW-to-CCW or CCW-to-CW transitions, measured relative to the onset of the stimulus, were stored as records in a PDP 11/34 computer for subsequent analysis. These numbers were accurate to within about 55 msec, with errors arising from delays due to the electronics, from uncertainties in the positions of the phase discontinuities on the strip-chart records or from random slippage of the paper in the digitizing apparatus.

Data Analysis

Over 1700 records, containing more than 35,000 events, were digitized in all. An array of computer programs was developed to collate, analyze and display data reduced from these records. Each record contained a list of numbers corresponding to the times at which reversals in the direction of rotation occurred. A chronological list of all such numbers in a set of n records was compiled by concatenating the records and sorting the numbers with the Shell-Metzner algorithm (see, for example, Wirth, 1976). A function was constructed whose initial value was taken to be equal to the total number of records in which the cell was spinning CCW at time zero. The value of the function for subsequent times was computed by changing the previous value by unity at every reversal: +1 for a CW-to-CCW transition, −1 for a CCW-to-CW transition. An estimate of the probability of spinning CCW was obtained by dividing all the values in this function by n (Figure 1). Prior to display, this probability function was passed to a cubic spline-fit smoothing routine (Reinsch, 1967, 1971), which fits an array of cubic segments to the data. The endpoints of each segment are constrained to pass close to (but not necessarily through) the data, in such a way that the spline-fit curve fits the data in a least-squares sense. A smoothing parameter, specifying a χ^2 measure of the fit, governs the degree of smoothing. The routine was used to smooth data and to perform interpolation (see below).

The (uneven) density of points along the time axis in the probability function provided a measure of the total number of reversals occurring in the group of records at any instant. The average number of reversals per second per cell is this density divided by n. The density was computed by counting the total number of events up to a given time, and treating that number as a function of time. The time derivative (slope) of this curve gives the density of reversals. The derivative was computed by fitting the function with cubic splines, the coefficient of the linear term for each cubic giving the derivative. Smoothing was used to eliminate discontinuities in the density function.

The two-state model described in the text can be solved to give the fraction of time that a cell runs, f_r, and the reversal rate, ρ. When the system is at equilibrium, one obtains $f_r = k_t/(k_r + k_t)$ and $\rho = 2k_rk_t/(k_r + k_t)$. Even when the system is out of equilibrium, these quantities can be derived from a knowledge of f_r, its time derivative, df_r/dt, and ρ. Since

$$df_r/dt = -k_rf_r + k_t(1 - f_r) \tag{1}$$

and

$$\rho = k_rf_r + k_t(1 - f_r), \tag{2}$$

it follows that

$$k_r = \frac{\rho - df_r/dt}{2f_r} \tag{3}$$

and

$$k_t = \frac{\rho + df_r/dt}{2(1 - f_r)}. \tag{4}$$

The rate constants in Figure 9 were calculated according to equations (3) and (4) with the use of the impulse response, its time derivative and the reversal rate. The impulse response and reversal rate were determined as previously described. The time derivative of the impulse response was obtained from the cubic spline-fit to the rotational data by a method similar to that described for the reversal rate. Both the reversal rate and the impulse response data were smoothed prior to the computation; no smoothing was performed on the result.

The Fourier transform of the impulse response was performed on an array of 1024 points with a Fast Fourier Transform Module (Digital Equipment Corporation). The magnitude of the transform was computed from the real and complex parts. The input array of equally spaced points was obtained by interpolation of 400 unevenly spaced points from Figure 3A with the cubic spline-fit smoothing routine. Some smoothing was done to eliminate excessive noise at high frequencies. Low-frequency trends were eliminated by choosing a baseline and subtracting out the best-fit straight line prior to transformation. Aliasing was reduced by choosing the length of the transformed record (20 sec) to be close to an integral multiple of the impulse response period (approximately 4 sec).

The predicted response to a small step was computed by a routine that performs the convolution integral of an experimentally determined impulse response with a step function of adjustable amplitude. The impulse response was interpolated and smoothed as described above, and the integration was carried out numerically by Romberg extrapolation (Acton, 1970).

Acknowledgments

S. M. B. and J. E. S. contributed equally to the work. We are grateful to Robert Smyth for discussion and for providing computer routines. We also thank Markus Meister for theoretical contributions to the two-state model, and Paul Meyer for discussion of small-step stimuli. This work was supported by a grant from the National Institute of Allergy and Infectious Diseases. J. E. S. acknowledges support as an NSF predoctoral fellow.

The costs of publication of this article were defrayed in part by the payment of page charges. This article must therefore be hereby marked "*advertisement*" in accordance with 18 U.S.C. Section 1734 solely to indicate this fact.

Received July 13, 1982

References

Acton, F. S. (1970). Numerical Methods That Work. (New York: Harper & Row), pp. 100–129.

Armstrong, J. B., Adler, J. and Dahl, M. M. (1967). Nonchemotactic mutants of *Escherichia coli*. J. Bacteriol. *93*, 390–398.

Berg, H. C. and Brown, D. A. (1972). Chemotaxis in *Escherichia coli* analysed by three-dimensional tracking. Nature *239*, 500–504.

Berg, H. C. and Purcell, E. M. (1977). Physics of chemoreception. Biophys. J. *20*, 193–219.

Berg, H. C. and Tedesco, P. M. (1975). Transient response to chemotactic stimuli in *Escherichia coli*. Proc. Nat. Acad. Sci. USA *72*, 3235–3239.

Berg, H. C., Manson, M. D. and Conley, M. P. (1982). Dynamics and energetics of flagellar rotation in bacteria. Symp. Soc. Exp. Biol. *35*, 1–31.

Boyd, A. and Simon, M. (1980). Multiple electrophoretic forms of methyl-accepting chemotaxis proteins generated by stimulus-elicited methylation in *Escherichia coli*. J. Bacteriol. *143*, 809–815.

Boyd, A. and Simon, M. (1982). Bacterial chemotaxis. Ann. Rev. Physiol. *44*, 501–517.

Brown, D. A. and Berg, H. C. (1974). Temporal stimulation of chemotaxis in *Escherichia coli*. Proc. Nat. Acad. Sci. USA *71*, 1388–1392.

Chelsky, D. and Dahlquist, F. W. (1980). Structural studies of methyl-accepting chemotaxis proteins of *Escherichia coli*: evidence for multiple methylation sites. Proc. Nat. Acad. Sci. USA *77*, 2434–2438.

DeFranco, A. L. and Koshland, D. E., Jr. (1980). Multiple methylation in processing of sensory signals during bacterial chemotaxis. Proc. Nat. Acad. Sci. USA *77*, 2429–2433.

Dreyer, F. and Peper, K. (1974). Iontophoretic application of acetylcholine: advantages of high resistance micropipettes in connection with an electronic current pump. Pflügers Arch. ges. Physiol. *348*, 263–272.

Engström, P. and Hazelbauer, G. L. (1980). Multiple methylation of methyl-accepting chemotaxis proteins during adaptation of E. coli to chemical stimuli. Cell *20*, 165–171.

Goy, M. F., Springer, M. S. and Adler, J. (1977). Sensory transduction in *Escherichia coli*: role of a protein methylation reaction in sensory adaptation. Proc. Nat. Acad. Sci. USA *74*, 4964–4968.

Goy, M. F., Springer, M. S. and Adler, J. (1978). Failure of sensory adaptation in bacterial mutants that are defective in a protein methylation reaction. Cell *15*, 1231–1240.

Hazelbauer, G. L., Mesibov, R. E. and Adler, J. (1969). *Escherichia coli* mutants defective in chemotaxis toward specific chemicals. Proc. Nat. Acad. Sci. USA *64*, 1300–1307.

Kihara, M. and Macnab, R. M. (1981). Cytoplasmic pH taxis and weak-acid repellent taxis of bacteria. J. Bacteriol. *145*, 1209–1221.

Kobayasi, S., Maeda, K. and Imae, Y. (1977). Apparatus for detecting rate and direction of rotation of tethered bacterial cells. Rev. Sci. Instr. *48*, 407–410.

Kondoh, H., Ball, C. B. and Adler, J. (1979). Identification of a methyl-accepting chemotaxis protein for the ribose and galactose chemoreceptors of *Escherichia coli*. Proc. Nat. Acad. Sci. USA *76*, 260–264.

Kort, E. N., Goy, M. F., Larsen, S. H. and Adler, J. (1975). Methylation of a membrane protein involved in bacterial chemotaxis. Proc. Nat. Acad. Sci. USA *72*, 3939–3943.

Koshland, D. E., Jr. (1981). Biochemistry of sensing and adaptation in a simple bacterial system. Ann. Rev. Biochem. *50*, 765–782.

Larsen, S. H., Reader, R. W., Kort, E. N., Tso, W.-W. and Adler, J. (1974). Change in direction of flagellar rotation is the basis of the chemotactic response in *Escherichia coli*. Nature *249*, 74–77.

Lovely, P. S. and Dahlquist, F. W. (1975). Statistical measures of bacterial motility and chemotaxis. J. Theor. Biol. *50*, 477–496.

Macnab, R. M. (1978). Bacterial motility and chemotaxis: the molecular biology of a behavioral system. CRC Crit. Rev. Biochem. *5*, 291–341.

Macnab, R. M. and Koshland, D. E., Jr. (1972). The gradient-sensing mechanism in bacterial chemotaxis. Proc. Nat. Acad. Sci. USA *69*, 2509–2512.

Macnab, R. and Koshland, D. E., Jr. (1973). Persistence as a concept in the motility of chemotactic bacteria. J. Mechanochem. Cell. Motil. *2*, 141–148.

Marmarelis, P. Z. and Marmarelis, V. Z. (1978). Analysis of Physiological Systems. (New York: Plenum), pp. 11–130.

Niwano, M. and Taylor, B. L. (1982). Novel sensory adaptation mechanism in bacterial chemotaxis to oxygen and phosphotransferase substrates. Proc. Nat. Acad. Sci. USA *79*, 11–15.

Papoulis, A. (1977). Signal Analysis. (New York: McGraw-Hill), pp. 3–25, 56–138.

Parkinson, J. S. (1978). Complementation analysis and deletion mapping of *Escherichia coli* mutants defective in chemotaxis. J. Bacteriol. *135*, 45–53.

Parkinson, J. S. (1981). Genetics of bacterial chemotaxis. Symp. Soc. Gen. Microbiol. *31*, 265–290.

Parkinson, J. S. and Parker, S. R. (1979). Interaction of the *cheC* and *cheZ* gene products is required for chemotactic behavior in *Escherichia coli*. Proc. Nat. Acad. Sci. USA *76*, 2390–2394.

Parkinson, J. S. and Revello, P. T. (1978). Sensory adaptation mutants of E. coli. Cell *15*, 1221–1230.

Reilley, C. N. and Vavoulis, A. (1959). Tetraethylenepentamine, a selective titrant for metal ions. Anal. Chem. *31*, 243–248.

Reinsch, C. H. (1967). Smoothing by spline functions. Numerische Mathematik *10*, 177–183.

Reinsch, C. H. (1971). Smoothing by spine functions II. Numerische Mathematik *16*, 451–454.

Segall, J. E., Manson, M. D. and Berg, H. C. (1982). Signal processing times in bacterial chemotaxis. Nature *296*, 855–857.

Sherris, D. and Parkinson, J. S. (1981). Posttranslational processing of methyl-accepting chemotaxis proteins in *Eshcerichia coli*. Proc. Nat. Acad. Sci. USA *78*, 6051–6055.

Silverman, M. and Simon, M. (1974). Flagellar rotation and the mechanism of bacterial motility. Nature *249*, 73–74.

Silverman, M. and Simon, M. (1977). Chemotaxis in *Escherichia coli*: methylation of *che* gene products. Proc. Nat. Acad. Sci. USA *74*, 3317–3321.

Springer, M. S., Goy, M. F. and Adler, J. (1977). Sensory transduction in *Escherichia coli*: two complementary pathways of information processing that involve methylated proteins. Proc. Nat. Acad. Sci. USA *74*, 3312–3316.

Springer, M. S., Goy, M. F. and Adler, J. (1979). Protein methylation in behavioral control mechanisms and in signal transduction. Nature *280*, 279–284.

Springer, W. R. and Koshland, D. E., Jr. (1977). Identification of a protein methyltransferase as the *cheR* gene product in the bacterial sensing system. Proc. Nat. Acad. Sci. USA *74*, 533–537.

Spudich, J. L. and Koshland, D. E., Jr. (1975). Quantitation of the sensory response in bacterial chemotaxis. Proc. Nat. Acad. Sci. USA *72*, 710–713.

Spudich, J. L. and Koshland, D. E., Jr. (1976). Non-genetic individuality: chance in the single cell. Nature *262*, 467–471.

Stock, J. B. and Koshland, D. E., Jr. (1978). A protein methylesterase involved in bacterial sensing. Proc. Nat. Acad. Sci. USA *75*, 3659–3663.

Tsang, N., Macnab, R. and Koshland, D. E., Jr. (1973). Common mechanism for repellents and attractants in bacterial chemotaxis. Science *181*, 60–63.

Wirth, N. (1976). Algorithms + Data Structures = Programs. (Englewood Cliffs, N. J.: Prentice-Hall), pp. 56–124.

Chapter III

FURTHER IMPULSE AND STEP RESPONSE STUDIES

Soon after submission of the impulse response paper, Steve turned to finishing up the paper describing responses of tethered cells to gradual changes in attractant concentration generated by a programmable mixer(see Block et al., 1983). I continued studying the responses of various strains to impulse and step stimuli, while working with Akira on filamentous cells (discussed in the next two chapters). This chapter summarizes the unpublished information that I have collected.

Responses of Wild-type Cells

Attractant Stimuli: L-Aspartate and α-methylaspartate. The accumulated responses of wild-type cells to brief pulses of L-aspartate and α-methylaspartate are plotted in Text-figure 4. Responses to pulses of α-methylaspartate at 22 or 32°C and responses to pulses of L-aspartate at 32°C were combined to produce this plot. These responses were quite similar, with the possible exception of the responses to pulses of α-methylaspartate at 32°C in which the initial lobe lasted 0.86 sec compared to 1.06 sec for the responses to the other two stimuli (data not shown). A possible explanation for this difference is that the responses to α-methylaspartate at 32°C were from cells adapted to 0.16 mM α-methylaspartate, which is roughly the dissociation constant for the receptor. The *tar* MCP, which mediates these responses would have a higher level of methylation. Perhaps the altered response kinetics reflect this difference in methylation level.

The accumulated responses to step increases in aspartate or α-methylaspartate are shown in Text-figure 5. The prediction of the step response kinetics by the impulse response shown in Text-figure 4 is also plotted and fits quite well. The step response shown in Text-figure 5 reflects the time course of responses to small step stimuli. Responses to large step stimuli can

Text-figure 4. The wild-type attractant impulse response

The dotted curve shows cumulative responses of strain AW405 to pulses of α-methylaspartate or L-aspartate at 22 or 32°C. The pulse begins at 5.06 sec (bar). Responses at 22°C were to pulses 0.034 - 0.12 sec long (-50 to -100 nA) with 1 - 7 mM α-methylaspartate in the pipette. Responses at 32°C were to pulses 0.12 sec long (-100 nA) with 1 - 3 mM α-methylaspartate in the pipette and 0.16 mM α-methylaspartate in the bath, or to pulses 0.016 - 0.019 sec long (-25 to -100 nA) with 1 mM L-aspartate in the pipette. The graph was constructed from 378 records containing 7,566 events from 17 different cells. The mean bias within a 0.05 sec window was determined and plotted every 0.05 sec.

The smooth curve is the fit of a sum of six exponentials to the impulse response with the additional constraint that the Fourier transform of the fit predict a response amplitude of about 0.2 for a sine wave modulation in receptor occupancy of 0.001 Hz and amplitude 0.265, as described in the text. The relative weights of the points in the impulse response were determined by their bias values, assuming that fluctuations in bias are normally distributed. The fit values were (amplitude and rate constant per sec) a_1,k_1 = 37.51,1.973; a_2,k_2 = -25.76,4.184; a_3,k_3 = -28.37,1.669; a_4,k_4 = 12.01,5.768; a_5,k_5 = 1.715,3.831; a_6,k_6 = 2.871,1.781.

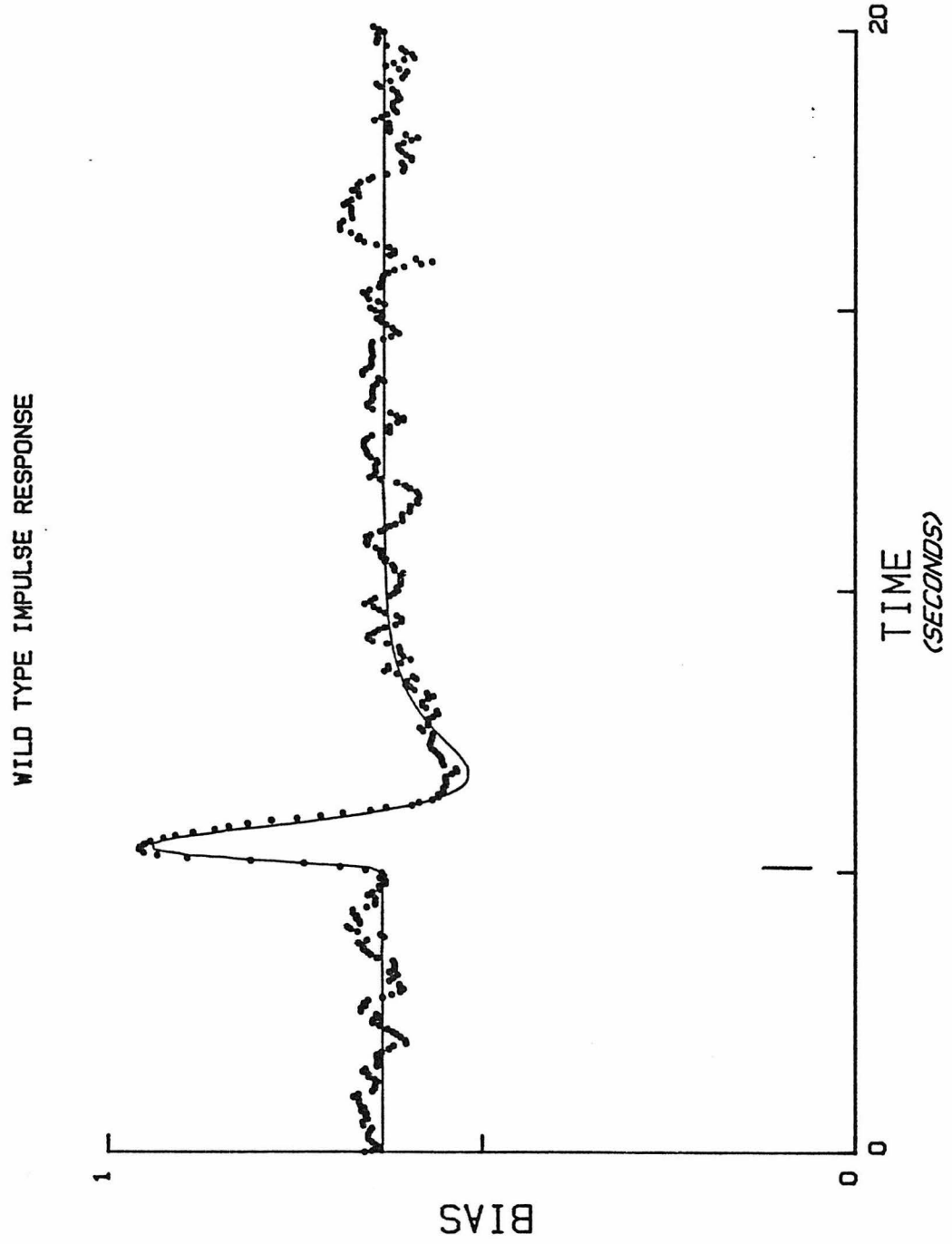
WILD TYPE IMPULSE RESPONSE
BIAS
1
0
0
20
TIME
(SECONDS)

Text-figure 5. Wild-type attractant step response

The heavy line shows the cumulative response of AW405 to long pulses (usually about 12 sec long) beginning at 1.0 seconds (bar). The response to the end of the pulse is not shown. Pulse sizes were -3 to -10 nA and the concentration in the pipette was 0.1 - 1 mM L-aspartate or 1 - 10 mM α-methylaspartate. In most cases there was 0.16 mM α-methylaspartate in the buffer. The graph was constructed from 227 records containing 5040 events from 10 cells. The mean bias during a 0.05 sec window was determined and plotted every 0.05 seconds.

The light line is the prediction of the wild-type attractant impulse response to a step change in receptor occupancy with the amplitude chosen to fit the data. The impulse response was smoothed and the baseline bias subtracted before performing the integration.

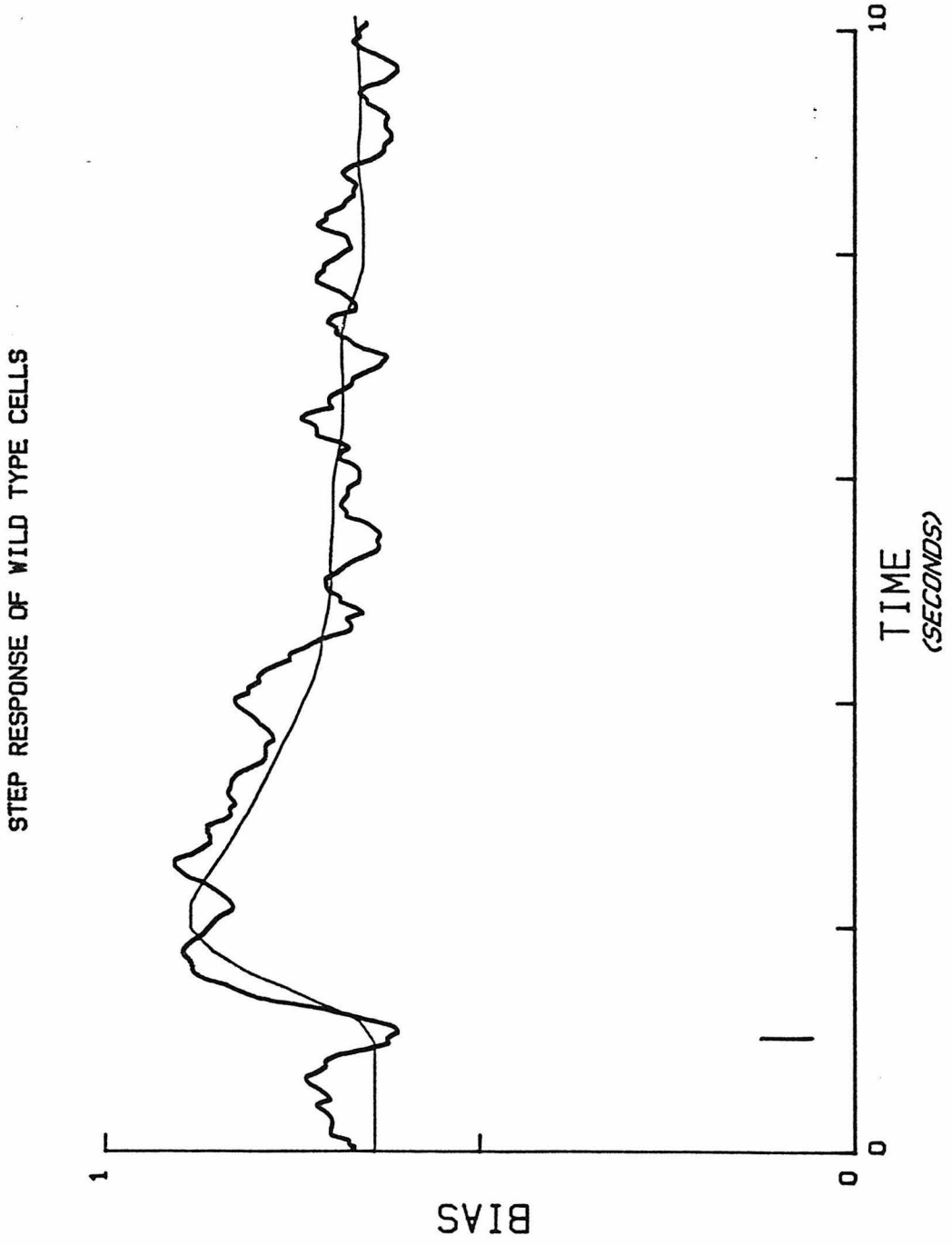
STEP RESPONSE OF WILD TYPE CELLS
BIAS
1
0
0
10
TIME
(SECONDS)

have different kinetics if one of the reactions involved in generating the impulse response becomes saturated. For example, it is quite likely that the rate of methylation becomes saturated with large step changes in attractant concentration, giving rise to the long times required for adaptation that were observed in earlier studies (Berg and Tedesco, 1975; Macnab and Koshland, 1972; Spudich and Koshland, 1975).

An estimate of the sensitivity of the chemotaxis system to small step changes in attractant concentration could be made from these data if the concentration change during the step were known. The concentration change for a subset of the responses shown in Text-figure 5 was determined in the following way. Pipettes were filled with 1 mM or 3.3 mM α-methylaspartate. Cells were stimulated by long -100 nA pulses at 32°C in the standard buffer containing 0.16 mM α-methylasparate - this is the apparent dissociation constant for the receptor as determined by transition time measurements in Berg and Tedesco, 1975; 0.13 mM was determined by Pfeffer assay by Mesibov et al., 1973. The α-methylaspartate was added in order to compare the results with the results from programmed flows (see below). The amount of attractant released by the -100 nA currents was estimated by the transition time (Berg and Tedesco, 1975) of tethered cells 5 microns from the tip of the pipettes. Some cells were stimulated with the same pipettes by 10 sec long pulses of smaller amplitude (-3 nA to -10 nA) and their responses were recorded. The responses were not saturated. Assuming that the amount of attractant released is proportional to the size of the current flowing through the pipette, the estimate of release at -100 nA by the transition times can be used to estimate the release for the smaller currents. Then the size of the averaged response can be compared with the estimated change in receptor occupancy due to the average change in concentration during the pulses. The peak change in bias in response to this

subset of long pulses was about 0.233. The average change in receptor occupancy was estimated to be 0.42%. Thus a dramatic change in bias was produced by a 0.4% change in receptor occupancy. Since there are 600 to 1000 *tar* molecules per cell (Clarke and Koshland, 1979; Hazelbauer and Harayama, 1983), a .4% change in receptor occupancy corresponds to about 3 more *tar* molecules binding. Each molecule binding attractant can cause a change in bias of 0.233/3 = 0.08.

It would be useful to be able to interpret changes in bias in terms of changes in run length, because change in run length produces net movement of swimming cells in a particular direction. Unfortunately, a direct comparison of changes in bias and changes in run length has not been made. The difficulties of such a study will be greatly reduced when equipment currently being developed in the lab is ready for use. One possible way to get a rough estimate is by using data of Doug Brown showing the dependence of run length on rate of change of receptor occupancy (D. Brown, thesis; Brown and Berg, 1974), and comparing it with Steve's data on the dependence of bias on rate of change of receptor occupancy (Figure 6A in Block et al., 1983). From Steve's data the rate of change of receptor occupancy for a particular change in bias can be estimated, and then the corresponding change in run length for that rate of change in receptor occupancy can be gotten from Doug Brown's data. The data are sketchy because the experiments were quite difficult. However, I estimate that a change in bias of 0.08 (binding of attractant to one more receptor) corresponds to a change in run length by a factor of 2 to 4 - about the size of the increase in run length that was observed for cells swimming in spatial gradients of aspartate. This indicates an exquisite sensitivity to very small changes in the number of receptors binding attractant, or equivalently, the fraction of time that receptors bind attractant.

It is interesting to note that the threshold change in receptor occupancy for responses to α-methylaspartate as measured by Pfeffer assay was also about .4% (Mesibov et al., 1973). However, this is the total change in receptor occupancy between cells inside the capillary tube and those outside far from the capillary. The cells actually responding to the spatial gradients established near the end of the capillary will be measuring smaller changes in receptor occupancy, consistent with the conclusions drawn in the preceding paragraph.

Knowledge of the sensitivity of the system to a step change in receptor occupancy, combined with the use of the impulse response, allows us to predict the response to any type of change in receptor occupancy. As discussed in the impulse response paper, the response of a linear system to any stimulus is the convolution of the impulse response with the stimulus. If only the kinetics of the response are desired, the size of the stimulus is arbitrary, because the kinetics of the response to a particular stimulus do not depend on the size of the stimulus. If one wishes to predict the size of the response, then the size of the stimulus convoluted with the impulse response must be calibrated. This can be done using the responses to the 0.4% change in receptor occupancy. The size of the step that produces a peak change in bias of 0.233 when convoluted with the impulse response corresponds to a 0.4% change in receptor occupancy. The convolution of a step 1/2 that large with the impulse response predicts the response to a 0.2% change in receptor occupancy. Convolution of a sine wave of that amplitude predicts the response to a sinusoidal change in receptor occupancy of amplitude 0.4%, and convolution of a linear ramp that changes by that amount every second with the impulse response predicts the response to a linear ramp in receptor occupancy with a slope of 0.4% per second. The ramp and sine wave predictions can be compared with the measurements made by Steve (Block et al., 1983) of responses to linear ramps and sine waves of receptor occupancy.

Convolution of a linear ramp with the impulse response produces a steady state change in bias (data not shown), with the amplitude of the change in bias varying linearly with ramp rate, as shown in Text-figure 6A. The slope is quite similar to the slope of Steve's data. (The threshold shown by Steve's data is evidence for departure from linearity at small ramp rates. A possible explanation for this nonlinearity is discussed in Appendix C of Block et al., 1983.).

An alternate way to study the response of the system to the rate of change of receptor occupancy is to measure the response to low-frequency sine wave changes in receptor occupancy. The amplitude of the response should be predicted by the response to the maximum rate of change of receptor occupancy during the sine wave (using the plot of change in bias versus ramp rate). The thresholds seen in Figure 6 of Block et al., 1983, and Text-figure 6A should produce distortions in the response (which are seen, e.g., Figure 7 of Block et al., 1983). Convolution of sine waves with the impulse response produces sine wave changes in bias (data not shown). The variation in amplitude of the response with frequency is given by a Bode plot of the fourier transform of the impulse response. Text-figure 6B shows the Bode plot along with the data collected by Steve on responses to sine waves. Again there is reasonably good correspondence between the prediction of the impulse response and the actual responses, when the effects of the thresholds seen in Figure 7 of Block et al., 1983, are compensated for. It is clear that although the impulse response can predict the general behavior of bacterial chemotactic responses, the nonlinearities reflected in the thresholds to linear ramps and the asymmetry of responses to sine waves are not predicted by the linear impulse response analysis and give new information about the system not contained in the impulse response data.

Text-figure 6. Comparison of the predictions of the impulse response with responses to linear ramps and sine waves

A. The data of figure 6A in Block et al., 1983 replotted as change in bias during ramp versus rate of change of fraction of receptor occupied. The solid line is the prediction of the impulse response. The dashed line is the prediction of the impulse response with an offset of 0.15. The slope of both lines is 114 seconds. The slope of the best fit line through the data (points equally weighted, the point on the far right not included) is 76 seconds.

B. The Bode plot - $\log_{10}$(response amplitude) versus $\log_{10}$(frequency) - of the absolute magnitude of the complex Fourier transform of the wild-type impulse response. The line is the Bode plot of the linefit in Text-figure 3, scaled so that the value at 3 Hz is $\log_{10}(21.1)$ - the response predicted by the linefit to a 3 Hz sine wave in fraction of receptors occupied of amplitude 0.265. The dots are the Bode plot of the wild-type impulse response, calculated as described in Block et al., 1982, placed by eye over the solid line. The stars show the unsaturated changes in bias of cells exposed to sine waves in fraction of receptor occupied of amplitude 0.265 (from data in Block et al., 1983). To compensate for thresholds in responses(the large threshold to down ramps essentially eliminates responses to the portion of the sine wave in which receptor occupancy is decreasing), the difference between the maximum and the minimum values of the bias are plotted, not 1/2 that value (which is the normal definition of the amplitude of the response).

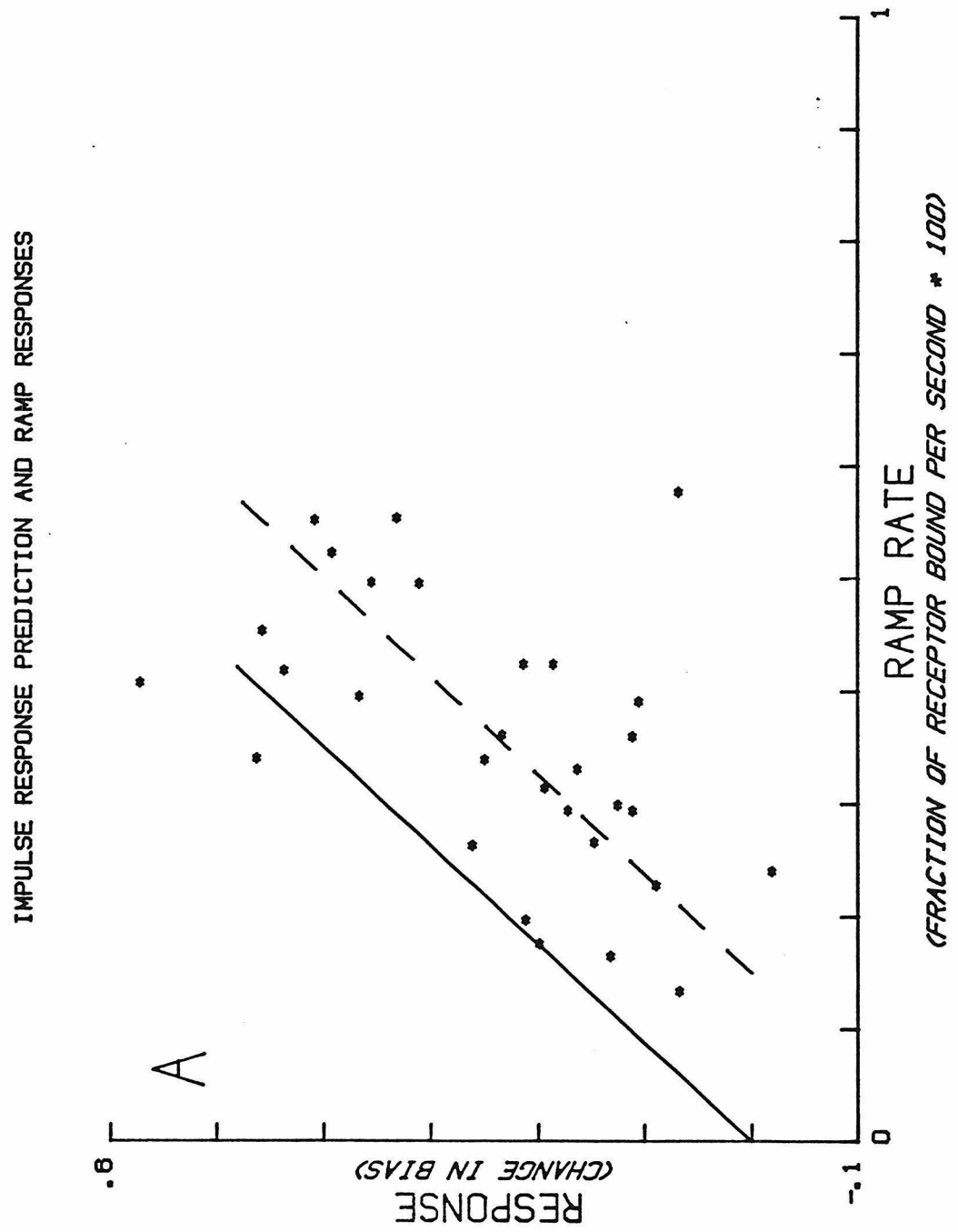
IMPULSE RESPONSE PREDICTION AND RAMP RESPONSES
A
.8
-.1
0
1
RESPONSE
(CHANGE IN BIAS)
RAMP RATE
(FRACTION OF RECEPTOR BOUND PER SECOND * 100)

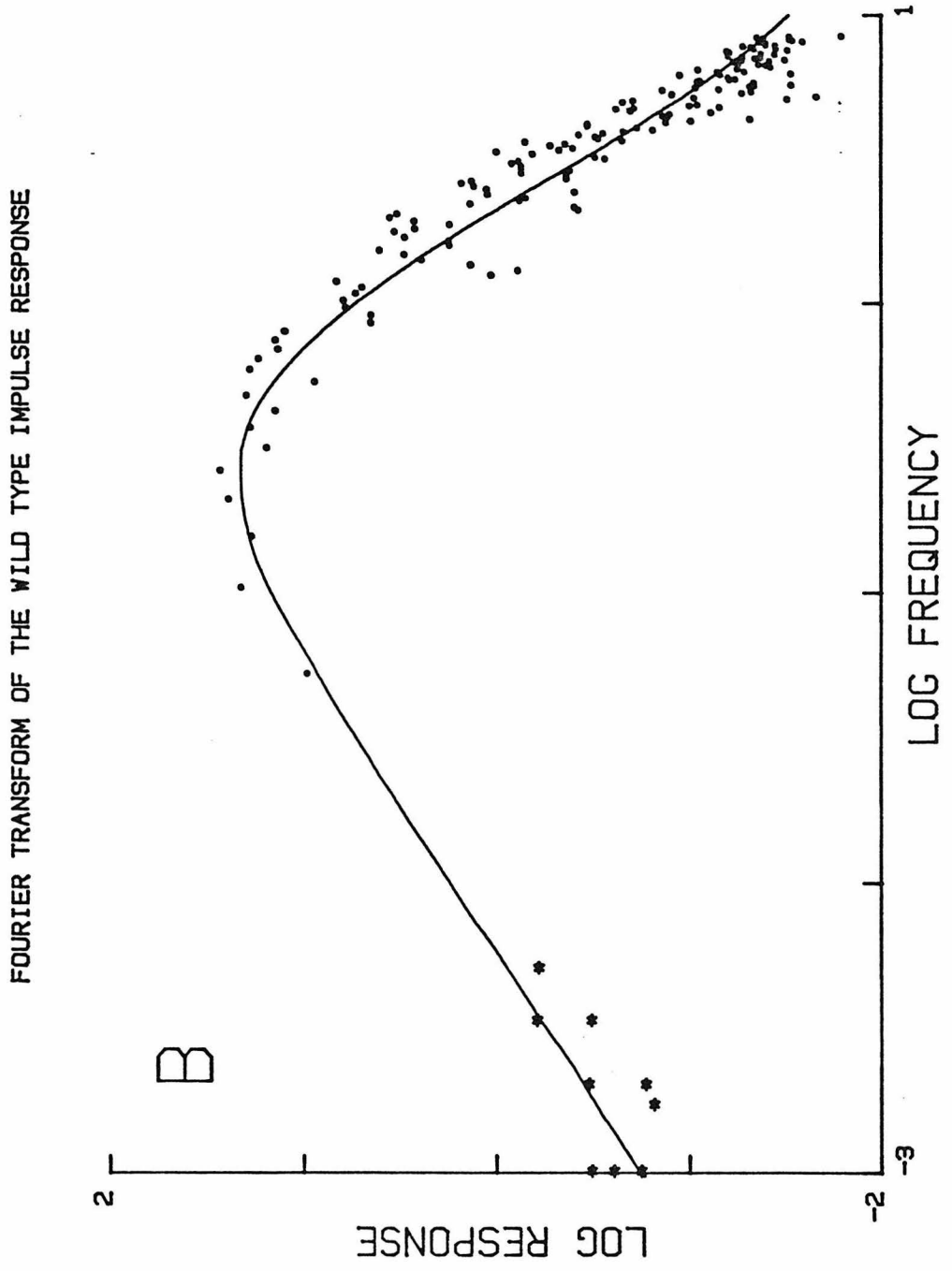
FOURIER TRANSFORM OF THE WILD TYPE IMPULSE RESPONSE
B
LOG RESPONSE
LOG FREQUENCY
2
-2
-3
1

Attractant Data: D-glucosamine. Text-figure 7 shows responses to brief pulses of D-glucosamine at 32°C. The response to D-glucosamine is probably mediated by the mannose enzyme II of the PTS sugar system (Adler and Epstein, 1974). The data are preliminary, but the width of the initial lobe is quite similar to that for responses to aspartate and α-methylaspartate (shown in Text-figure 4). The second lobe, or undershoot, is not visible, but more responses are necessary to determine if this adaptive portion of the impulse response is different from that in Text-figure 4. The response to D-glucosamine of a *cheZ* mutant (RP5007) is lengthened, perhaps even more than responses to aspartate are lengthened in this mutant (data not shown). The responses of other *cheZ* mutants to D-glucosamine have not been determined. These initial studies suggest that the kinetics of chemotactic signalling for D-glucosamine are similar to the kinetics of signalling for aspartate, and may reflect a similar mechanism for signalling the flagellar motor.

Repellent Data. Three types of repellent impulses have been used--addition of benzoate or nickel, or removal of aspartate. The accumulated response to all three is shown in Text-figure 8 and is quite similar to the attractant impulse response in Text-figure 4. All three individual responses had initial downward lobes with similar kinetics. The second lobes seemed to have more varied kinetics (data not shown), the second lobe of the benzoate response being briefer than the second lobe of the nickel response; the data for aspartate removal were too noisy to distinguish a second lobe. I noticed that it was important with nickel to give pulses of small amplitude, because large pulses would give a normal initial lobe, but then an extremely large second lobe, often saturated. This probably reflects the asymmetry in the kinetics of adaptation to attractant and repellent stimuli. A large nickel pulse could produce a very rapid, large

Text-figure 7. Wild-type impulse response to D-Glucosamine

Cumulative response of AW405 to pulses of D-glucosamine at 32°C starting at 5.06 sec (bar). Pulses of amplitude +10 - +100 nA and length 0.019 - 0.029 sec long were delivered from pipettes containing 10 mM D-glucosamine. The graph was constructed from 115 records containing 2898 events from 3 cells. The mean bias during a 0.05 sec window was calculated and plotted every 0.05 sec.

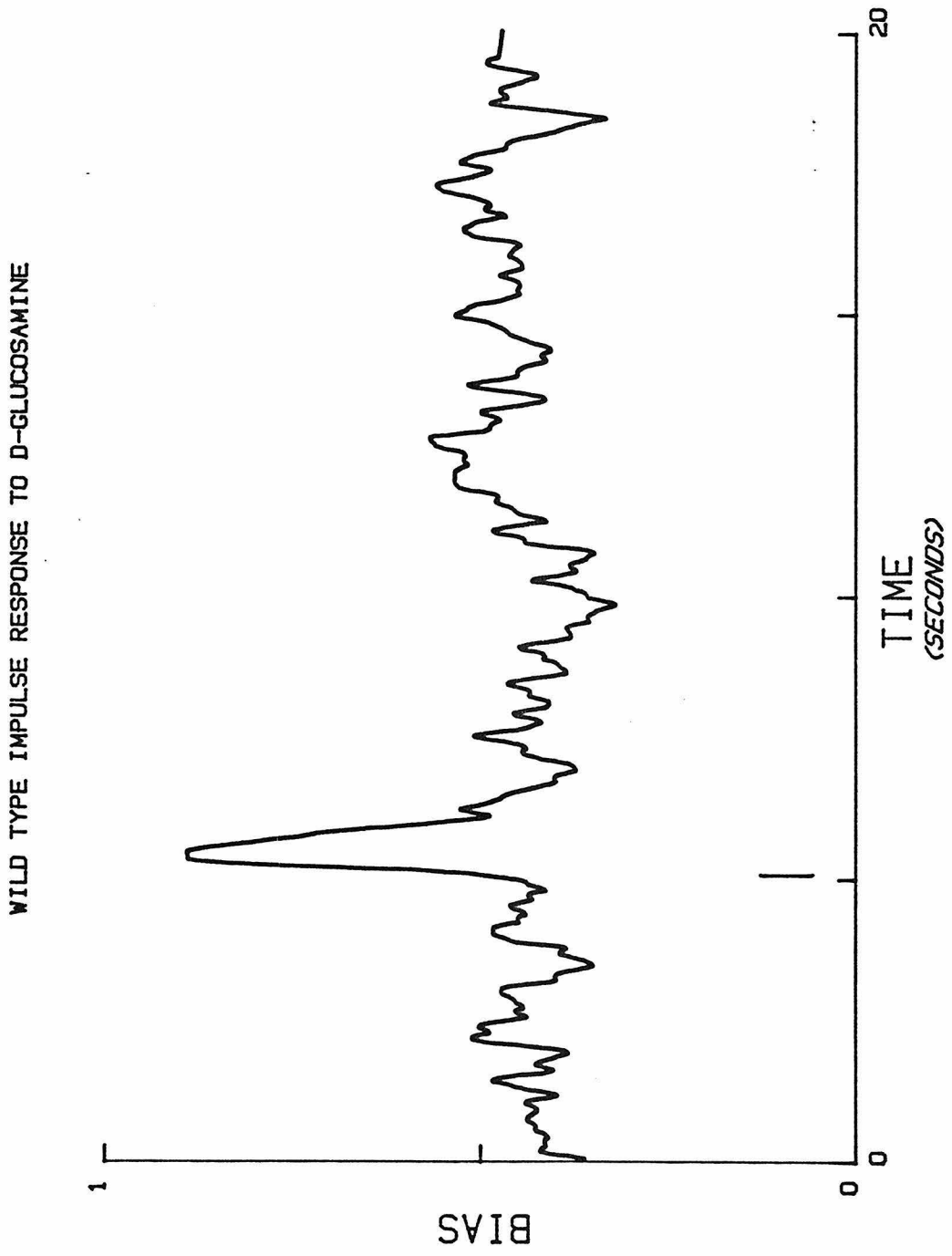
WILD TYPE IMPULSE RESPONSE TO D-GLUCOSAMINE
BIAS
1
0
0
20
TIME
(SECONDS)

Text-figure 8. Wild-type repellent impulse response

Cumulative response of AW405 to repellent pulses at 22 and 32°C. Pulses began at 5.06 sec (bar). Pulses were either addition of benzoate or nickel, or removal of aspartate. Pulses of amplitude -100 nA and length 0.04 - 0.12 sec were delivered with 0.1 M or 0.2 M benzoate in the pipette. Pulses of amplitude +2.5 - +40 nA and length 0.028 - 0.12 sec were delivered with 0.1 - 1 mM $NiCl_2$ in the pipette. For aspartate, cells were adapted to -2 - -6 nA currents from pipettes containing 1mM L-aspartate and shifts in current to +1 - +4 nA for 0.019 - 0.06 seconds were delivered. The graph was constructed from 465 records containing 9,644 events from 12 cells. The mean bias during a 0.05 sec window was determined and plotted every 0.05 sec.

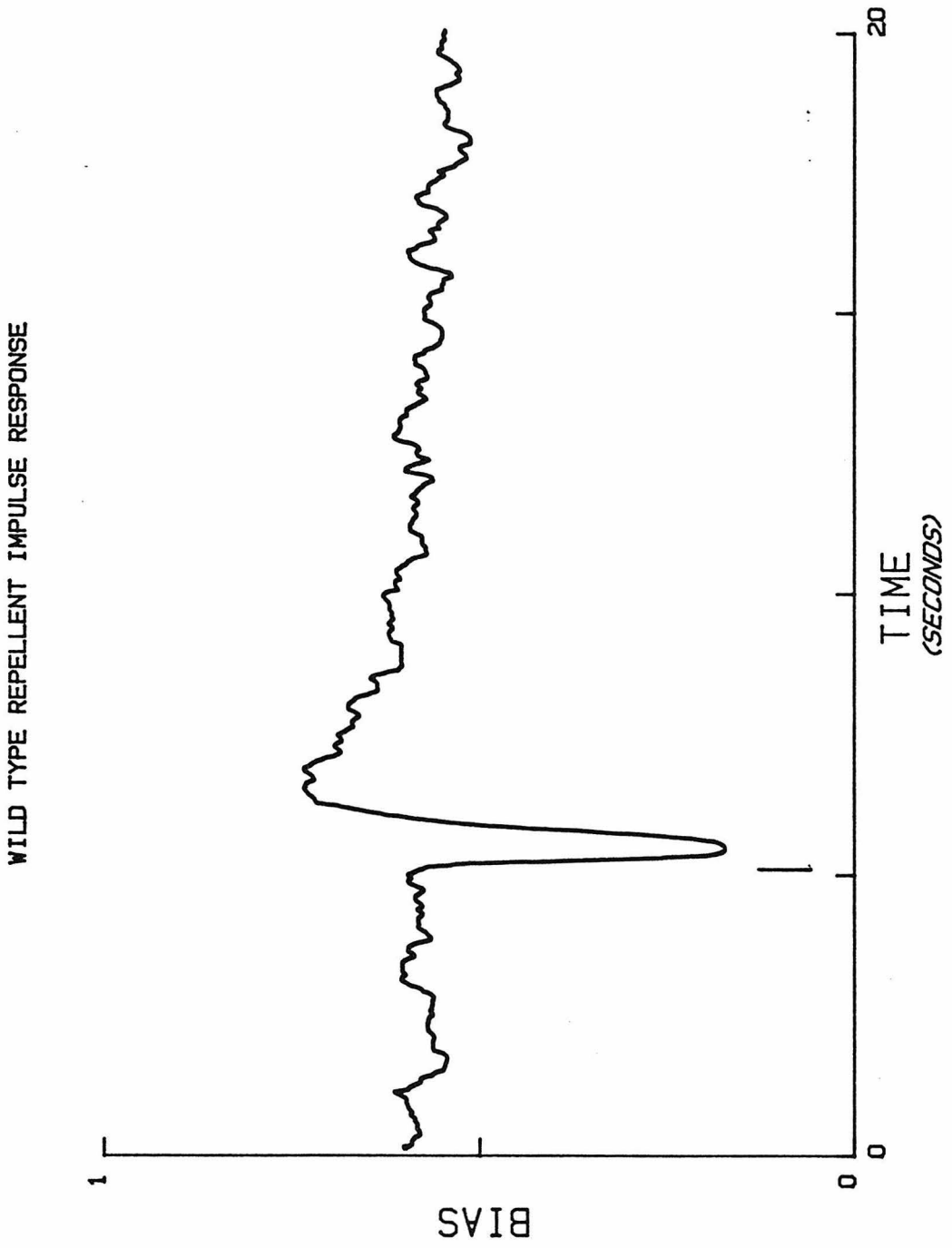
WILD TYPE REPELLENT IMPULSE RESPONSE
BIAS
1
0
0
20
TIME
(SECONDS)

demethylation of the *tar* MCP, and then the remethylation could not occur as rapidly, resulting in a very large and long second lobe.

The only responses to repellent step stimuli available are the responses to the shutting off of a long pulse of aspartate(the pulses used to collect the data in Text-figure 5). The responses to the beginning and the end of the pulse are compared in Text-figure 9. The kinetics of the initial phases of the responses are similar, though opposite in sign. However, the adaptation kinetics are different. This difference is reflected to some extent in the second lobe of the impulse response to benzoate (see Figure 3B of Block et al., 1982), but is not very clear in the average impulse response to repellent pulses (Text-figure 8). The asymmetry in adaptation kinetics for attractant and repellent steps may reflect the asymmetry in response thresholds to linear up and down ramps in attractant concentration, discussed above. Those data show the change in bias required to activate the methylation or demethylation enzymes in order to keep up with the rate of change of receptor occupancy. A positive change in bias corresponds to the rate of methylation required to offset a certain rate of increase in receptor occupancy. The same negative change in bias corresponds to a larger rate of demethylation and a greater rate of decrease in receptor occupancy. Thus the methylation rate while the bias is shifted above the steady-state value is less than the demethylation rate when the bias is shifted an equivalent amount below the steady state value, perhaps giving rise to the observed difference.

Mutant Responses

***che*RB deletion strains.** The response of *che*RB deletions (RP2867 and RP4969) to impulse and step stimuli using L-aspartate are shown in Text-figures 10 and

Text-figure 9. Wild-type step responses

The light line again shows the response to a long pulse of L-aspartate or α-methylaspartate shown in Text-figure 5, but the pulse begins at 2.56 sec (bar). The heavy line shows the response to the end of the pulse, the pulse ending at 2.56 (bar). The heavy line is constructed from 222 records containing 1,989 events from 10 cells. The mean bias during a 0.05 second window was calculated and plotted every 0.05 seconds.

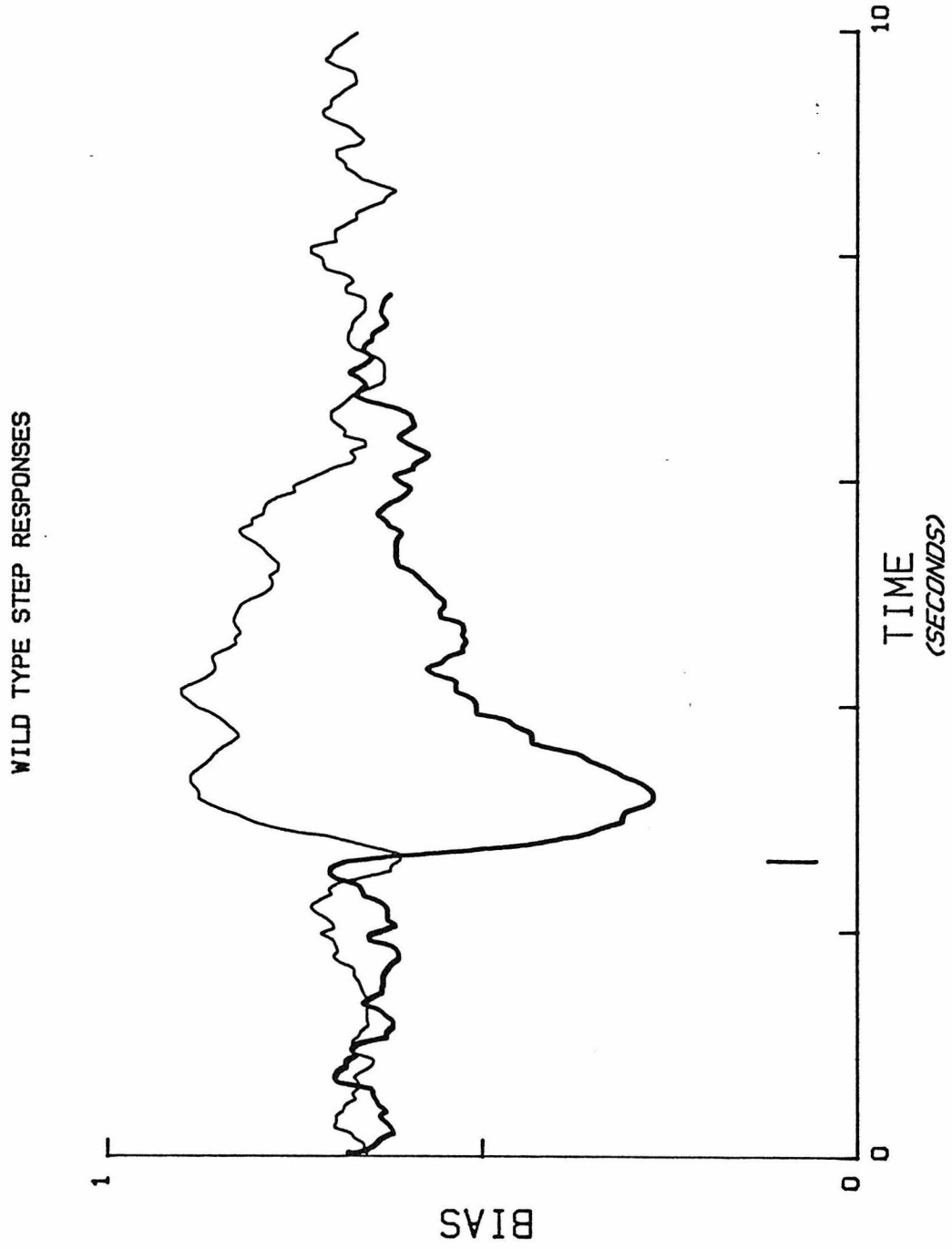
WILD TYPE STEP RESPONSES
BIAS
1
0
0
10
TIME
(SECONDS)

Text-figure 10. ***Che*RB attractant impulse response**

Cumulative responses at 22 and 32 ^{o}C to pulses of aspartate of strains containing a deletion of the cheR and cheB genes (RP2867 and RP4969). Pulses begin at 5.06 seconds (bar). Pulse amplitudes were -50 - -100 nA and lengths were 0.009 - 0.387 seconds. Pipettes contained 3 - 20 mM L-aspartate. The graph was constructed from 207 records containing 5,006 events from 13 cells. The mean bias during a 0.05 second window was calculated and plotted every 0.05 seconds.

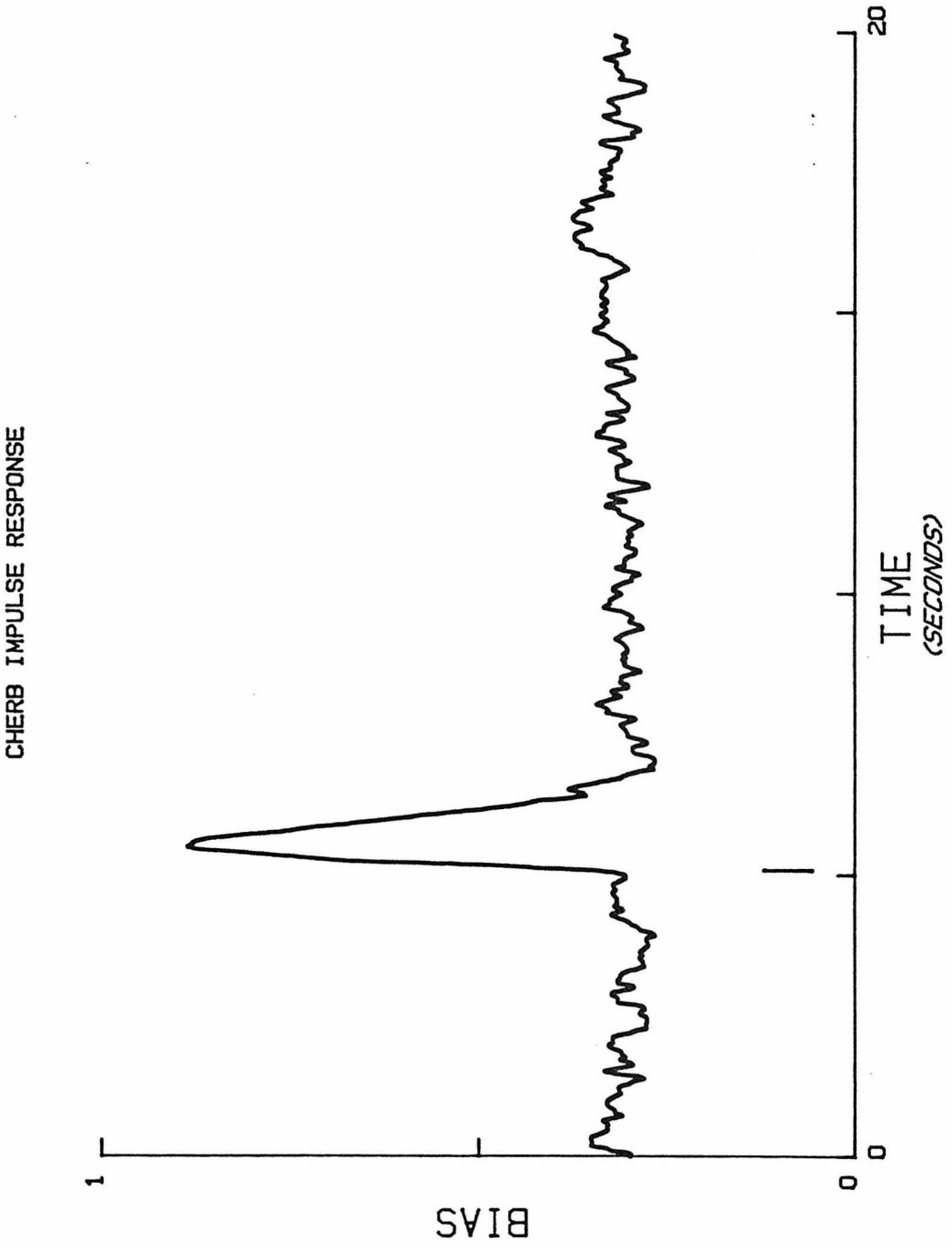
CHERB IMPULSE RESPONSE
BIAS
1
0
0
20
TIME
(SECONDS)

Text-figure 11. *Che*RB attractant step response

Response at 32°C to long pulses of attractant by a strain containing a deletion of the *che*R and *che*B genes (RP2867). Pulses begin at 5.06 seconds (first bar). Because pulses of different length (5 - 12 sec) were used in different experiments, the cumulative response to the ends of the pulses (second bar) was plotted starting at 10.6 seconds (break in plot). Pulse amplitudes were 0.0 to -4.5 nA or -3 to -20 nA. Pipettes contained 2 - 5 mM L-aspartate. The graph was constructed from 178 records containing 5,184 events from 6 cells. The mean bias in a 0.05 second window was calculated and plotted every 0.05 seconds.

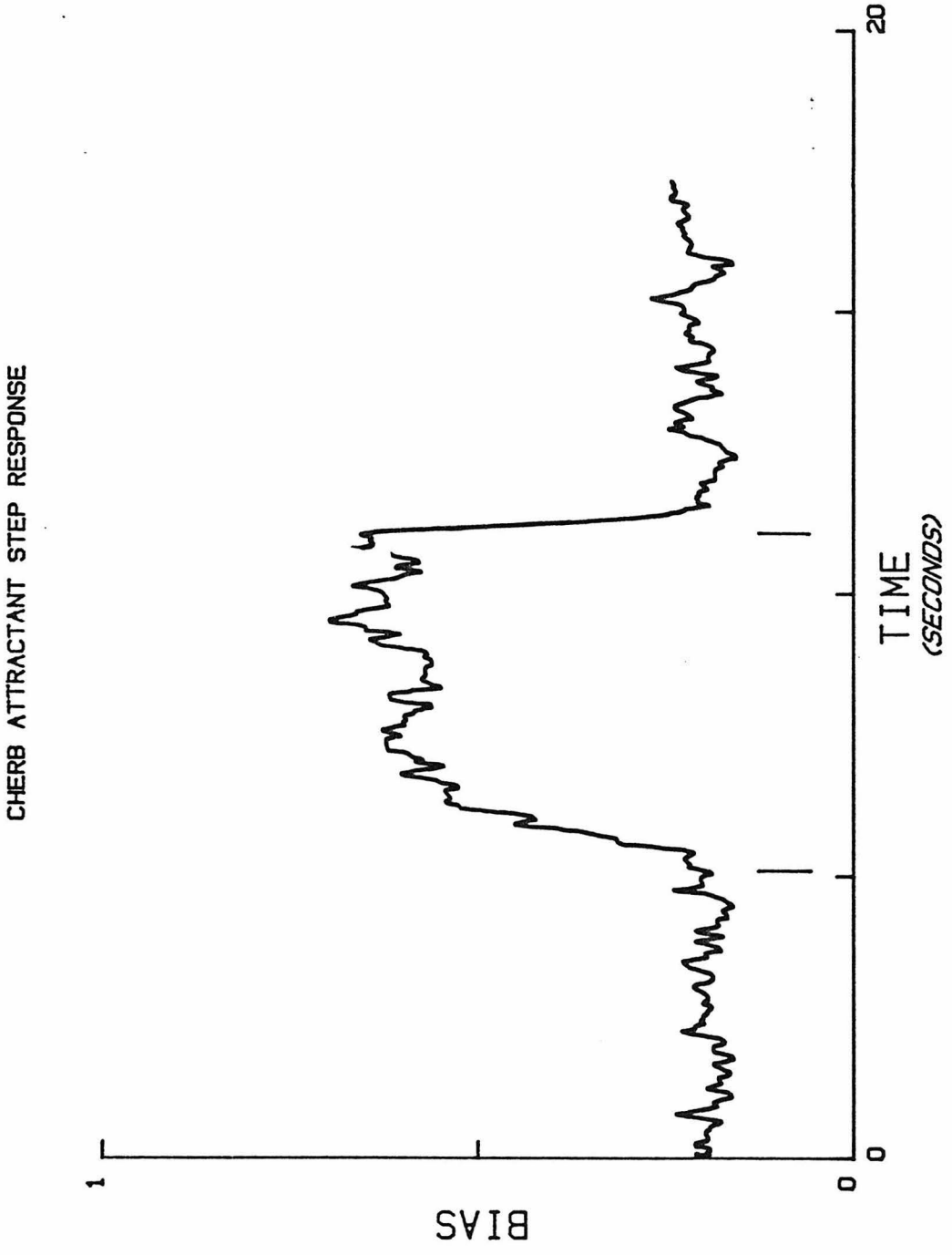
CHERB ATTRACTANT STEP RESPONSE
BIAS
1
0
0
20
TIME
(SECONDS)

11. The impulse response shows only an initial lobe and little or no second lobe. Such an impulse response predicts that this strain should not adapt to long pulses of L-aspartate. The response to a 5 sec pulse is shown in Text-figure 11 and shows no evidence of adaptation. Responses to 11 sec pulses (not shown) also show no adaptation. However, this response does provide evidence for a response threshold, as described in Chapter 5. The response to the start of the pulse has a lag, while the response to the end of the pulse is quite rapid.

I find that *che*RB strains are less sensitive to L-aspartate than wild type by a factor of 10 to 100. There are few responses to α-methylaspartate, possibly for this reason. All the results described above were obtained with L-aspartate. The reason for this decreased sensitivity is unknown. *Che*B mutants show the same decreased sensitivity, implying that this might be because the tar MCP has not been modified by the *che*B gene product, as normally occurs in the wild-type. Whether there is a change in the binding of the receptor for aspartate or a decrease in the efficiency of signal transmission across the membrane is uncertain.

***CheZ* strains.** The impulse responses of *cheZ* and *cheZ cheC* mutants are very similar and have been combined in Text-figure 12. The initial lobe has slower rising and falling phases than the wild-type. The kinetics of the second lobe are also slower than the wild-type. The responses to small step changes in attractant concentration show kinetics consistent with the impulse response (Text-figure 13). The response to the start of the pulse rises with a time constant of about 3.2 sec and slowly decays, and has not returned to baseline by the end of the pulse. The response to the end of the pulse falls with a time constant of about 2.3 sec and also returns slowly to the baseline. The anomalous results reported in Block et al., 1982, were probably caused by not waiting long

Text-figure 12. ***Che*Z and *che*Z *che*C attractant impulse response**

Cumulative response of cheZ cheC(RP2734) and cheZ(RP5006, RP5007) mutants to pulses of L-aspartate at 32°C. Pulses begin at 5.06 seconds (bar). Pulse amplitudes were -100 nA, pulse lengths were 0.67 to 1.24 seconds. Pipettes contained 0.3 or 1 mM L-aspartate. The graph was constructed from 175 records containing 13,653 events from 6 cells. The mean bias in a 0.6 second window was calculated and plotted every 0.3 sec.

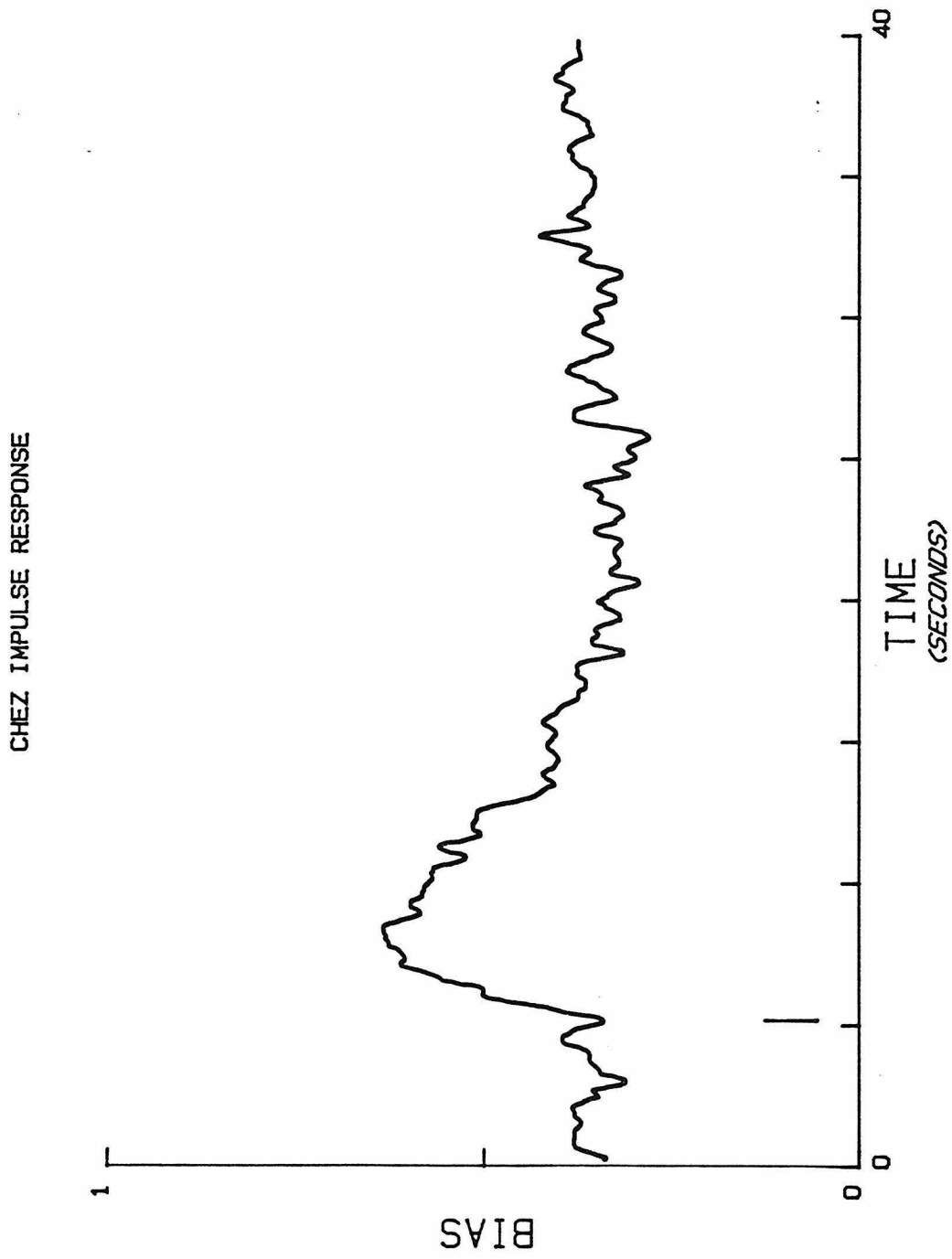
CHEZ IMPULSE RESPONSE
BIAS
1
0
0
40
TIME
(SECONDS)

Text-figure 13. *CheZ* **attractant step responses**

Response of a *cheZ* mutant (RP5007) to long pulses (about 50 seconds long) of L-aspartate at 22°C. The responses to the start (heavy line) and end (light line) of the pulses are shown with the start or end beginning at 9.06 seconds (bar). The response to the end of the pulse was moved down 0.17 so that it was separate from the heavy line. Pulse amplitudes were -8 to -20 nA and pipettes contained 0.1 or 0.2 mM L-aspartate. The external buffer contained 1 μM serine or 10 mM L-cysteic acid. (Wild-type cells do not fully adapt to large shifts in the concentration of serine, and I hoped to increase the bias of cheZ cells in the same way with serine. The L-cysteic acid should block L-aspartate transport (Schellenberg and Furlong, 1977) and thus might reduce effects due to uptake and metabolism of L-aspartate.) The graphs were constructed from 53 records containing about 6,000 events from 3 cells. The mean bias during a 0.6 second window was calculated and plotted every 0.3 seconds.

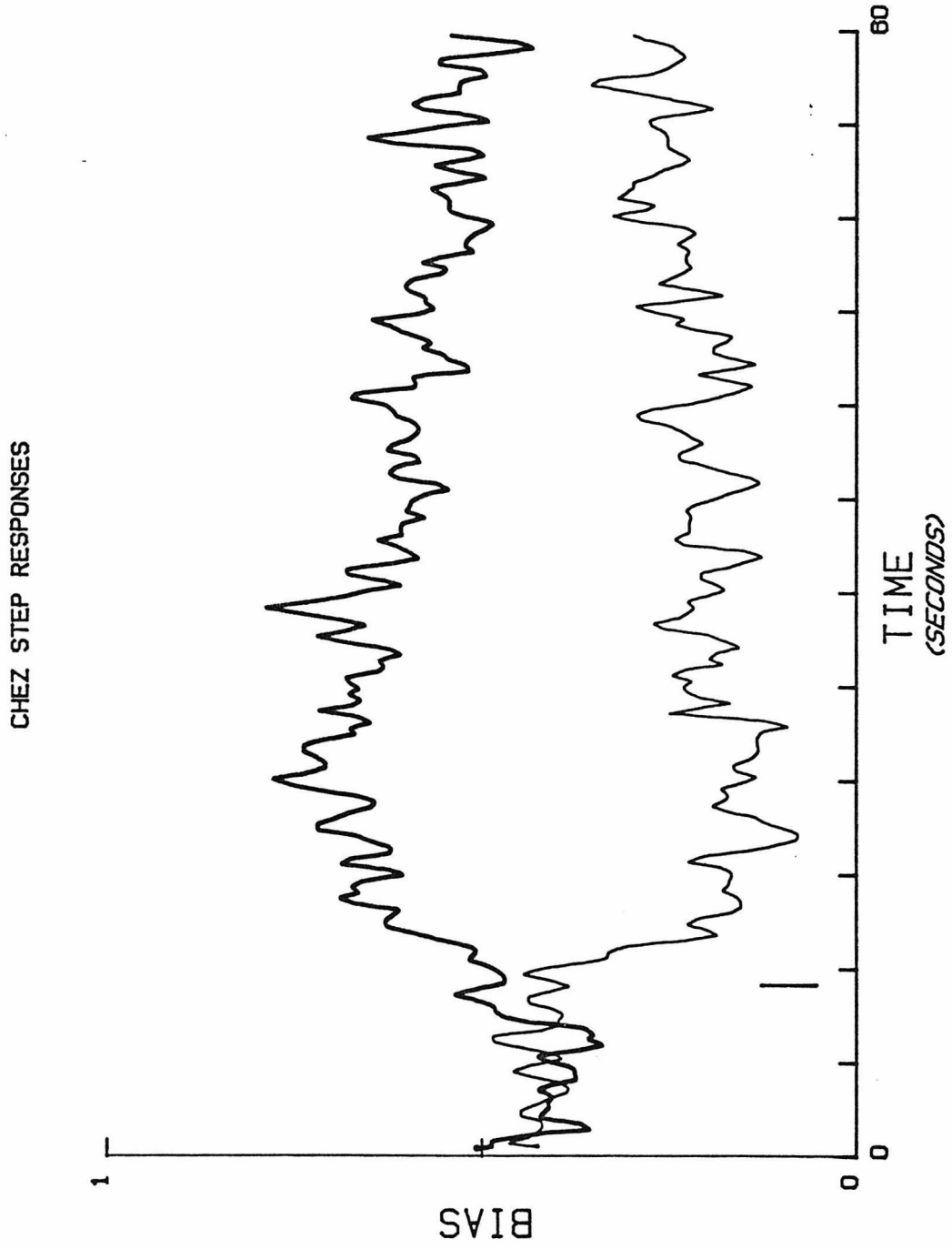
CHEZ STEP RESPONSES
BIAS
1
0
0
60
TIME
(SECONDS)

enough between pulses. The suggestion that *cheZ cheC* double mutants were nonchemotactic because the kinetics of responses were delayed (Segall et al., 1982; Block et al., 1982) is most likely correct.

***CheA* and *cheW* strains.** These strains rotate CCW continuously and do not respond to either nickel or benzoate stimuli. These strains will rotate CW if exposed to 10-50 mM acetate at pH 5.5, but I did not attempt to do this with iontophoresis. This response requires a large change in the internal pH of the cell, and it is unclear what stage of the transduction pathway is affected.

***CheY* and suppressor strains.** Although most *cheY* strains tested were identical in behavior to the cheA and cheW strains, one strain did respond to nickel pulses, with kinetics very similar to the wild-type, although the cells still rotated exclusively CCW if not stimulated. Sandy Parkinson has also sent us some *cheY* strains containing extragenic suppressors in the *cheC* and *cheV* proteins (Parkinson et al., 1983). The strains containing the suppressors have motors with a more normal bias, and a variety of attractant impulse response kinetics. Some seem very similar to wild-type, while others seem intermediate between wild-type and *cheZ* (data not shown).

Chapter IV

COORDINATION OF FLAGELLA ON FILAMENTOUS CELLS OF *ESCHERICHIA COLI*

This paper introduces the techniques that Akira developed for tethering markers to filamentous cells. That task was non-trivial. My contributions dealt mainly with theory, and involved the analysis and interpretation of the data, along with considerations of the voting hypothesis described in the appendix.

JOURNAL OF BACTERIOLOGY, July 1983, p. 228–237
0021-9193/83/070228-10$02.00/0

Vol. 155, No. 1

Coordination of Flagella on Filamentous Cells of *Escherichia coli*

AKIRA ISHIHARA, JEFFREY E. SEGALL, STEVEN M. BLOCK, AND HOWARD C. BERG*
Division of Biology, California Institute of Technology, Pasadena, California 91125

Received 24 February 1983/Accepted 27 April 1983

Video techniques were used to study the coordination of different flagella on single filamentous cells of *Escherichia coli*. Filamentous, nonseptate cells were produced by introducing a cell division mutation into a strain that was polyhook but otherwise wild type for chemotaxis. Markers for its flagellar motors (ordinary polyhook cells that had been fixed with glutaraldehyde) were attached with antihook antibodies. The markers were driven alternately clockwise and counterclockwise, at angular velocities comparable to those observed when wild-type cells are tethered to glass. The directions of rotation of different markers on the same cell were not correlated; reversals of the flagellar motors occurred asynchronously. The bias of the motors (the fraction of time spent spinning counterclockwise) changed with time. Variations in bias were correlated, provided that the motors were within a few micrometers of one another. Thus, although the directions of rotation of flagellar motors are not controlled by a common intracellular signal, their biases are. This signal appears to have a limited range.

Escherichia coli is propelled by about six flagellar filaments arising at random points on the surface of the cell. Each filament is powered by a rotary motor at its base (7, 28). When the motors turn counterclockwise (CCW), the filaments work together in a bundle that drives the cell steadily forward—the cell runs; when the motors turn clockwise (CW), the bundle flies apart, and the motion is highly erratic—the cell tumbles (20, 23). Runs and tumbles occur in an alternating sequence, each run constituting a step in a three-dimensional random walk (8). When the cell swims in a spatial gradient of a chemical attractant, runs up the gradient are extended; this imposes a bias on the random walk that carries the cell in a favorable direction (8, 22). Changes in concentration of attractants are sensed by specific receptors (1). CCW rotation is favored as more attractant is bound (9, 31). The bias of the flagellar motors (the fraction of time spent spinning CCW) increases in proportion to the rate of change of receptor occupancy (11). The nature of the signal that controls the direction of flagellar rotation is not known.

Is this signal a global signal? Do different flagellar motors on the same cell reverse synchronously? This assumption is implicit in a model, developed extensively by Koshland (17–19), in which CCW and CW rotational states are determined according to whether the value of an intracellular response regulator is above or below some critical value. Transitions between states occur in the absence of chemotactic stimulation, because the regulator (or the critical value) is subject to statistical fluctuation.

An alternative hypothesis asserts that the flagellar motors exist as two-state systems, one state generating CCW rotation and the other CW rotation, with transitions between states governed by first-order rate constants (10, 15). These transitions occur spontaneously, with probabilities that depend on the level of the chemotactic signal. The chemotactic signal affects the bias of the motor, not the particular times at which transitions occur. The motors are autonomous; a correlation should exist between the biases of different flagellar motors but not between their directions of rotation.

The experiments described here were designed to determine whether the motors are autonomous. We grew long, filamentous cells and attached inert, asymmetric markers to their flagella. The markers spun alternately CCW and CW. Transitions between CCW and CW modes occurred asynchronously, whereas variations in bias were correlated, as predicted by the two-state model.

This work confirms and extends that of Macnab and Han (21), who observed asynchronous motion of flagellar filaments on cells of *Salmonella typhimurium* of normal size (nonchemotactic mutants with a strong CW bias observed under conditions of reduced proton motive force). They argued that the asynchrony could be explained by a two-state model or by a response regulator mechanism, provided in the

latter case that fluctuations occur locally, i.e., in a different manner at each flagellar motor. However, as shown elsewhere (11), any threshold-crossing mechanism would be expected to generate CCW and CW interval distributions with many long events, whereas the distributions that are observed are exponential and do not show such events. Again, this behavior is predicted by the two-state model (10, 11).

If the flagellar motors are autonomous, how are their filaments able to work synchronously in a bundle? Which sets of motor states are occupied when cells run or tumble? This problem is discussed in an appendix.

MATERIALS AND METHODS

Strains. All strains were derivatives of *E. coli* K-12. Strain AW405 (wild type) was the gift of J. Alder (24); MS778 (*flaI*, no flagellar structures), YK4105 (*flaE*, polyhooks), and YK4106 (*hag*, no flagellar filaments) were gifts of M. Simon (16, 29, 30, 32); and TOE1 (*ftsQ*, normal growth at 30°C but no septa at 42°C) was the gift of K. J. Begg (4). HB174 (chemotactic at 42°C) was a derivative of AW405 picked from the edge of a tryptone swarm plate at 42°C; wild-type cells grown at this temperature have few flagella (2). HB9 (*flaE hag*) and HB162 (*flaE hag ftsQ*) were constructed from AW405 by P1 cotransduction with *his* or *leu*. HB203 (*flaE hag ftsQ*, chemotactic at 42°C) was constructed in a similar manner from HB174.

Reagents and buffers. All solutions were prepared from reagent-grade chemicals and glass-distilled water. Chloramphenicol, lysozyme (egg white, crystallized three times), and cephalexin were purchased from Sigma Chemical Co. Poly-D-lysine (molecular weight, 151,700) and glutaraldehyde (E.M. grade, 8%) were obtained from U.S. Biochemical and Polyscience, respectively. Rabbit anti-hook antibody was prepared against isolated polyhooks and preadsorbed with cells of strain MS778. Tethering buffer was 90 mM NaCl–10 mM KCl–10 mM potassium phosphate (pH 7.0)–0.1 mM EDTA.

Preparation of filamentous cells. Filamentous cells were prepared in three different ways. Strain HB9 was grown at 35°C in tryptone broth (Difco Laboratories) until early exponential phase, cephalexin (a β-lactam antibiotic) was added (50 μg/ml), and the cells were grown at the same temperature for another 2 h (13, 26). Strain HB162 was grown at 33°C in tryptone broth until early-exponential phase and then shifted to 42°C and grown for 30 min. Strain HB203 was grown at 30°C in tryptone broth until early exponential phase and then shifted to 42°C and grown for 1.5 or 2 h. In all cases, chloramphenicol was added (100 μg/ml), and the cultures were held at their final temperatures for another 20 min; this prevented formation of septa when strains carrying the *ftsQ* mutation were cooled to room temperature.

Preparation of spheroplasts. Spheroplasts were prepared from filamentous cells of strain HB162 and HB203 by a method adapted from Onitsuka et al. (25). Cells were washed twice with 50% sucrose (wt/vol) and resuspended in the same solution. Lysozyme and EDTA were added to final concentrations of 0.09 mg/ml and 12 mM, respectively. The suspension was incubated at 37°C for 10 min and diluted 10-fold with Penassay broth (Difco).

Preparation of markers. Strain HB9 was grown at 35°C in tryptone broth. The cells were treated with 0.1% glutaraldehyde for 30 min, washed three times with tethering buffer, and resuspended in the same buffer (about 10^{10} cells per ml).

Tethering. Markers were attached to filamentous cells that were fixed to a cover slip with poly-D-lysine. The cover slip was dipped in poly-D-lysine (0.2 mg/ml) and air dried. It was then sealed at opposite edges to two other cover slips (0.15 mm thick) greased to a glass slide (all with Apiezon L) to form a flow chamber with a volume of about 50 μl. When solutions were added to the chamber, it was held cover slip up, and the eluent was taken up with a piece of filter paper. Otherwise, it was placed upside down on spacers in a wet petri dish. Fifty microliters of culture medium was added, and the filamentous cells were allowed to settle for 20 min. Then, 50 μl of anti-hook antibody (preadsorbed antisera diluted about 1:500 with tethering medium) was added, and the mixture was allowed to stand for 1 h. Next, 30 μl of the marker suspension was added, and the mixture was allowed to stand for 30 min. Finally, the assembly was turned right-side up and placed on the microscope stage for observation.

Data acquisition and analysis. The motion of the markers was recorded on videotape by inverse phase-contrast microscopy with a Nikon Optiphot microscope (Plan 40 BM objective, Photo 8× eyepiece), a Sanyo VC1620X video camera, and a Sanyo VTC7100 cassette recorder. In some experiments, the temperature of the stage and objective were controlled at 22°C with an aluminum block coupled to a water-cooled Peltier element (14a). A digital time display was included in the recording. It was pulsed from black to white once every 45 s as an additional timing signal (see below).

The videotapes were played back at one-quarter speed. An operator scored the directions of rotation of the markers by eye, depressing or releasing a pushbutton that tripped a pen on a strip-chart recorder (11). A photodiode placed on the screen over the time display tripped a second pen when this display changed from black to white. This made it possible for records obtained with different markers to be synchronized and for slippage of the charts that occurred in readings of long records to be corrected. The strip charts were digitized (10), and the data, a list of numbers representing the time of CW-to-CCW and CCW-to-CW transitions, were analyzed with a PDP 11/34 computer. The cumulative error in the timing of events was less than 0.3 s, based on errors arising from operator response time (about 0.1 s) and from slippage of the chart paper while digitizing segments of length 45 s (about 0.2 s).

Pairs of records, designated $x(t)$ and $y(t)$, each of length T, were considered as a function of time and assigned the value +1 whenever the marker spun CCW and −1 whenever it spun CW. The direction correlation function, the time average $\langle x(t)y(t+\tau)\rangle$, provides a measure of interrelation between the rotational sense of the two records at any lag (or lead) time, τ (5). This function was computed by dividing T into equal time intervals, δt (generally 0.2 s), and computing the average:

$$\frac{1}{N}\sum_{k} x(k\delta t)y(k\delta t + \tau) \quad (1)$$

where, for $\tau > 0$, k ranged from 0 to $N = (T - \tau)/\delta t$, and for $\tau < 0$, k ranged from $-\tau/\delta t$ to $T/\delta t$; τ assumed values that were integral multiples of δt. When the two records computed were the same, i.e., when $x(t) = y(t)$, we obtained the direction autocorrelation function, which decays from 1 at zero lag—since $x(t)$ is either +1 or −1, its mean square value is 1—to an asymptotic value at infinite lag equal to the square of the mean value of $x(t)$. When transitions between rotational states occur at random, this decay is exponential, with a time constant equal to the reciprocal of the sum of the rates of transition between the two states. Computation of the direction correlation function enables systematic interrelations between different markers to be detected, even if the two markers do not reverse simultaneously, but do so with a relative lag, and even if reversals are not coupled with very high probability.

The rotational bias of a marker, defined as the fraction of time that it spins CCW, was computed over periods of 20 s. A running average, made in steps of 2 s, provided a smoothed estimate of the bias over the complete record. Bias correlation functions were computed in the same way as direction correlation functions (using δt = 2 s), except that the mean bias for each marker was first subtracted out; i.e., the relative biases $x(t) - \langle x \rangle$ and $y(t) - \langle y \rangle$ were used.

The means and standard deviations in direction or bias correlation expected for a given pair of markers, assuming that they were not cross-correlated, were estimated by using a Monte Carlo method. Thirty pairs of simulated records were constructed by a random-number process that generated exponential distributions of CCW and CW intervals. The mean CCW and CW intervals were chosen to match those measured for the pairs of markers under study. These data were analyzed in the same way as the real data, and standard deviations were estimated from the scatter in the 30 direction or bias correlation functions. To determine the extent to which a bias correlation was statistically significant, a bias correlation ratio was computed by dividing the amplitude of the correlation of the real markers at zero lag by the standard deviation in this quantity obtained from the simulation. A bias correlation ratio of 4.0 or greater indicates a high degree of synchronization near zero lag.

The angular velocities of the markers were measured by playing the video tapes back at one-quarter speed and timing 10 revolutions with a stop watch. This measurement was repeated several times during the course of each experiment.

RESULTS

Markers rotated when on filamentous cells. The markers, cells of strain HB9 fixed with glutaraldehyde, were inert when attached to glass, but they spun when attached to the filamentous cells. Thus, torque was generated by the filamentous cells, not by the markers. To learn whether the markers might contaminate the preparation in some way, we exposed wild-type cells tethered to glass to a suspension of markers at a density of about 10^{10} cells per ml. No changes were observed in the behavior of the tethered cells. The markers were much shorter than the filamentous cells, so there was no problem in distinguishing the two (Fig. 1). The lengths of the filamentous cells used in this study ranged from 20 to more than 120 μm (Table 1, column 2).

The filamentous cells did not adhere strongly to the cover slip; therefore, some markers were free to rotate even when attached to the sides of a cell (Fig. 2). The markers rotated alternately CCW and CW, at angular velocities comparable to those observed when wild-type cells are tethered to glass (Table 1, columns 5, 7, and 8). The CCW intervals tended to be longer than those observed with wild-type cells (9, 11), yielding somewhat higher biases (Table 1, column 6), but the angular velocities fell in a comparable range, with short markers (or short wild-type cells) rotating more rapidly than long markers (or long wild-type cells). As many as three markers were followed on a single cell (Table 1, experiments 7 and 8). The records for the last 134 s of experiment 8 are shown in Fig. 3.

The filamentous cells responded to temperature shifts and to chemotactic stimuli. Adaptation occurred in either case. The markers spun CCW for a time when the cells were heated and CW when they were cooled. They spun CCW when the cells were exposed to aspartate, delivered iontophoretically (27). In many cases, it was difficult to tell whether a marker was attached to the near side or the far side of a filamentous cell. In experiments 8 through 14, thermal responses were used to verify directions of rotation. In experiments 1 through 7, the determination was made by assuming that the bias was greater than 0.5. Errors made in this

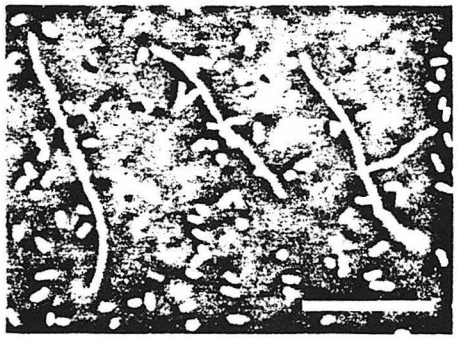

FIG. 1. Filamentous cells of strain HB203 mixed with glutaraldehyde-fixed cells of strain HB9 in the presence of anti-hook antibody. The filamentous cells picked up 0, 2, 1, and 1 markers, respectively (left to right). The plane of focus was near the surface of the cover slip. Most of the markers were attached to the glass. Bar, 20 μm.

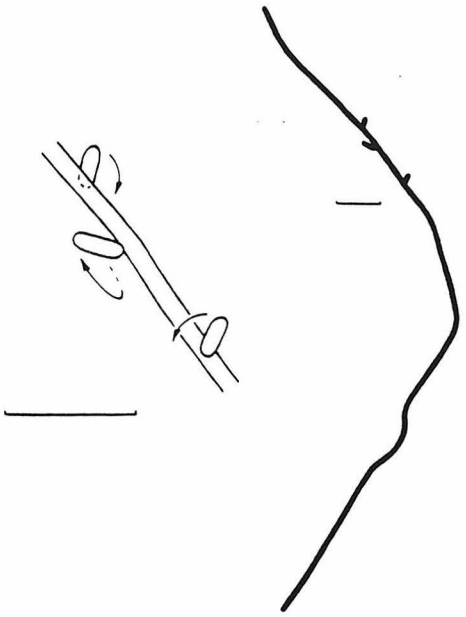

FIG. 2. Tracing from the video screen of a filamentous cell of strain HB203 carrying three markers (Table 1, experiment 8). The markers are shown in the inset (enlarged ×3) at a time when each was rotating CCW. Marker A (top) was on the far side of the filamentous cell, marker B (middle) on the left side, and marker C (bottom) on the near side, between the filamentous cell and the cover slip. Each bar, 5 μm.

way, if any, affect the signs of correlation calculations, not their amplitudes.

Filamentous cells had a single cytoplasmic space. Spheroplasts were prepared from filamentous cells of strains HB162 and HB203. When the cells were grown at 42°C, preparations with long cells gave large spheres, and preparations with short cells gave small spheres. For example, filamentous cells about 40 μm long gave spheres about 4 μm in diameter, and cells about 3 μm long gave spheres about 1 μm in diameter. This indicates that the cytoplasmic space was enclosed by one continuous membrane. When these strains were grown at 35°C, many septa could be seen along the filamentous cells. Spheroplasts of these cells consisted of clusters of small spheres. Thus, the presence of septa could be determined visually. No septa were seen between any of the markers included in this study.

Dramatic evidence for the continuity of the cytoplasmic space was obtained in experiment 8 when the three markers (Fig. 2) slowed down over an interval of about 1.5 s and stopped, coming to rest within about 0.1 s of one another (Fig. 3, arrow). About 1 min later, the markers began to rotate again, starting up slowly and reaching their original speeds after about 1.5 min. They started CCW and continued to spin in this direction for about 20 s after reaching top speed before switching back and forth between the CW and CCW modes. This behavior is consistent with the sudden collapse and gradual restoration of proton motive force that would be expected if a hole were to open up and close in the cytoplasmic membrane. This was a rare event; all of the other markers that we observed rotated continuously.

Motors on the same cell changed directions asynchronously. When records for different markers on the same cell were placed in register, as in Fig. 3, no synchronization was apparent. This was confirmed by computing the direction correlation function, as described above. Figure 4 compares the direction autocorrelation function for marker A of experiment 1 with the direction cross-correlation function for markers A and B. There was no correlation at any lag between any of the pairs of markers in Table 1 greater than that expected by chance, assuming that each motor changed directions at random (allowing for the slow drifts in bias described below).

Biases were not constant. Different motors on the same cell tended to have similar biases (Table 1, column 6), but this also was true for motors on other cells in the same preparation (compare the biases of markers labeled X). Larger differences occurred from preparation to preparation.

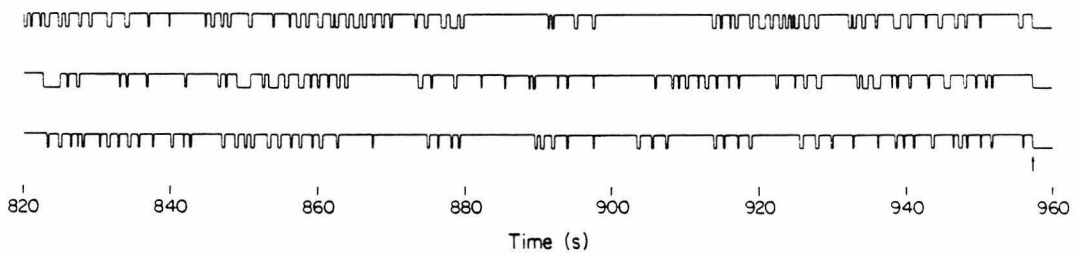

FIG. 3. Strip-chart records for markers A (top), B (middle), and C (bottom) of Fig. 2 (CCW direction, up; CW direction, down) for the last 134 s of experiment 8. The markers stopped within about 0.1 s of one another at the point shown by the arrow.

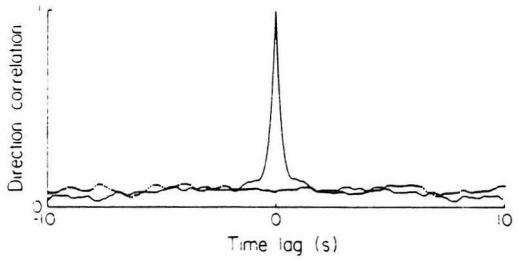

FIG. 4. Direction autocorrelation function for marker A of experiment 1 (solid curve) and the cross-correlation function for markers A and B of experiment 1 (dotted curve), shown for time lags ranging from −10 to +10 s.

Variations in bias of a given motor were examined by computing a running average. These functions fluctuated in a manner expected for averages of two-state systems that change states at random, as shown in the bottom panel of Fig. 5, but in some cases, as shown in the top panel, the variations in bias were larger than expected and occurred over a longer time span. Precise temperature control was introduced in experiments 8 through 14 in an attempt to reduce these variations, but without effect. The variations in bias were not due to changes in proton motive force because the angular velocities of the motors remained constant (15). For example, 50 measurements were made of the angular velocities of each of the markers whose biases

TABLE 1. Properties of the filamentous cells used in this study[a]

Expt. no.	Cell length (μm)	Data length (s)	Marker label[b]	Angular velocity (Hz)	Bias[c]	Mean interval		No. of CCW and CW events	Marker separation (μm)	Bias correlation ratio
						CCW (s)	CW (s)			
1	>80	891	A	3.6	0.59	0.83	0.56	1,283	14	5.6
			B	4.8	0.65	2.12	1.16	544		
2	66	166	A	7.6	0.71	1.38	0.59	168	6	0
			B	6.5	0.77	2.93	0.87	87		
3[d]	95	366	A	4.7	0.75	1.11	0.37	496	6	8.8
			B	6.8	0.70	0.97	0.41	533		
4[d]	20	163	A	7.1	0.75	2.71	0.95	89	6	1.2
			B	ND[e]	0.59	2.19	1.56	87		
5	60	385	A	10.2	0.84	5.24	0.99	123	18	2.6
			B	9.4	0.85	4.50	0.79	145		
6	>120	377	A	3.8	0.83	2.56	0.52	244	5	4.7
			B	4.1	0.84	2.82	0.54	223		
7[f]	34	703	A	2.4	0.67	1.97	0.96	479	5 (AB)	7.1
			B	6.1	0.85	4.01	0.71	297	16 (BC)	2.0
			C	6.8	0.93	5.89	0.44	222	21 (AC)	0.3
8	80	954	A	9.3	0.82	3.88	0.83	405	3 (AB)	7.9
			B	2.8	0.83	3.94	0.81	402	5 (BC)	5.8
			C	7.2	0.90	5.33	0.60	322	8 (AC)	4.3
9	80	207	A	2.8	0.84	2.99	0.58	116	3 (AB)	4.0
			B	8.0	0.88	10.2	1.41	35	25 (BX)	−0.3
			X	1.4	0.93	12.9	0.98	29	23 (AX)	−0.1
10	100	405	A	9.8	0.29	1.05	2.57	224	47	−0.3
			B	4.5	0.09	1.08	11.2	65		
11	45	787	A	ND	0.95	24.3	1.14	62	11 (AB)	1.6
			B	ND	0.91	6.58	0.64	218	4 (BX)	−3.4
			X	ND	0.97	19.1	0.58	78	11 (AX)	−0.5
12	54	278	A	3.7	0.83	7.18	1.49	64	8 (AB)	0.8
			B	3.6	0.83	2.30	0.48	199	8 (BX)	0.1
			X	2.5	0.87	7.35	1.10	65	4 (AX)	−1.7
13	55	252	A	ND	0.41	0.79	1.15	260	30	−2.8
			B	7.6	0.47	1.42	1.58	168		
14	37	474	A	4.0	0.65	2.19	1.17	281	9	0.8
			B	6.9	0.59	1.15	0.79	488		

[a] Cells of strain HB203 grown at 42°C in tryptone broth, except as noted. The experiments were done at room temperature (22°C), with precise temperature control for experiments 8 through 14.

[b] A, B, and C indicate markers on the same cell, and X indicates a marker on a second nearby cell.

[c] The fraction of time spent spinning CCW.

[d] Strain HB162 grown at 42°C in tryptone broth.

[e] ND, Not determined.

[f] Strain HB9 grown at 35°C in tryptone broth in the presence of cephalexin.

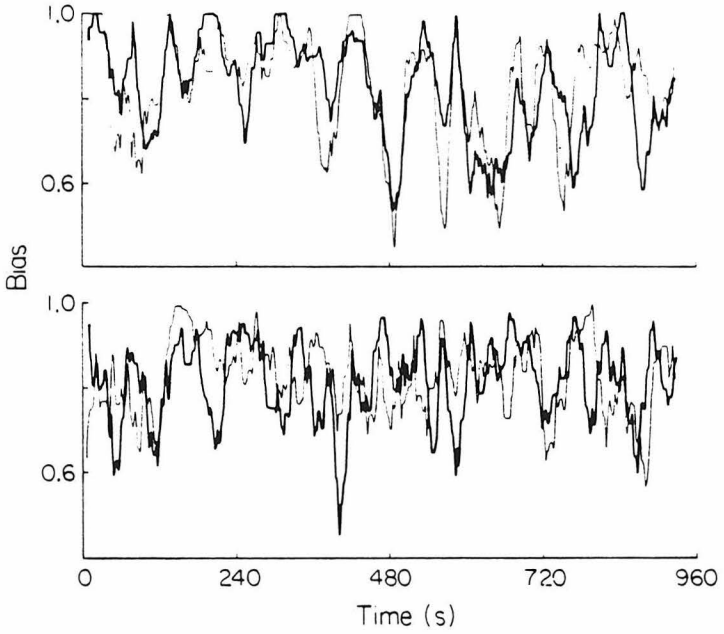

FIG. 5. (Top) Biases of markers A (thick curve) and B (thin curve) of experiment 8. (Bottom) Biases of two simulated markers with the same mean biases as markers A and B.

are shown in the top panel of Fig. 5 over a 130-s interval centered at 480 s, an interval during which the biases varied by as much as 50%. No deflections in angular velocity were apparent (mean ± 1 standard deviation, 9.3 ± 0.7 and 2.8 ± 0.2 Hz, respectively).

Some biases were correlated. Another feature apparent in the data shown in the top panel of Fig. 5 is that the biases of the two motors rose and fell synchronously. This was confirmed by computing the bias correlation function, with the results shown in Fig. 6. The bias correlation ratio, defined above, was 7.9 for experiment 8 (Table 1, last column). This value indicates a high degree of correlation between the biases of the motors at zero lag. A scatter plot of bias correlation ratio as a function of motor separation is shown in Fig. 7. There was a clear correlation for some, but not all, motors separated by 10 μm or less. In experiments 7 and 8, in which three markers were attached to each cell, the correlation decreased with distance. None of the markers on different cells were correlated, even when these markers were close to one another. We conclude that variations in the bias of the flagellar motors can be correlated, provided that the motors are on the same cell and no more than a few micrometers apart.

DISCUSSION

In summary, we attached markers to different flagellar motors on single filamentous cells (Fig. 1 and 2, Table 1). The cells responded to chemical and thermal stimuli. They were fully energized, as judged by speed and direction of flagellar rotation, and they contained a single cytoplasmic space, as judged by the formation of giant spheroplasts and by a fortuitous event in which three adjacent markers stopped synchronously (Fig. 3, arrow). The markers were far enough apart that they did not interact mechanically. We were unable to find any correlation in the directions of rotation of different flagellar motors (e.g., Fig. 4, dotted curve). The biases of the motors shifted with time (e.g., Fig. 5, top

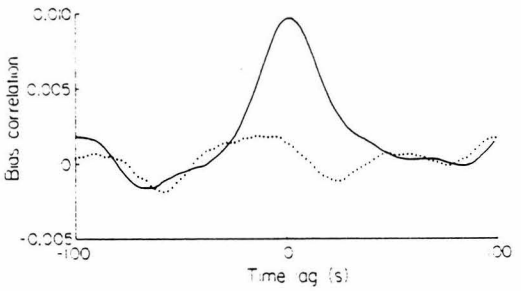

FIG. 6. Bias correlation functions for the data shown in the top and bottom panels of Fig. 5 (solid and dotted curves, respectively) for time lags ranging from −100 to +100 s. The standard deviation in bias correlation expected for uncorrelated markers was ±0.0012 (not shown).

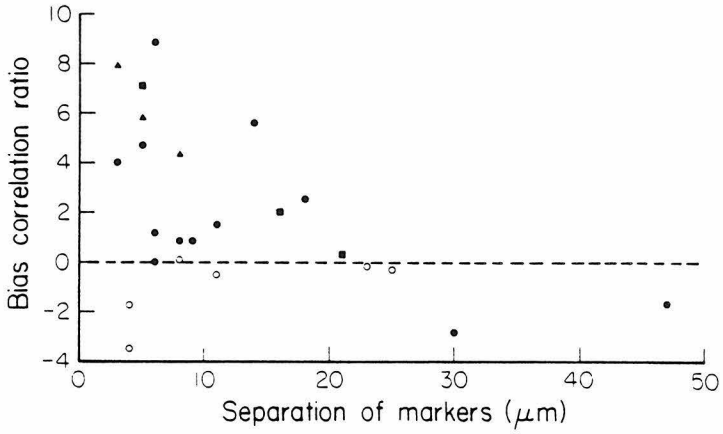

FIG. 7. Bias correlation ratio as a function of marker separation for pairs of markers on the same cell (closed symbols) or on different cells (open symbols). Three markers were observed on the same cell in experiments 7 (■) and 8 (▲).

panel). The biases of different motors tended to shift in synchrony, provided that the motors were on the same cell and within a few micrometers of one another (Fig. 6 and 7).

A global signal does not synchronize flagellar motors. The absence of direction correlation at any lag shows that the times at which flagellar reversals occur are not subject to coordinate control. If such control were exerted either chemically or electrically on motors, say, 3 μm apart (the closest pairs examined), coordination would be expected on time scales of milli- or microseconds, respectively. The time required for a motor to change the direction of rotation of a tethered cell once a reversal is initiated is 10 ms or less (6), so this delay is not important. The possibility that coordination occurs when motors are closer to one another than 3 μm is ruled out by the data of Macnab and Han (21), who observed asynchronous reversals of flagellar filaments on single cells of *S. typhimurium*. However, their experiments are not strictly equivalent to ours, because they used mutants with an extreme CW bias under conditions of reduced proton motive force. This allowed reversals to occur at torques below those that generate polymorphic transitions (23). The motors of their cells frequently stopped, a behavior not observed here. Whether this was due to the reduced proton motive force, to mechanical interactions between different flagellar filaments, or to interactions between these filaments and the glass is not known.

A global signal does control motor bias. Although transitions between CCW and CW states occur at random times, the rates at which these transitions occur are subject to coordinate control. This is shown by the strong bias correlation between some motors on the same cell (as represented by the points in the upper left-hand corner of Fig. 7). The reasons for the changes in bias leading to this correlation are not known. These changes were not due to drifts in external variables, such as temperature, because there was no bias correlation between markers on different cells. Note, in experiments 8 through 14, that the correlation persisted when the temperature was carefully controlled.

This signal has a finite range. The fact that the bias correlation was strongest for motors only a few micrometers apart indicates that the signal has a finite range, long compared to the length of a normal cell but short compared to the length of a filamentous cell. If the signal is electrogenic and the filamentous cell has cable properties similar to those of a nerve axon of the same diameter, then a space constant for potential of several hundred micrometers is expected (3). Thus, an electrogenic signal seems unlikely, but it cannot be ruled out. If the signal is some chemical, then it must be inactivated or removed from the cell. It is not able to equilibrate over distances much larger than about 10 μm in times less than about 1 min, the time scale on which the variations in bias occurred. Note that a small molecule can diffuse 10 μm in water in about 0.1 s.

Flagellar motors function as two-state systems. These results argue for a two-state model (10), in which a motor exists either in a state that generates CCW rotation (runs) or in a state that generates CW rotation (tumbles). Transitions between these states are governed by first-order rate constants, which are the probabilities per unit time that the occupation of a state is terminated. These are the parameters that are subject to global control.

An alternative hypothesis asserts that transitions are generated by threshold crossings of a

signal subject to statistical fluctuation (17–19). The lack of synchronization could be explained in this model if fluctuations were local rather than global (21), especially if they occurred in the threshold rather than in the signal, since the thresholds could be set independently at each motor. However, as shown elsewhere (11), threshold-crossing mechanisms lead to CCW and CW interval distributions with extended tails, i.e., with relatively large numbers of long events. The CCW and CW interval distributions observed experimentally are exponential; they do not show these events (11). Exponential distributions are the hallmark of two-state systems.

We do not know how transitions between rotational states are generated. They could occur through changes in protein conformation, through the binding and unbinding of a ligand at a receptor, or the like. If so, the signal affects the stabilities of alternate conformations, the on and off rate constants, or the like. It does not generate the transitions per se.

Discrepancies between run/tumble and CCW/CW statistics remain unresolved. If the flagellar motors are autonomous, how do their filaments work synchronously in a bundle? In *E. coli* strain AW405, the mean run and tumble lengths are about 1 and 0.1 s, respectively (8), whereas the mean CCW and CW intervals are both about 1 s (9, 11). As discussed in the Appendix, one possibility is that a cell runs when half or more than half of its filaments rotate CCW and tumbles otherwise. However, the fit to the data is not very good. A more elaborate mechanism seems to be required.

APPENDIX

Voting hypothesis. If the motors driving the flagellar filaments reverse independently, and therefore asynchronously, how does a flagellar bundle form to allow a concerted run in one direction? The simplest possibility is that a stable bundle is formed when a certain fraction (e.g., greater than or equal to one-half) of the motors rotate in the CCW direction. Once the bundle is formed, individual filaments whose rotational sense does not coincide with the majority (i.e., those trying to spin CW) are driven against their preferred rotational sense, and the bundle remains stable. When a sufficient number of flagella have, by chance, changed their preferred sense of rotation from CCW to CW (so as to reduce the number CCW below the fixed fraction required for stability), the bundle flies apart, and the cell tumbles. According to this hypothesis, the overall state of the several individual motors determines whether the cell runs or tumbles. This possibility will be referred to as the "voting hypothesis," in that independent flagella vote upon whether the cell is in the run or tumble mode by attempting to turn CCW or CW, respectively. The fraction required for a stable run, i.e. the "rules" for determining what constitutes a majority, remains to be determined. A version of this hypothesis was first advanced by Khan and Macnab (15), who suggested that a tumble might be initiated when more than one flagellum in a bundle tried to reverse. However, their assumption that the system can be treated as if at steady state is not valid, so that the run times that they were led to predict are in error.

Predictions of the voting hypothesis. The voting hypothesis assumes that individual flagella are completely autonomous; each is endowed with a set of switching probabilities for transitions between CCW and CW states. Once these probabilities are known, then it is possible to derive an expression for the length of time during which a number n or more of f flagella are trying to rotate CCW. Such an expression is obtained below; it defines the mean run and tumble times for a cell in terms of the mean CCW and CW intervals of the separate motors.

For wild-type *E. coli*, mean run times are about 1.1 s (0.86 s adjusted upward by the 0.24-s interval required to detect a run; see reference 8, addendum), whereas mean tumble times are about 0.14 s. A swimming cell therefore spends almost 90% of the time running. When tethered, however, individual flagellar filaments spend nearly equal amounts of time rotating in the CCW and CW directions (9). For the wild type, mean CCW times are about 1.20 s, whereas mean CW times are about 1.06 s (11). All of these values were obtained with cells of the same wild-type strain in similar media at the same temperature (strain AW405 in dilute phosphate buffer at 32°C). We assume that cells of *E. coli*, like those of *S. typhimurium* (14), have, on average, about six flagella.

Are these figures consistent with the predictions of the voting hypothesis? The results of computations given in Table 2 and discussed below suggest that they are not; the observed tumble times are too short to be accommodated by the voting hypothesis, given the measured values for mean rotational times. Conversely, given the measured values for run and tumble times, one is led to predict mean CW intervals that are much shorter than those generally seen. Similar results were obtained in computations assuming numbers of flagella ranging from four to nine. The possibility remains that the published values are inconsistent because of the way in which the cells were selected for study, but we view this as unlikely.

In addition, the voting hypothesis would require runs and tumbles to be distributed as sums of several exponential processes, whereas experimental evidence indicates that runs and tumbles are distributed as single exponentials (8), just as are CCW and CW intervals (11). Under certain conditions, sums of exponentials can be difficult to distinguish from pure exponentials, but again we view this possibility as unlikely. Although mean run times have a large biological variability in swimming cells, mean tumble times are remarkably constant (8). On the other hand, both mean CCW and CW intervals show variability in tethered cells. This asymmetry is not easily explained by the voting hypothesis.

The voting hypothesis also predicts that the torque produced by a rotating bundle should vary with time, as the number of flagella asserting CCW rotation within the bundle changes. Under conditions in which torque is limiting, e.g., in a medium of high viscosity, changes in torque will be reflected in changes in angular velocity, so one would expect to see fluctua-

TABLE 2. Predicted run and tumble times for the voting hypothesis[a]

Case	Minimum no. of flagella required to be in CCW mode for a run	Predicted mean run time (s)	Predicted mean tumble time (s)
1[b]	1	16.42	0.18
	2	2.69	0.24
	3	**0.92**	**0.37**
	4	0.46	0.68
	5	0.29	1.74
	6	0.20	8.72
2[c]	1	553.52	0.07
	2	31.55	0.08
	3	4.41	0.11
	4	**1.12**	**0.17**
	5	0.44	0.29
	6	0.23	0.82

[a] The numbers shown in boldface provide the closest match of observed and predicted interval times. The calculations assume six flagella per cell.

[b] In this case, we assume a mean CCW interval of 1.20 s and a mean CW interval of 1.06 s (measured values, see the text).

[c] In this case, we assume a mean CCW interval of 1.4 s and a mean CW interval of 0.4 s (values adjusted to give prediction of times close to the measured values for the mean run and tumble times, see the text).

tions in the speed of swimming cells. Preliminary measurements of the speeds of swimming cells in a medium containing 9.5% Ficoll (4.0 cP) do not show such fluctuations (J. E. Segall, unpublished data). Therefore, it appears unlikely that the voting hypothesis, in the simple form presented here, is correct. More complicated voting rules seem to be required. For example, when a flagellum is outvoted, it might simply change its vote. Mechanical interactions between flagellar filaments, acting through some kind of feedback process, might cause the motor to assert the opposite torque. But tethered cells do not reverse direction when their rotation is suddenly blocked by a micropipette or when they become stuck briefly on the tethering surface (M. D. Manson and S. M. Block, unpublished data). However, this observation does not rule out the possibility of feedback under conditions of less limiting torque. Somehow, tumbles are terminated prematurely. Too little is known at present about the interactions of flagellar filaments to explain the disparity between run/tumble interval times and CCW/CW interval times.

Mathematics of the voting hypothesis. A cell with f flagella can exist in $(f + 1)$ states, ranging from $n = 0$ up to $n = f$ flagella rotating CCW at any instant. Assuming that the rates for CCW-to-CW and for CW-to-CCW transitions are the same for all the flagella and equal to k_r and k_t, respectively, we have the system:

$$[0] \underset{k_r}{\overset{fk_t}{\rightleftharpoons}} [1] \underset{2k_r}{\overset{(f-1)k_t}{\rightleftharpoons}} \cdots \underset{nk_r}{\overset{(f-n-1)k_t}{\rightleftharpoons}} [n] \underset{(n+1)k_r}{\overset{(f-n)k_t}{\rightleftharpoons}}$$

$$[n+1] \underset{(n+2)k_r}{\overset{(f-n+1)k_t}{\rightleftharpoons}} \cdots \underset{fk_r}{\overset{k_t}{\rightleftharpoons}} [f] \qquad (2)$$

where the states represent various numbers of flagella asserting the CCW direction. If the critical number of flagella spinning CCW is n or more, then run times will correspond to the lifetime of the compound state consisting of all individual states greater than or equal to n. The complete system can be solved as a set of $f + 1$ coupled differential equations (an eigenvalue problem); the solution for the compound (run) state, above, will consist of a weighted sum of $f - n + 1$ exponentials, whereas the solution for the companion compound (tumble) state will consist of a weighted sum of n exponentials. The problem can be solved by standard methods (cf. reference 12). However, a simple recursion relationship can be developed to obtain the lifetime of each state by using the theory of the random walk. One obtains for the mean time for passage from the state n to the $n + 1$st state:

$$t_{(n,n+1)} =$$

$$[k_{(n,n-1)}/k_{(n,n+1)}]t_{(n-1,n)} + 1/k_{(n,n+1)} \qquad (3)$$

where the k values are the transition rate constants among the subscripted states. The lifetime of the 0th state is simply $1/k_{(0,1)}$. Lifetimes for other states are obtained by recursion. Experimentally determined mean CCW and CW interval times give the reciprocals for k_r and k_t in equation 2. Using these values, and assuming six flagella per cell, we obtain the results shown in Table 2. If the rules for the voting hypothesis are such that half or more of the flagella are required to assert the CCW direction for a run to occur, we obtain run and tumble times of 0.92 and 0.37 s, respectively (Table 2). Although the run time agrees reasonably well with the observed mean run length of 1.1 s, the tumble time differs by almost a factor of three; 0.37 s is predicted whereas the measured value is 0.14 s. To get values close to the measured run and tumble times, we are forced to assume a mean CCW interval of 1.4 s and a mean CW interval of 0.4 s (Table 2).

Derivation of equation 3. The coupled system in equation 2 can be viewed as a random walk among states, with transition probabilities whose values depend upon the number of the state. We seek a mean time to passage across a boundary between state n and state $n + 1$. Let P_m be the probability that the system moves from state n to state $n - 1$ exactly m times before stepping from n to $n + 1$. Let T be the waiting time in the nth state before a step. T will be given by the reciprocal of the sum of the rate constants leaving the state, i.e., by:

$$T = 1/[k_{(n,n-1)} + k_{(n,n+1)}] \qquad (4)$$

The mean waiting time for a cell in state n to move to the $(n + 1)$st state is given by:

$$t_{(n,n+1)} = \left\{\sum_m mP_m[t_{(n-1,n)} + T]\right\} + T \qquad (5)$$

Let p be the probability of a step from n to $n - 1$. Then:

$$P_m = p^m(1 - p) \quad (6)$$

where $p = k_{(n,n-1)}/[k_{(n,n-1)} + k_{(n,n+1)}]$. Substituting this expression into equation 5 and summing over all m gives:

$$t_{(n,n+1)} = \frac{p}{1 - p}\,[t_{(n-1,n)} + T] + T \quad (7)$$

Further substitution of the expression for p in terms of the rates k gives equation 3. A similar recursion expression can be derived for transitions from a higher to a lower state. All rate constants for transitions to higher states will be multiples of k_r, whereas all rate constants for transitions to lower states will be multiples of k_r, the multiplicity being determined by the number of flagella rotating CCW.

ACKNOWLEDGMENTS

We thank M. P. Conley for help in strain constructions, M. Meister for developing the recursion relation used in the Appendix, and R. M. Macnab and D. P. Han for sending us a preprint of their manuscript.

This work was supported by Public Health Service grant AI16478 from the National Institutes of Health.

LITERATURE CITED

1. **Adler, J.** 1969. Chemoreceptors in bacteria. Science **166**:1588–1597.
2. **Adler, J., and B. Templeton.** 1967. The effect of environmental conditions on the motility of *Escherichia coli*. J. Gen. Microbiol. **46**:175–184.
3. **Aidley, D. J.** 1978. The physiology of excitable cells, 2nd ed, p. 47–53. Cambridge University Press, Cambridge.
4. **Begg, K. J., G. F. Hatfull, and W. D. Donachie.** 1980. Identification of new genes in a cell envelope-cell division gene cluster of *Escherichia coli*: cell division gene *ftsQ*. J. Bacteriol. **144**:435–437.
5. **Bendat, J. S., and A. G. Piersol.** 1971. Random data: measurement and analysis procedures. Wiley-Interscience, New York.
6. **Berg, H. C.** 1976. Does the flagellar rotary motor step?, p. A47–A56. *In* R. Goldman, T. Pollard, and J. Rosenbaum (ed.), Cold Spring Harbor Conferences on Cell Proliferation, vol. 3, cell motility. Cold Spring Harbor Laboratory, Cold Spring Harbor, N.Y.
7. **Berg, H. C., and R. A. Anderson.** 1973. Bacteria swim by rotating their flagellar filaments. Nature (London) **245**:380–382.
8. **Berg, H. C., and D. A. Brown.** 1972. Chemotaxis in *Escherichia coli* analysed by three-dimensional tracking. Nature (London) **239**:500–504. Reprinted with an addendum, 1974, p. 55–78, *In* E. Sorkin (ed.), Antibiotics and chemotherapy, vol. 19, chemotaxis: its biology and biochemistry. S. Karger, Basel.
9. **Berg, H. C., and P. M. Tedesco.** 1975. Transient response to chemotactic stimuli in *Escherichia coli*. Proc. Natl. Acad. Sci. U.S.A. **72**:3235–3239.
10. **Block, S. M., J. E. Segall, and H. C. Berg.** 1982. Impulse responses in bacterial chemotaxis. Cell **31**:215–226.
11. **Block, S. M., J. E. Segall, and H. C. Berg.** 1983. Adaptation kinetics in bacterial chemotaxis. J. Bacteriol. **154**:312–323.
12. **Colquhoun, D., and A. G. Hawkes.** 1977. Relaxation and fluctuations of membrane currents that flow through drug-operated channels. Proc. R. Soc. London Ser. B **199**:231–262.
13. **Greenwood, D., and F. O'Grady.** 1973. Comparison of the responses of *Escherichia coli* and *Proteus mirabilis* to seven β-lactam antibiotics. J. Infect. Dis. **128**:211–222.
14. **Iino, T.** 1974. Assembly of Salmonella flagellin in vitro and in vivo. J. Supramol. Struct. **2**:372–384.

14a. **Khan, S., and H. C. Berg.** 1983. Isotope and thermal effects in chemiosmotic coupling to the flagellar motor of *Streptococcus*. Cell **32**:913–919.

15. **Khan, S., and R. M. Macnab.** 1980. The steady-state counterclockwise/clockwise ratio of bacterial flagellar motors is regulated by protonmotive force. J. Mol. Biol. **138**:563–597.
16. **Komeda, Y., and T. Iino.** 1979. Regulation of expression of the flagellin gene (*hag*) in *Escherichia coli* K-12: analysis of *hag-lac* gene fusions. J. Bacteriol. **139**:721–729.
17. **Koshland, D. E., Jr.** 1977. A response regulator model in a simple sensory system. Science **196**:1055–1063.
18. **Koshland, D. E., Jr.** 1979. A model regulatory system: bacterial chemotaxis. Physiol. Rev. **59**:811–862.
19. **Koshland, D. E., Jr.** 1980. Bacterial chemotaxis as a model behavioral system. Raven Press, New York.
20. **Larsen, S. H., R. W. Reader, E. N. Kort, W.-W. Tso, and J. Adler.** 1974. Change in direction of flagellar rotation is the basis of the chemotactic response in *Escherichia coli*. Nature (London) **249**:74–77.
21. **Macnab, R. M., and D. P. Han.** 1983. Asynchronous switching of flagellar motors on a single bacterial cell. Cell **32**:109–117.
22. **Macnab, R. M., and D. E. Koshland, Jr.** 1972. The gradient-sensing mechanism in bacterial chemotaxis. Proc. Natl. Acad. Sci. U.S.A. **69**:2509–2512.
23. **Macnab, R. M., and M. K. Ornston.** 1977. Normal-to-curly flagellar transitions and their role in bacterial tumbling. Stabilization of an alternative quartenary structure by mechanical force. J. Mol. Biol. **112**:1–30.
24. **Mesibov, R., and J. Adler.** 1972. Chemotaxis toward amino acids in *Escherichia coli*. J. Bacteriol. **112**:315–326.
25. **Onitsuka, M. O., Y. Rikihisa, and H. B. Maruyama.** 1979. Biochemical and topographical studies on *Escherichia coli* cell surface. IV. Giant spheroplast formation from a filamentous cell. J. Bacteriol. **138**:567–574.
26. **Robinson, G. N.** 1980. Effect of β-lactam antibiotics on bacterial cell growth rate. J. Gen. Microbiol. **120**:317–323.
27. **Segall, J. E., M. D. Manson, and H. C. Berg.** 1982. Signal processing times in bacterial chemotaxis. Nature (London) **296**:855–857.
28. **Silverman, M., and M. Simon.** 1974. Flagellar rotation and the mechanism of bacterial motility. Nature (London) **249**:73–74.
29. **Silverman, M., and M. Simon.** 1974. Characterization of *Escherichia coli* flagellar mutants that are insensitive to catabolite repression. J. Bacteriol. **120**:1196–1203.
30. **Silverman, M. R., and M. I. Simon.** 1972. Flagellar assembly mutants in *Escherichia coli*. J. Bacteriol. **112**:986–993.
31. **Spudich, J. L., and D. E. Koshland, Jr.** 1975. Quantitation of the sensory response in bacterial chemotaxis. Proc. Natl. Acad. Sci. U.S.A. **72**:710–713.
32. **Suzuki, T., and Y. Komeda.** 1981. Incomplete flagellar structures in *Escherichia coli* mutants. J. Bacteriol. **145**:1036–1041.

Chapter V

IONTOPHORETIC STUDIES OF CHEMOTACTIC SIGNALING IN FILAMENTOUS CELLS OF *ESCHERICHIA COLI*

The experiments described in this paper were the most difficult that I have done to date. Markers very seldom remained tethered to filamentous cells for as long as was necessary to acquire the data. The bias of the markers fluctuated dramatically, and variation of the size of responses forced us to try to average many responses from each filamentous cell. Akira's patience and willingness to continue to try to make better preparations were an important asset in performing these experiments.

Iontophoretic Studies of Chemotactic Signaling in Filamentous Cells of *Escherichia coli*

Jeffrey E. Segall, Akira Ishihara, and Howard C. Berg*

Division of Biology, California Institute of Technology,
Pasadena, California 91125

Running title: Chemotactic signaling in *Escherichia coli*

*To whom requests for reprints should be sent

Abstract

Video techniques were used to record chemotactic responses of filamentous cells of *Escherichia coli* stimulated iontophoretically with aspartate. Long nonseptate cells were produced from polyhook strains either by introducing a cell division mutation or by growth in the presence of cephalexin. Markers indicating rotation of flagellar motors were attached with anti-hook antibodies. Aspartate was applied by iontophoretic ejection from a micropipette, and the effects on the direction of rotation of the markers were measured. Motors near the pipette responded, while those sufficiently far away did not, even when the pipette was near the cell surface. The response of a given motor decreased as the pipette was moved away, but it did so less steeply when the pipette remained near the cell surface than when it was moved out into the external medium. This shows that there is an internal signal, but its range is short, only a few microns. These experiments rule out signaling by changes in membrane potential, by simple release or binding of a small molecule, or by diffusion of the receptor-attractant complex. A likely candidate for the signal is a protein or ligand that is activated by the receptor and inactivated as it diffuses through the cytoplasm. The range of the signal was found to be substantially longer in a *cheZ* mutant, suggesting that the product of the *cheZ* gene contributes to this inactivation.

Escherichia coli is propelled by about six flagellar filaments that emerge at random points on the surface of the cell. Each filament is powered by a rotary motor at its base (11, 59). When the motors turn counterclockwise (CCW), the filaments work together in a bundle that drives the cell steadily forward--the cell runs; when the motors turn clockwise (CW), the bundle flies apart and the motion is highly erratic--the cell tumbles (38, 40). Runs and tumbles occur in an alternating sequence, each run constituting a step in a three-dimensional random walk (12). When the cell swims in a spatial gradient of a chemical attractant, runs up the gradient are extended; this imposes a bias on the random walk that carries the cell in a favorable direction (12, 39).

Within a few tenths of a second after the addition of a large amount of attractant, the flagella spin exclusively CCW, but the bias (the fraction of time spent spinning CCW) eventually returns to its prestimulus level: the system adapts to the attractant (14, 38, 39, 62). The response and adaptation to a number of attractants, including aspartate, is mediated by proteins that span the cytoplasmic membrane, called transducers or methyl-accepting chemotaxis proteins (for reviews, see 17, 30, 49, 61). The transducer for aspartate, which also contains the receptor binding site, is the product of the *tar* gene (named for *t*axis to *a*spartate and certain *r*epellents). Adaptation to an increase in the concentration of aspartate results from carboxymethylation of a set of glutamyl residues located on a cytoplasmic domain of this molecule. This is catalyzed by a methyltransferase, the product of the *che*R gene. Adaptation to a decrease in the concentration of aspartate results from demethylation of these sites, catalyzed by a methylesterase, the product of the *che*B gene. Evidently, binding of aspartate produces a signal that changes the rotational bias of the flagellar motors, and methylation shuts off this signal. Strains deleted for the *che*R and/or the *che*B genes respond to aspartate, but they do not adapt (28, 51, 66);

their biases can be set at will by addition of suitable concentrations of attractants and/or repellents (32). The response to the sudden addition of aspartate is markedly delayed in strains carrying mutations in the *cheZ* gene (16, 57), but the reasons for this have not been determined. However, there is evidence that both the *cheY* and *cheZ* gene products interact with other components of the chemotaxis system (52).

The nature of the signal that couples the transducers to the flagella is not known. However, it is clear that signaling does not require metabolism of the attractant (1, 43), protein synthesis (5, 7), or growth (2). Signals that have been proposed include membrane potential (63), free calcium ion (45), cyclic GMP (15), and transmembrane ion fluxes (24, 37, 63). Several studies have shown that membrane potentials are not likely to be involved in signaling in *E. coli* (e.g., 44, 60), although this mechanism remains viable for some longer bacteria, e.g., spirochetes (26, 27).

In order to learn more about the properties of the signal that couples the transducers to the flagella, and in particular its range, we combined techniques for iontophoretic stimulation (16, 57) with those for attaching markers to the flagellar motors of long filamentous cells (33). Markers (ordinary polyhook cells fixed with glutaraldehyde) were attached with anti-hook antibodies to the polyhooks of filamentous cells, so that the direction of rotation of their flagellar motors could be followed by phase-contrast microscopy. The filamentous cells have a single cytoplasmic space (33): any signal linking the receptors to the flagella should be free to travel internally from one end of the cell to the other. Iontophoretic ejection of a charged attractant, such as aspartate, from a micropipette produces a localized increase in concentration. We applied stimuli of this kind at various points in the vicinity of filamentous cells and measured the responses of their marked flagella.

Our results show that an internal signal exists, but that it has a short range. The range in a mutant deleted for *che*R and *che*B was about 2 μm, while the range in a *che*Z mutant was longer, about 6 μm. These results suggest that signaling is mediated by a substance generated at the transducers and destroyed in the cytoplasm, a substance that reaches the flagellar motors by diffusion.

MATERIALS AND METHODS

Strains. All strains were derivatives of *E. coli* K-12. AW405 (wild type; 6) was the gift of J. Adler. RP2867 (deleted for *che*R and *che*B; 50), RP5007 (*cheZ* 293; 47), and RP5099 (Tn10 insertion near *eda*) were gifts of J. S. Parkinson. HB9 (*fla*E *hag*) and HB203 (*fla*E *hag fts*Q, chemotactic at 42°) were described previously (33). The latter strain was reported as *fla*E *hag*, but subsequent complementation tests suggest that it is either *hag* and not *fla*E or that the *fla*E phenotype is suppressed by the mutation(s) allowing chemotaxis at 42°C. HB238 (*che*R *che*B *fla*E *hag*), HB241 (*che*R *che*B *fla*E), and HB254 (*cheZ fla*E *hag*) were constructed from HB9 by P1 transduction with *eda*. A tetracycline-resistant *eda*$^-$ clone was picked after infection of HB9 with P1 phage grown on RP5099, and *eda*$^+$ transductants were selected following infection with P1 grown on RP2867 or RP5007, respectively. The strains are listed in Table 1.

Reagents and buffers. All solutions were prepared from reagent-grade chemicals and glass distilled water. Reagents were obtained as described previously (16, 33). Motility medium contained 90 mM NaCl, 10 mM KCl, 10 mM Tris-Cl (pH 7.0), 10 mM sodium lactate, 0.1 mM tetraethylpentamine (tetren; 54) and 0.001 mM L-methionine.

Preparation of marked filamentous cells. Strain HB203 was grown in tryptone broth (Difco) at 30°C until early exponential phase, then shifted to 42°C for an additional 1 or 2 h. Chloramphenicol (100 μg/ml) was added to prevent formation of septa on cooling; this concentration was maintained throughout the course of an experiment. Strains HB9, HB238, HB241, and HB254 were grown on tryptone broth at 35°C until early exponential phase, cephalexin (50 μl/ml) was added, and growth was continued at 35°C for 1 or 2 h. This concentration of cephalexin or chloramphenicol (100 μg/ml) was maintained throughout the course of an experiment. Markers were prepared from cells of

strain HB9 and attached to the filamentous cells, as described previously (33), except that open coverslips were used instead of flow chambers, and filamentous cells attached to coverslips were rinsed with motility medium prior to the addition of anti-hook antibody. The final preparation was covered with a drop of motility medium of volume about 0.2 ml.

Data acquisition. The cells were viewed by phase contrast through a 40X water immersion objective (Zeiss) mounted on a Nikon S-Ke microscope. The experiments were done at room temperature (22°C). Iontophoretic pipettes were filled with motility medium containing 0.01 mM thorium chloride and either L-asparate or nickel chloride, as described previously (57). Pipette resistances were 15-60 megohms. A current-injection circuit (21) was used to pass current (-1 to -200 nA for aspartate and +3 to +50 nA for nickel) through the pipettes via AgCl coated Ag wires. Pipettes were positioned with a micromanipulator (Narishige MO-103).

The motion of the markers was recorded on videotape with a vidicon camera (Ikegami ITC-47) and a VHS recorder (Panasonic NV 8590) and displayed on a 9-inch monitor (Hitachi VM-910U). The overall magnification at the monitor was about 4000x. Calibration of the micromanipulator was checked by comparing recordings of the tip of the pipette as it was moved from position to position against the recording of an objective micrometer. The micromanipulator was used, in turn, to verify the magnification for each experiment: a recording was made of the tip of the pipette as it was displaced 10 μm. A digital time display was included in the recording that pulsed from black to white whenever the pipette current was turned on or off. Digital records of the direction of rotation of the markers were obtained from the video recordings, as described previously (33).

Concentration changes near filamentous cells. In searching for an internal chemotactic signal by comparing responses to step stimuli applied near the cell body or far away, it is essential to know that the concentration of attractant near the cell is not perturbed strongly by the presence of the cell, in particular, that it is not elevated by reflection of molecules from the cell body. Naively, one would expect the molecules to be absorbed rather than reflected, but to be absolutely certain, we determined the magnitude of the effect of reflection by appeal to an electrical analogue. The equation determining concentrations during steady-state diffusion (the Laplace equation) is the same as the equation determining electrical potentials in charge-free (electrically neutral) space, e.g., in solution of an electrolyte. With diffusion, the concentration at the tip of the pipette is constant, the concentration far away is zero, and gradients in concentration vanish normal to reflecting boundaries. With electrical currents, the potential at a point electrode is constant, the potential far away is zero, and gradients in potential vanish normal to insulating boundaries. Therefore, in a problem involving steady-state diffusion, one can determine concentrations by arranging suitable electrodes in a solution of an electrolyte, injecting current, and measuring electrical potentials. Measurements of this kind, described in detail below, showed that perturbations due to reflection were quite small.

A circular glass dish (12.5 cm in diameter, 6.5 cm deep) was filled with 0.1 M NaCl. To simulate a semi-infinite container, Ag/AgCl wire loops were placed near the side and top boundaries of this solution. Current was injected in the body of the solution from a 0.05 to 0.1 cm bead of AgCl at the tip of an insulated Ag wire and collected by the loops. A similar bead electrode was used to measure the potentials. To avoid artifacts due to buildup of ions at the AgCl/water interface, alternating currents were used (17 Hz). The resistance of the system was constant at about 40,000 ohms for frequencies between 10 and

1000 Hz. Potentials measured by the sensing electrode (input resistance 1 megohm) were recorded with an accuracy of about 1% on the 0.1-volt scale of a strip-chart recorder running at 12.5 cm/min. All measurements were made near the bottom surface of the dish, since filamentous cells are attached to an analogous boundary. As expected, the potential varied inversely with the distance from the current injecting electrode (10). The effect of a non-absorbing filamentous cell was modelled with a glass rod (0.3 cm diameter). The diameter of the rod provided the scale on which comparisons could be made; for example, when the current injecting electrode was one diameter from the rod, the situation modelled was that in which the tip of the pipette was one cell diameter from the surface of the filamentous cell. The potential-sensing electrode was placed at various points on the glass rod to measure the potential corresponding to the concentration near the surface of the cell. For each configuration of rod and electrodes, the potential was measured with the rod in place, and then the rod was removed without moving the electrodes, and the potential was measured again. This provided an estimate of the relative change in potential due to the presence of the rod, or analogously, the relative change in concentration due to the presence of a reflecting filamentous cell. For the configurations used to determine differences in response for stimuli applied close to the cell body or far away (Table 2), we found that the presence of the cell had less than a 2% effect on the difference in concentration of attractant or repellent expected at the marked flagellar motor.

RESULTS

General properties of filamentous cells. We began with strains carrying *fla*E *hag* mutations in order to produce filamentous cells with polyhooks but without flagellar filaments. Our hope was that these cells would be nonmotile but would have appendages to which glutaraldehyde-fixed polyhook markers could readily be attached. We introduced a temperature sensitive mutation in septation, *fts*Q (8), and produced filaments by growing the cells at 42°C. Although we used these cells for measurements of impulse responses (see below), their rotational biases proved to be highly variable and the yield of spinning markers was low. Therefore, we produced filaments by growing *fla*E *hag* cells at 35°C in the presence of the β-lactam antibiotic cephalexin (29, 55). Compared to cells of normal size (Table 1), these filamentous cells tended to have higher CCW biases and lower sensitivities to aspartate (as judged by the size of the stimulus required to produce a response). Relatively late in the course of this work we found that cells which were *fla*E rather than *fla*E *hag* had normal biases and sensitivities. Markers could be attached to these cells, even though some of their polyhooks presumably carried flagellar filament stubs (58). Experiments were done on both *fla*E *hag che*RB and *fla*E *che*RB cells (Table 1); similar results were obtained in either case (see below).

Impulse responses and transition times of strains wild-type for chemotaxis. The peak concentration for a diffusive wave of an attractant or repellent generated by a short iontophoretic pulse is inversely proportional to r^3, where r is the distance from the tip of the pipette (10). Thus, only receptors close to the pipette are strongly affected. Impulse responses (16) obtained when the tip of the pipette was near the surface of the cell but either close to a marker or far away were compared, as illustrated in Fig. 1A. The results are given in Fig. 2A. The positive lobe of the impulse response obtained when the

pipette was close to a marker was about 50% wider than normal, and the negative lobe appeared relatively shallow and prolonged (compare with Fig. 2B). The impulse response obtained when the pipette was 27 μm or farther from the marker was barely discernible. Responses of intermediate size could be obtained when the pipette was closer to the marker than this, but similar responses were observed when the pipette was moved out from the cell surface (data not shown); evidently, these responses arose primarily from changes in concentration of aspartate near the marker in the external medium.

We also measured transition times (the time between the onset of a large stimulus and the first reversal) for adaptation to step stimuli delivered iontophoretically (57). When an iontophoretic pipette is switched on, the concentration of attractant or repellent a distance r away approaches its steady-state value in a time of order $t = r^2/6D$, where D is the diffusion coefficient of the chemical (10); for $r = 10$ μm and $D = 10^{-6}$ cm^2/sec, this time is relatively short, 0.2 sec. The steady-state concentration is inversely proportional to r (not r^3), so receptors are strongly affected over a longer range. The transition time decreased as the pipette was moved along the surface of a filamentous cell (strain HB203) 15 to 35 microns from a marker, as illustrated in Fig. 1B. Near the lower end of this range, similar transition times were obtained when the pipette was moved out from the cell surface (data not shown). A similar distance dependence was observed with the repellent Ni^{++} (with strain HB9). These experiments show that *E. coli* does not have a long-range chemotactic signaling system.

Changes in rotational biases of strains defective in adaptation. Accurate determination of the chemotactic impulse response requires the use of as many as 100 repetitive stimuli (16), and preparations of marked filamentous cells were too fragile to make work on this scale very practical. Therefore, we used an

alternative approach: measurements of changes in bias generated by small step stimuli, using mutants defective in adaptation (e.g., *che*R *che*B mutants, that fail to adapt at all, or *che*Z mutants that adapt slowly; 16). We established, first, that there is an internal chemotactic signal, and then we determined its range.

A small step change in the concentration of asparate applied near the marker of a *che*RB filamentous cell (*fla*E or *fla*E *hag*) generated a step change in bias that persisted for the longest step tested (60 sec), while the bias of a *che*Z filamentous cell returned about one-fourth of the way to its prestimulus level in a similar period of time. Shifts in bias to small step changes in concentration applied either on the cell or off the cell at about the same distance from a marker at the end of the cell were compared, as illustrated in Fig. 1C. Examples of the response are shown in Fig. 3, and the results are summarized in Table 2. In every case, responses were larger with the pipette on the cell than off the cell, by as much as 100% (Table 2, last column). This was true even when the pipette was farther from the marker when on the cell than when off the cell (Table 2, cells 1, 4, 5, 8, 9/first pair, 10). As discussed at the end of **MATERIALS AND METHODS**, given equal pipette-to-marker distances, reflection of aspartate from the cell body would raise the concentration of aspartate at the marker when the pipette was on the cell relative to the value expected when the pipette was off the cell by no more than 2%. This effect is more than offset by the difference in displacement of the pipettes, which, through the inverse dependence of steady-state concentration on distance, gives rise to larger changes in concentration. In any event, since aspartate is taken up and metabolized under chemotaxis conditions (43), the cells probably lower rather than raise the concentration of asparate at the marker. Why, then, should the response be larger with the pipette on the cell than off the cell? When the pipette is on the cell, more receptors in regions away from the marker bind

attractant than when the pipette is off the cell. Evidently, these extra receptors contribute to the change in bias of the flagellar motor at the end of the cell. Therefore, *E. coli* must have a short-range signaling system.

Accurate determination of the range of this system proved more difficult. The ideal experiment, illustrated in Fig. 1D, would be one in which comparisons were made of responses with the pipette on or off the cell for a series of different pipette-to-marker distances. In practice, this could not always be done because of variations in response from stimulus to stimulus, shifts in prestimulus bias, and episodes in which markers stopped spinning or fell off. Therefore, we combined data from all cells in which stimuli were given at more than one position on the cell body.

In order to interpret the effect of small concentration changes on responses, we measured the dose response curves of *che*RB and *che*Z filamentous cells. One type of measurement was made by placing the pipette near a marker on a filamentous cell and recording the responses to currents of different amplitude. From earlier studies of transition times of tethered wild-type cells (J.E.S., unpublished), we know that the change in concentration varies linearly with current, particularly for currents less than 20 nA. The other type of measurement was made on markers at the end of a filamentous cell by fixing the amplitude of the stimulus current and moving the pipette to different points off the end of the cell. The *che*RB filamentous cells had a dose response curve with a clear threshold (Fig. 4A). This probably accounts for the relatively low sensitivity of *che*RB strains to attractant stimuli (Table 1; 16). The *che*Z filamentous cells, on the other hand, had a dose response curve that was reasonably linear (Fig. 4B). These cells were more sensitive to attractant stimuli than *che*RB cells (Table 1).

The decay of the internal signal with distance was measured by comparing the sizes of the responses produced to identical step stimuli when the tip of the pipette was placed near the surface of a cell at different distances from the marker, as illustrated in Fig. 1B and 1D (both with small step stimulation). The stimuli were small enough that the response was not saturated at the point of closest approach. The responses of *che*RB filamentous cells decayed very rapidly with distance (Fig. 5A). When the effects of the nonlinear dose response curve were included, the response was found to decay roughly as expected for a space constant of 2 μm (thick curve; see below). The response of *che*Z filamentous cells decayed more slowly with distance (Fig. 5B), roughly as expected for a space constant of 6 μm (thick curve; see below).

DISCUSSION

Our principal findings from iontophoretic stimulation of filamentous cells (Fig. 1) are as follows. (1) *E. coli* does not have a long range chemotactic signaling system. Pulse stimuli applied within a few microns of the cell surface about 30 μm away from a flagellar motor did not affect its rotational bias (Fig. 2). (2) *E. coli* does have a short range chemotactic signaling system. Step stimuli applied within about 10 μm of a flagellar motor at the end of a cell were more effective when applied near the cell surface than off the end of the cell (Fig. 3, Table 2). (3) The range of this signal is substantially smaller with *che*RB cells than with *che*Z cells (Fig. 5). These findings are consistent with our earlier observations that correlations in bias fluctuations of motors on the same cell have a range of at most a few microns (33). They suggest that these fluctuations are, in fact, due to variations in strength of a chemotactic signal.

Nature of the chemotactic signal. Our results rule out signaling by changes in membrane potential. Such changes have a long range which can be estimated from the specific resistances of the cell membrane and cytoplasm (4). The specific resistance of the cytoplasmic membrane of *E. coli* is at least 2000 ohm-cm^2 (25). The specific resistance of the cytoplasm of *E. coli* is not known, but that for the squid giant axon is about 60 ohm-cm (4). The space constant (the distance over which changes in membrane potential decrease by 1/e) for a cell 0.5 μm in diameter having these specific resistances is 205 μm. If the specific resistance of the cytoplasm were actually 10 times larger, the space constant would still be 65 μm, much greater than the range that we have observed for the chemotaxis signal. This does not contradict the observation that changes in membrane potential affect the flagellar motors of *E. coli* (35, 44) or rule out the possibility that such changes are used for signaling in other species, such as *Spirochaeta aurantia* (25, 26) or *Spirillum volutans* (36).

However, chemotactic responses of *E. coli* to aspartate are not mediated by any such long range signaling system.

Simple release or binding of a small molecule (such as Ca^{++}) when attractant is bound to receptor also is unlikely as a signaling mechanism. With such a mechanism, the signal would simply diffuse away from the point of release: the initial change in bias of nearby markers would decline, and the bias of distant markers would increase. This was not observed when *che*RB filamentous cells were given step stimuli lasting 30 s; the biases of markers about 4 μm from the pipette shifted rapidly and remained high for this period, while the biases of markers 7 μm away remained low. Since a molecule of diffusion coefficient D can diffuse in one dimension a mean-square distance x^2 in time $t = x^2/2D$, a signal molecule of this kind would remain localized within 3 μm for 30 s only if its diffusion coefficient were smaller than about $D = 1.5 \times 10^{-9}$ cm^2/sec. This is several hundred times smaller than the diffusion coefficient of, say, Ca^{++} in axoplasm (31).

To account for the kind of decay shown in Fig. 5 (or found for the bias correlation ratio described earlier, 33) the signal must be inactivated as it moves away from its point of origin, either by conversion to some inert form or by transport out of the cell. The smaller the signal's diffusion coefficient and the higher its rate of inactivation, the shorter the range. A model for diffusion with decay is discussed in the Appendix. The decay length of such a signal (the range for an e-fold diminution) is the square root of the ratio of the diffusion coefficient and the inactivation rate constant (or of the product of the diffusion coefficient and the signal decay time).

These considerations allow us to rule out signaling by diffusion of the receptor-attractant complex. The decay time of the receptor-aspartate complex can be estimated from its dissociation constant (6 μM for *Salmonella*

typhimurium, which has the same sensitivity to aspartate as *E. coli*; 19) and from the on rate constant, which for small ligands is typically in the range 10^7 to 10^8 $M^{-1}s^{-1}$ (18). This gives an off rate constant for aspartate of 60 to 600 sec^{-1}, or a decay time of the complex of about 20 to 2 ms, respectively. Maximum values of diffusion coefficients of membrane proteins are about 10^{-8} cm^2/s (42), yielding a decay length of 0.13 μm or less. This is much smaller than the range that we observed with *che*Z cells. In addition, there is no evidence in *E. coli* that transducers are this closely associated with the flagellar motors (23).

As noted in the Introduction, it is generally agreed that binding of attractant to transducers changes the level of a signal that affects the rotational bias of the flagellar motors, and that methylation of transducers returns this level to its prestimulus value (17, 30, 49, 56, 61). We favor an hypothesis in which the signal is a molecule that diffuses through the cytoplasm and raises the CW bias of the motor. If inactivation of this molecule were enhanced by the *che*Z gene product, a possibility suggested by P. Engstrom (22), then *che*Z cells would have responses with slower kinetics than wild-type (or *che*RB) cells, as observed in measurements of response latencies and impulse responses (16, 57; compare the rise and fall times of the *che*Z and *che*RB step responses shown in Fig. 3). This also would explain why the signal has a longer range in the *che*Z cells: the decay time is about 10 times longer in *che*Z cells than in wild-type cells, so the decay length should be 10 times as long, which is roughly the factor that we observed. According to this model, *che*Z mutants have a strong CW bias because they have a higher concentration of signal: the signal shifts the bias CW. Since strains lacking transducers are CCW biased (53), the transducers appear to be involved in the synthesis of the signal. Furthermore, since addition of attractant shifts the bias CCW, generation of the signal must be depressed

when the transducer binds attractant. Methylation then returns the activity of the signal-generation site to its initial value.

An estimate of the diffusion coefficient of the signal can be made from measurements of signal decay times (3 s in *cheZ* cells, as deduced from measurements of step response kinetics) and decay lengths (about 6μm in *cheZ* cells, Fig. 5B), which give $D \approx 10^{-7}$ cm^2/s. An estimate of the size of the signal molecule can be made given the viscosity of the cytoplasm. Estimates of this parameter for *E. coli* range from 5 to more than 10 times the viscosity of water (J. E. Tanner, 64, and private communication; 34), implying a diffusion coefficient for the signal molecule in water of 5×10^{-7} to 10^{-6} cm^2/s. This range of diffusion coefficients corresponds roughly to those for globular proteins in the molecular weight range 80,000 to 10,000 daltons (18). Unfortunately, this estimate of molecular weight is very sensitive to the size of the diffusion coefficient. There is enough uncertainty in the above analysis, including the measurements of cytoplasmic viscosity, that we cannot rule out the possibility that the signal is a small molecule, perhaps one that binds to larger molecules in the cytoplasm or on the cell membrane, and thus, undergoes buffered diffusion. If the signal is a protein that is reversibly modified, an obvious candidate would be one or more of the chemotaxis-related gene products for which there is no known function, such as *cheA* (68,000 daltons), *cheW* (15,000 daltons) or *cheY* (11,000 daltons; 48). The suggestion that a complex of the *cheB* and *cheZ* proteins is the signal (46) is unlikely to be correct (J. S. Parkinson, private communication), since *cheRB* deletion strains still respond to attractants. Strains carrying defects in the *cheA*, *cheW* or *cheY* genes are extremely CCW-biased, as would be expected if one of the missing gene products were a signal that decreases the CCW bias (46). Since the *cheY* gene is in the same operon as

the tar, tap *che*R, *che*B and *che*Z genes and is expressed at a higher level (20), it is currently the strongest candidate for such a signal.

We note, finally, that a signaling system with a short range is quite reasonable for *E. coli*, which is normally less than 3 μm long. It is more important for such a cell to be able to respond quickly (to have a signal with a short decay time) than to signal over a long range (to have a signal with a long decay length). On the other hand, by using a signal that can diffuse a few microns before being inactivated, the cell can both couple inputs from receptors of the same kind, improving the precision with which it measures concentrations (13), and integrate inputs from receptors of different kinds (3, 14, 65).

APPENDIX

Signaling by diffusion with decay. This model assumes that an internal chemotactic signal is generated by the transducers at a rate that varies with the local external attractant concentration and decays throughout the cell at a rate proportional to the signal concentration. A filamentous cell is modeled as a linear structure that does not change the concentration of attractant in its neighborhood. The time-independent diffusion equation for this model is

$$Dd^2S/dx^2 - k_dS = k_p(A), \qquad (1)$$

where D is the diffusion coefficient of the signal molecule, S is its concentration, x is the position along the filamentous cell, k_d is the first order rate constant for inactivation of the signal molecule, and k_p is the rate constant for its production, which depends on the attractant concentration, A. Note that both S and A are functions of x. Eq. (1) implies that the concentration of signal molecules produced at one point in the cell decays as $\exp(-x/(D/k_d)^{1/2})$, where x is the distance from that point. The decay length is $(D/k_d)^{1/2}$. To calculate the total concentration of S at a particular point in the cell, one sums the contributions from all the points at which S is produced, taking into account the boundary conditions at the ends of the cell, i.e., the Green's function for Eq. (1) is determined, multiplied by k_p, and then integrated over the length of the cell (41).

The problem then reduces to determining the dependence of flagellar bias on S and of k_p on A. The best that can be done at this stage is to use the dose response curves shown in Fig. 4. Since the dose response curve for *cheZ* filamentous cells is reasonably linear, this procedure is likely to be valid for these cells. In these experiments, A is much smaller than the dissociation constant of the receptor, so the rate of production of S is proportional to A under the assumption that k_p depends linearly on the fraction of receptor

occupied. We assume, as well, that the change in bias depends linearly on S. For the *che*RB cells, we assume that the threshold occurs in the dependence of k_p on A, not in the dependence of bias on S--the result is about the same if the threshold is assumed to occur in the dependence of bias on S. The thick curves shown in Fig. 5 were computed from the model with these assumptions.

One assumption made in formulating this model is that the rate of production of S is independent of S. This is reasonable if S is a small molecule that is synthesized *de novo*, but it might not be correct if S is a protein that is cycled between a signaling and an inactivated state. The only alteration to Eq. (1) would be the addition to k_d of a term dependent on A, so that k_d would no longer be constant. Such an alteration would increase the rate of destruction of S and shorten the signaling space constant, and thus strengthen our argument against the membrane receptor serving as the signal.

ACKNOWLEDGMENTS

J. E. S. and A. I. contributed equally to the work presented here. We thank J. S. Parkinson for gifts of strains, phage, and for useful suggestions regarding strain constructions, M. Meister for suggesting the use of the electrical analogue for steady-state diffusion, and S. M. Block for comments on the manuscript. This work was supported by Public Health Service grant AI16478 from the National Institute of Allergy and Infectious Diseases. J. E. S. acknowledges support as a National Science Foundation predoctoral fellow during the early phase of this work.

TABLE 1. Behavioral properties of strains used in this study

Cell size	Strain	Genotype	Marker yield	Prestimulus bias[a]	Sensitivity to aspartate
Normal:					
	AW405	wild type		CW≈CCW	high
	HB9	*flaE hag*		CCW	high
	RP2867	*cheRB*$^{\Delta}$		CW to CW≈CCW	low
	RP5007	*cheZ*		CW	high
Filamentous[b]:					
	HB9	*flaE hag*	high	CCW[c]	N.D.[d]
	HB203	*flaE hag ftsQ*	low	CCW[e]	high
	HB238	*flaE hag cheRB*$^{\Delta}$	high	CCW	low[f]
	HB241	*flaE cheRB*$^{\Delta}$	high	CW≈CCW	low[g]
	HB254	*flaE hag cheZ*	high	CW≈CCW	high

[a]CW≈CCW roughly 50% CCW, CCW more than 75% CCW, CW less than 25% CCW.

[b]Strain HB203 by growth at 42°C; other strains by growth in the presence of cephalexin.

[c]Nearly 100% CCW.

[d]Not determined.

[e]Sometimes CCW, sometimes CW, depending on the preparation.

[f]Somewhat lower than strain RP2867.

[g]Somewhat higher than strain RP2867.

TABLE 2. Changes in rotational bias of motors at the ends of filamentous cells in response to step stimuli of aspartate applied on or off the cell

Cell[a] no.	Conc. in pipette (mM)	Step amplitude (nA)	Step duration (s)	Pipette[b] position	Distance to marker (μm)	Number of trials	Response[c] mean	Response[c] std. error	Difference[d] on-off (%)
1	2	-50	60	on	4.5	2	0.45	0.05	18
				off	3.2	1	0.37		
2	2	-50	60	on	2.4	3	0.33	0.05	6
				off	2.7	3	0.31	0.08	
3	2	-30	60	on	2.8	6	0.33	0.05	24
				off	3.1	4	0.25	0.07	
		-30	60	on	4.8	3	0.13	0.08	46
				off	4.8	1	0.07		
4	0.2	-49	12	on	6.2	3	0.84	0.04	33
				off	5.5	2	0.56	0.09	
		-47	12	on	6.2	5	0.83	0.02	64
				off	5.5	5	0.30	0.04	
5	0.2	-20	12	on	6.3	7	0.56	0.05	91
				off	5.9	5	0.05	0.06	
		-19	12	on	6.3	5	0.43	0.09	100
				off	5.9	3	-0.09	0.02	
6	0.1	-50	40	on	8.3	3	0.80	0.03	38
				off	9.5	3	0.50	0.12	
			40	on	16.5	2	0.56	0.09	48
				off	18.4	2	0.29	0.11	
7	0.2	-13	60	on	9.4	5	0.29	0.06	17
				off	9.7	5	0.24	0.03	
8	0.2	-17	12	on	6.7	4	0.12	0.02	33
				off	6.5	4	0.08	0.03	
		-15	12	on	6.7	3	0.11	0.01	100
				off	6.5	3	0.00	0.06	
9	0.2	-8	21	on	5.4	16	0.33	0.05	52
				off	5.1	16	0.16	0.02	
				on	9.5	10	0.20	0.03	55
				off	11.2	15	0.09	0.03	
10	0.2	-10	12	on	6.9	7	0.48	0.06	20
				off	5.3	7	0.40	0.08	

[a]Cells 1 to 5 were *che*RB (1 to 3 strain HB238, 4 and 5 strain HB241) >27 μm long with markers <1 μm from the end spinning >8 Hz. Cells 6 to 10 were *cheZ* (strain HB254) >18 μm long with markers <3 μm from the end spinning >4 Hz.
[b]On or off the cells, as illustrated in Fig. 1C.
[c]Change in rotational bias: mean value during the step less the mean value for 20 to 30 s before and after the step. The steps were spaced about 1 min apart.
[d]Change in bias on, less change in bias off, divided by change in bias on, times 100.

FIG. 1. Schematic illustration of different modes of iontophoretic stimulation of filamentous cells carrying flagellar markers. (A) Pulse stimulation with the pipette close to the cell surface either near the marker or far away. (B) Large step stimulation with the pipette close to the cell surface different distances from the marker. (C) Small step stimulation with the pipette close to the cell surface or far away at about the same distance from the marker. (D) As C but at more than one distance from the marker. Scale: the marker in A is 20 μm from the left end of the cell.

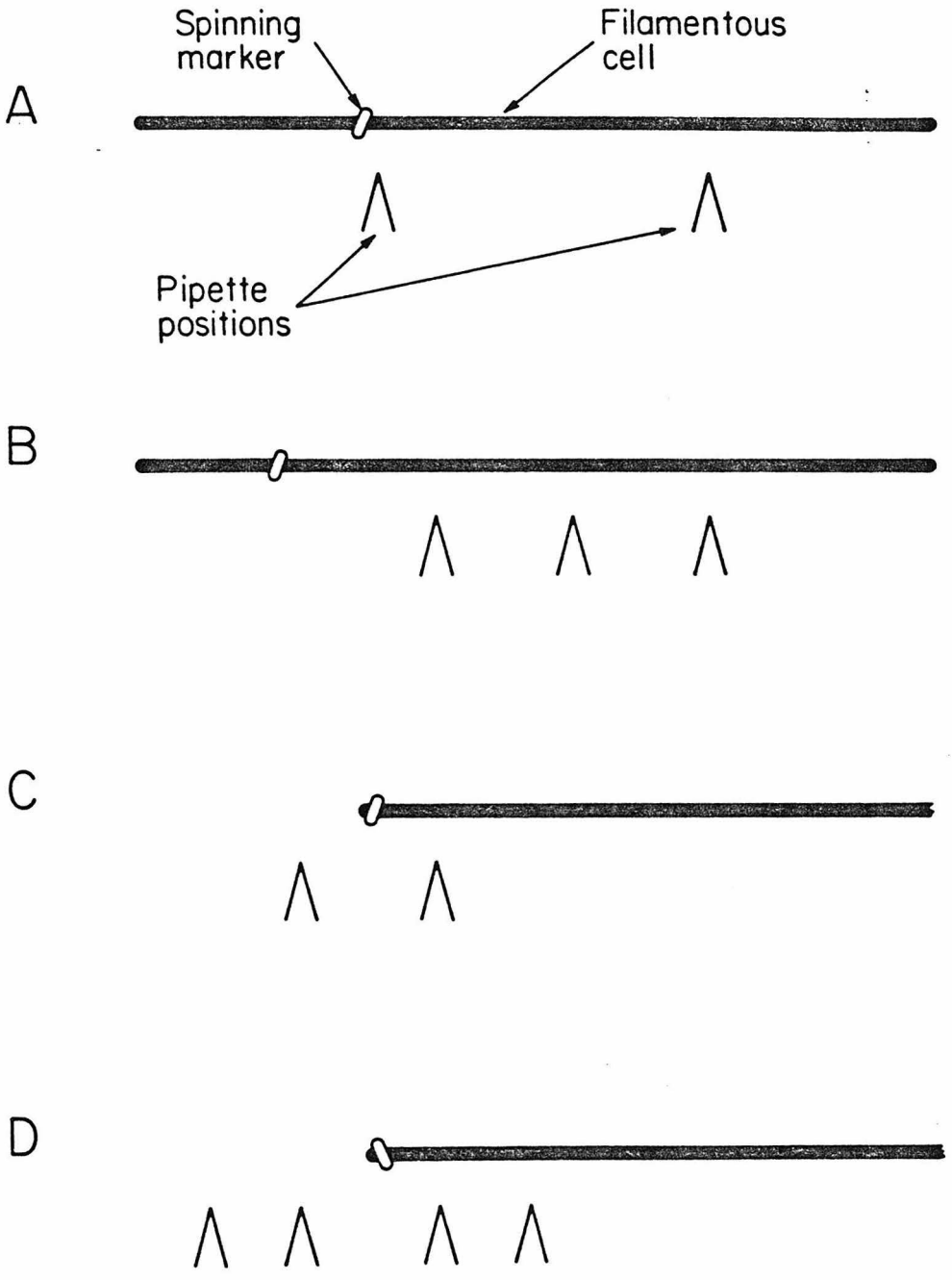
A
Spinning marker
Filamentous cell
Pipette positions
B
C
D

FIG. 2. Responses of wild-type cells for chemotaxis to brief pulses of L-aspartate (A) when the tip of the pipette was near the surface of a filamentous cell (strain HB203, *fla*E *hag fts*Q) either near the marker (thick curve) or far away (thin curve) and (B) when the tip of the pipette was near a normal tethered cell (strain AW405). The stimuli were given at 5 sec (vertical lines). All data were smoothed so that each point of a curve represents the average bias in a 0.1 s interval centered at that point (A). In all cases the pipette was within 4 μm of the cell surface. Pipettes containing 1 mM L-aspartate or 3.3 mM α-methylaspartate were placed near (less than 5 μm in 4 cases, 15 μm in one case) or far (27 to 40 μm) from a marker and pulses 20-62 ms long and -50 or -100 nA in amplitude were delivered. Pulses of the same duration and amplitude were used at either position on a given cell. Responses obtained when the pipette was near the marker (81 stimuli) or far away (93 stimuli) were obtained by averaging data from 5 cells. (B) The impulse response for strain AW405 was obtained by averaging data from 17 cells and 378 stimuli.

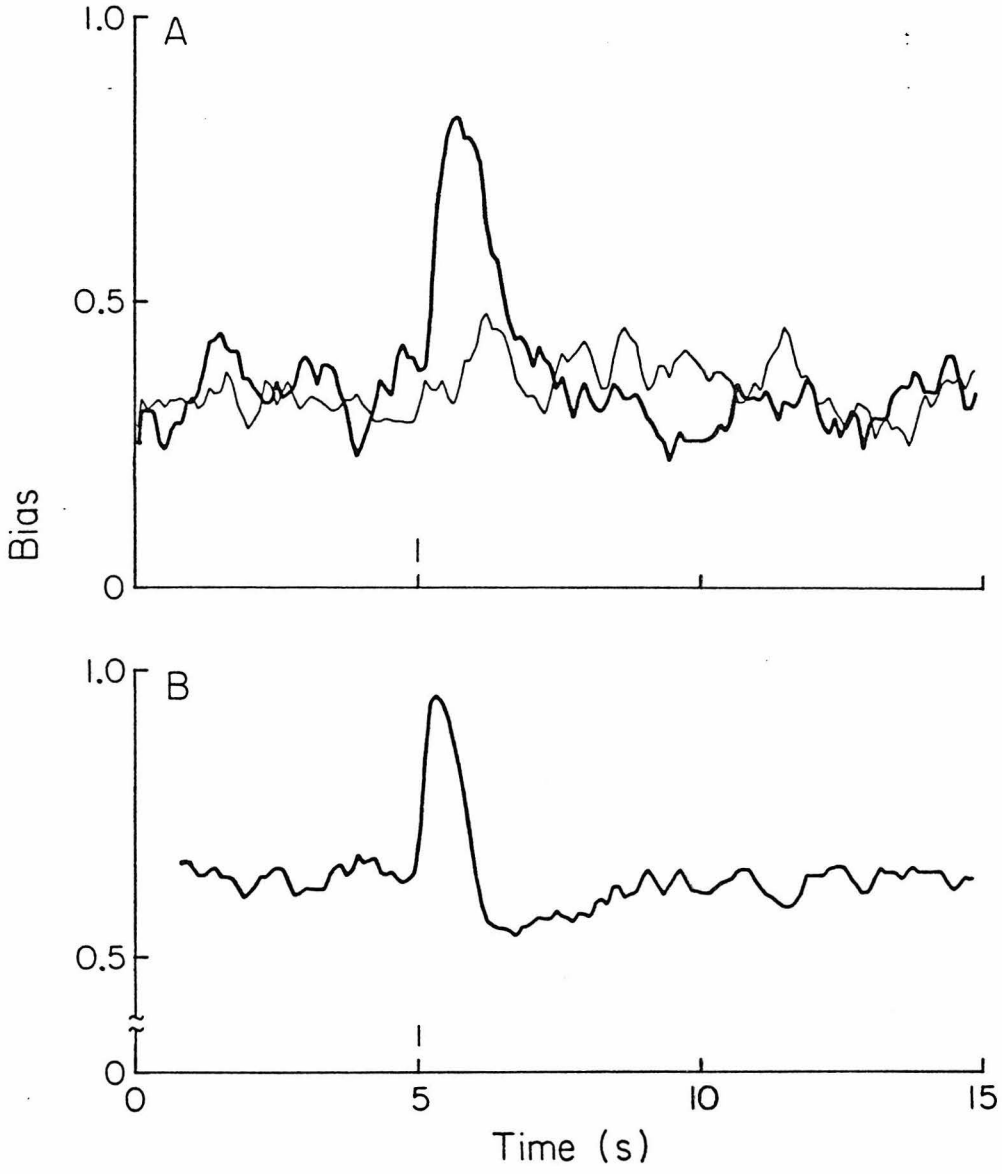
1.0
A
0.5
Bias
0
1.0
B
0.5
0
0
5
10
15
Time (s)

FIG. 3. Change in rotational bias of motors at the ends of filamentous cells to small step changes in concentration of aspartate applied on the cells (thick curves) or off the cells (thin curves) for a *che*RB cell (A) and a *che*Z cell (B). All data were smoothed, so that each point on a curve represents the average bias in a 2 s interval centered at that point. (A) Cell no. 5, Table 2. The current was on from 20 to 32 s (bar); 12 and 8 responses were averaged to generate the thick and thin curves, respectively. (B) Cell no. 9, Table 2, with the pipette at the positions closer to the marker. The current was on from 30 to 51 s (bar); 16 responses were averaged to generate each curve.

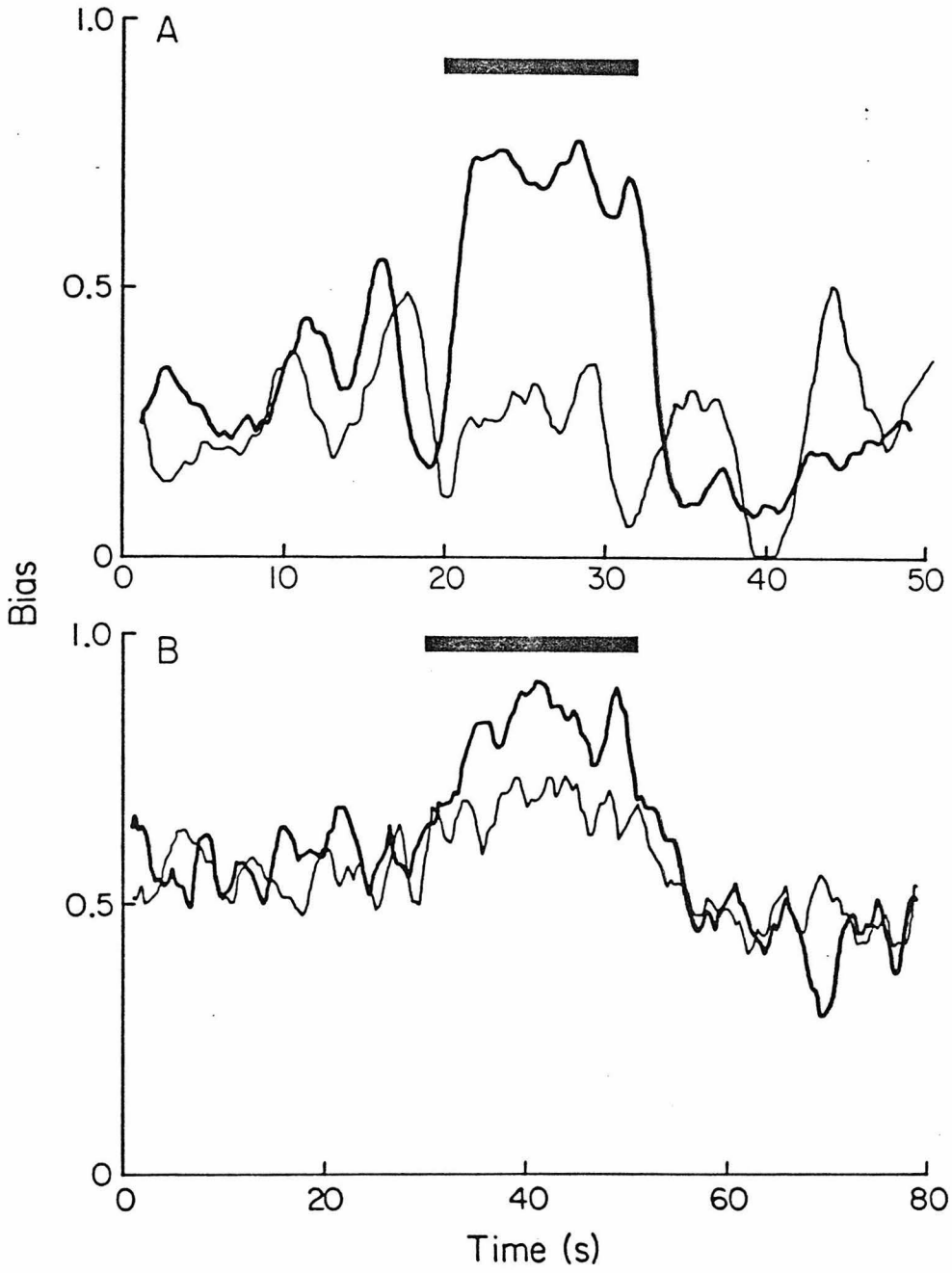
A
B
1.0
0.5
0
Bias
0
10
20
30
40
50
60
80
Time (s)

FIG. 4. Dose-response curves of *che*RB filamentous cells (A) and *che*Z filamentous cells (B). For each cell, the change in bias (Table 2, note c) generated by a given current or at a given position was averaged and scaled to the mean response to the largest stimulus given. The stimulus amplitudes were scaled to the largest stimulus amplitude. The error bars are the standard errors in each normalized response (including the uncertainty due to the standard error in the mean response to the largest stimulus). The different symbols identify different cells (6 in A, 1 strain HB238 and 5 strain HB241, and 8 in B, strain HB254). The thick curves were drawn by eye.

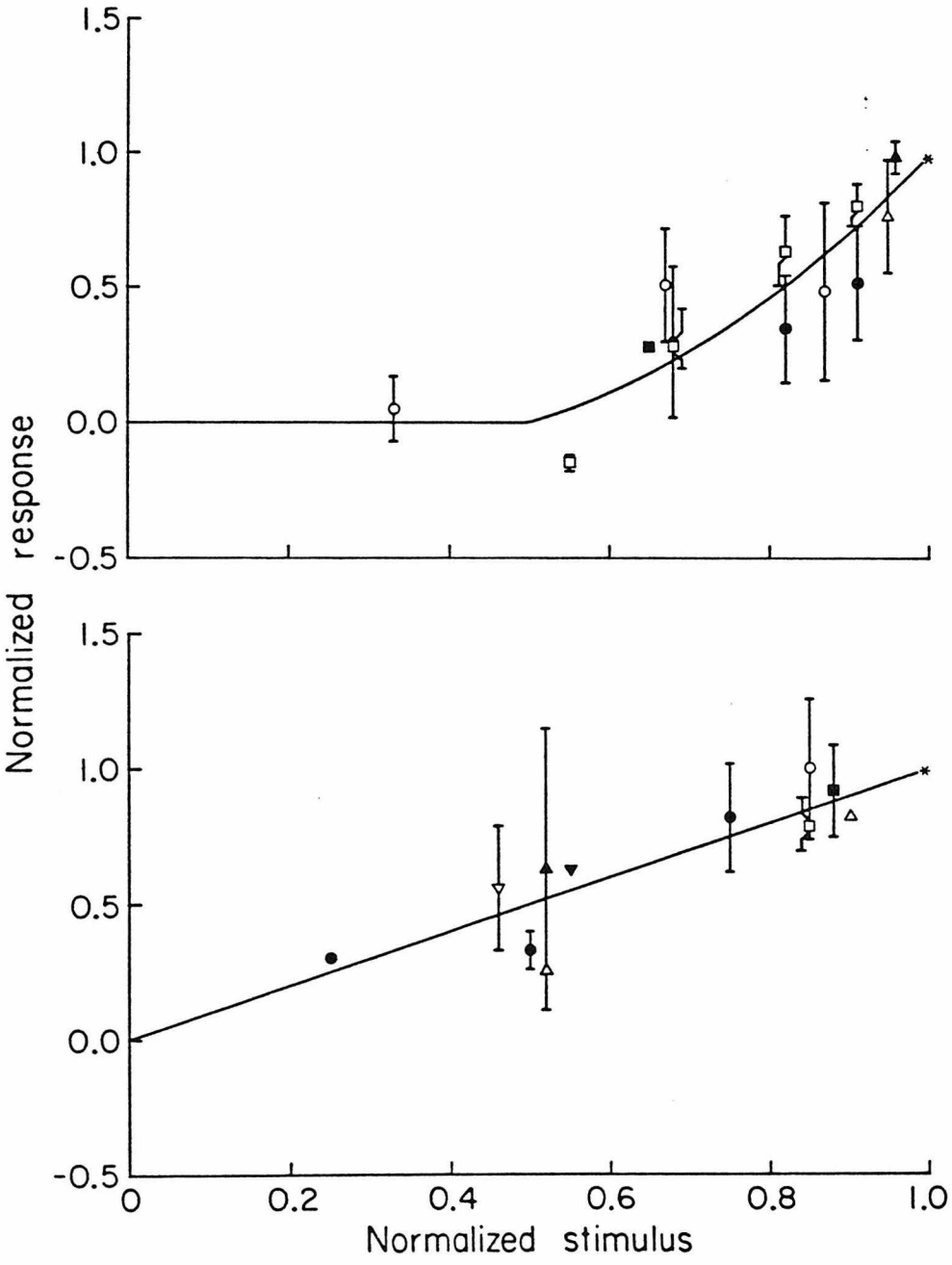
1.5
1.0
0.5
0.0
-0.5
Normalized response
1.5
1.0
0.5
0.0
-0.5
0
0.2
0.4
0.6
0.8
1.0
Normalized stimulus

FIG. 5. Distance dependence of the chemotactic signal in *che*RB filamentous cells (A) and *cheZ* filamentous cells (B). For each cell, the change in bias (Table 2, note c) generated by a fixed stimulus at a given position was averaged and scaled to the mean response obtained at the position of closest approach. The error bars are the standard errors in each normalized response. Since the position of closest approach varied from cell to cell, the distance for this position was scaled to 4 μm (roughly the mean value), and the other distances for the same cell were scaled by the same factor (so that their ratios remained constant). The thin curves are the predicted dependence of change in bias on distance if the response is determined solely by the concentration of attractant in the external medium at the marker in the manner specified by the dose response curves of Fig. 4. The thick curves are the predicted dependence for signaling by diffusion with decay, computed as described in the Appendix, for space constants of 2 μm (A) and 6 μm (B), respectively.

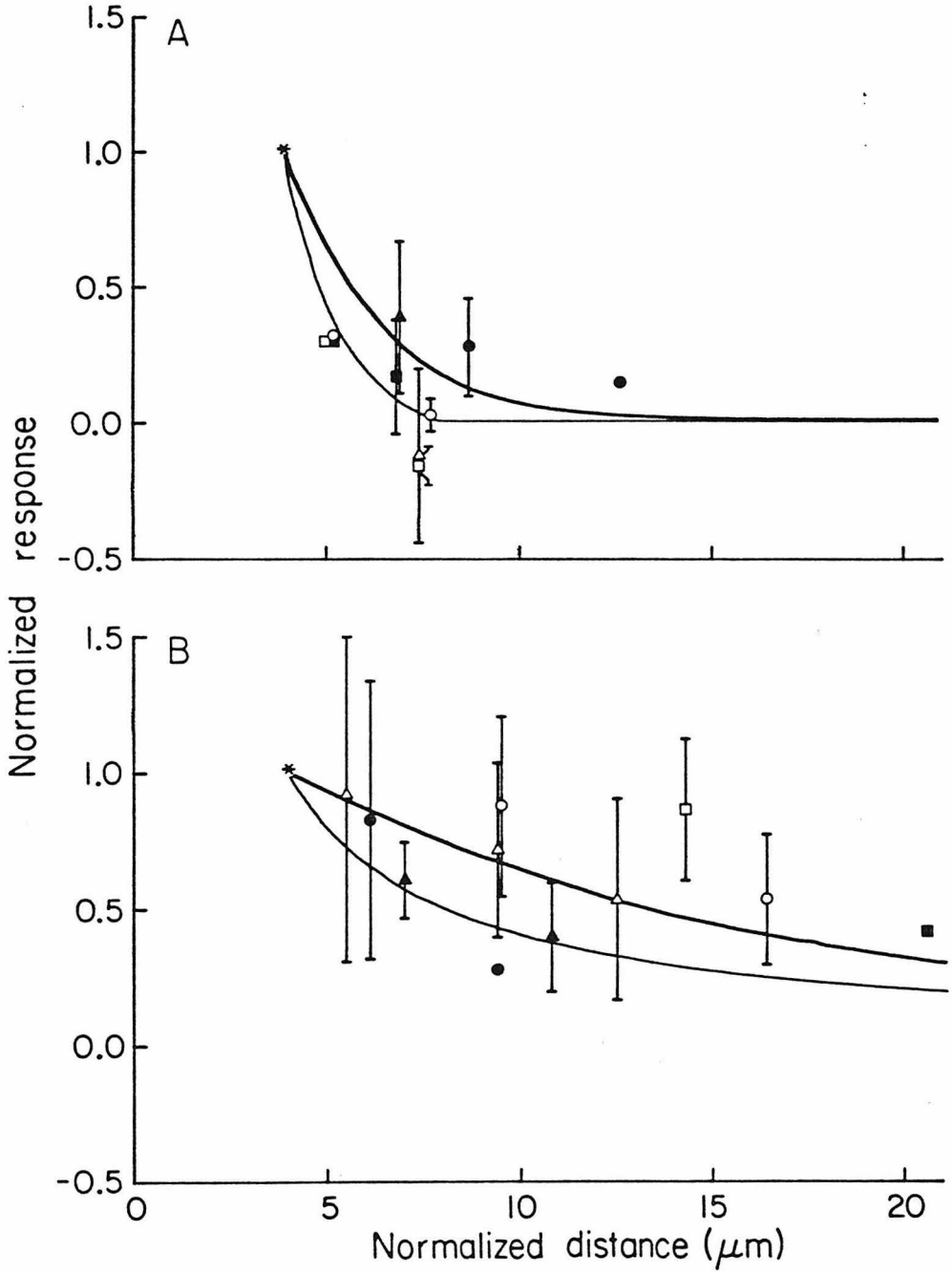
A
B
1.5
1.0
0.5
0.0
-0.5
Normalized response
0
5
10
15
20
Normalized distance (μm)

LITERATURE CITED

1. **Adler, J.** 1969. Chemoreceptors in bacteria. Science **166:** 1588-1597.
2. **Adler, J.** 1973. A method for measuring chemotaxis and use of the method to determine optimum conditions for chemotaxis by *Escherichia coli.* J. Gen. Microbiol. **74:** 77-91.
3. **Adler, J. and W. Tso.** 1974. "Decision"-making in bacteria; chemotactic responses of *Escherichia coli* to conflicting stimuli. Science **184:** 1292-1294.
4. **Aidley, D. J.** 1978. The physiology of excitable cells, 2nd ed., p. 47-53. Cambridge University Press, Cambridge.
5. **Armstrong, J. B.** 1972. Chemotaxis and methionine metabolism in *Escherichia coli.* Can. J. Microbiol. **18:** 591-596.
6. **Armstrong, J. B., J. Adler, and M. M. Dahl.** 1967. Nonchemotactic mutants of *Escherichia coli.* J. Bacteriol. **93:** 390-398.
7. **Aswad, D. W. and D. Koshland, Jr.** 1975. Evidence for an S-adenosylmethionine requirement in the chemotactic behavior of *Salmonella typhimurium.* J. Mol. Biol. **97:** 207-223.
8. **Begg, K. J., G. F. Hatfull and W. D. Donachie.** 1980. Identification of new genes in a cell envelope-cell division gene cluster of *Escherichia coli*: cell division gene *fts*Q. J. Bacteriol. **144:** 435-437.
9. **Berg, H. C.** 1975. Bacterial behavior. Nature (London) **254:** 389-392.
10. **Berg, H. C.** 1983. Random Walks in Biology, p. 22-23. Princeton University Press, Princeton.
11. **Berg, H. C. and R. Anderson.** 1973. Bacteria swim by rotating their flagellar filaments. Nature (London) **245:** 380-382.

12. **Berg, H. C. and D. A. Brown.** 1972. Chemotaxis in *Escherichia coli* analysed by three-dimensional tracking. Nature (London) **239:** 500-504.

13. **Berg, H. C. and E. M. Purcell.** 1977. Physics of chemoreception. Biophys. J. **20:** 193-219.

14. **Berg, H. C. and Tedesco, P. M.** 1975. Transient response to chemotactic stimuli in *Escherichia coli*. Proc. Nat. Acad. Sci. U.S.A. **72:** 3235-3239.

15. **Black, R. A., A. C. Hobson and J. Adler.** 1980. Involvement of cGMP in intracellular signaling in the chemotactic response of *Escherichia coli*. Proc. Nat. Acad. Sci. U.S.A. **77:** 3879-3883.

16. **Block, S. M., J. E. Segall and H. C. Berg.** 1982. Impulse responses in bacterial chemotaxis. Cell **31:** 215-226.

17. **Boyd, A. and M. Simon.** 1982. Bacterial chemotaxis. Ann. Rev. Physiol. **44:** 501-517.

18. **Canter, C. R. and P. R. Schimmel.** 1980. Biophysical Chemistry, Part III, p 921, and Part II, p. 584. W. H. Freeman and Company, San Francisco.

19. **Clarke, S. and D. E. Koshland, Jr.** 1979. Membrane receptors for aspartate and serine in bacterial chemotaxis. J. Biol. Chem. **254:** 9695-9702.

20. **DeFranco, A. L. and D. E. Koshland, Jr.** 1981. Molecular cloning of chemotaxis genes and overproduction of gene products in the bacterial sensing system. J. Bacteriol. **147:** 390-400.

21. **Dreyer, R. and K. Peper.** 1974. Iontophoretic application of acetylcholine: advantages of high resistance micropipettes in connection with an electronic current pump. Pflügers Arch. **348:** 263-272.

22. **Engström, P.** 1982. Thesis: Protein modifications in bacterial sensory adaptation. Acta Universitatis Upsaliensis. Abstracts of Uppsala Dissertaions from the Faculty of Science **650.** Uppsala Universitet, Uppsala.

23. **Engström, P. and G. L. Hazelbauer.** 1982. Methyl-accepting chemotaxis proteins are distributed in the membrane independently from basal ends of bacterial flagella. Biochim. Biophys. Acta **686:** 19-26.

24. **Eisenbach, M., Y. Margolin, A. Ciobotario and H. Rottenberg.** 1983. Distinction between changes in membrane potential and surface charge upon chemotactic stimulation of *Escherichia coli*. Biophys. J. **45:** 463-467.

25. **Felle, H., D. L. Stetson, W. S. Long and C. L. Slayman.** 1978. Direct measurement of membrane potential and resistance in giant cells of *Escherichia coli*, pp. 1399-1407. *In* P. L. Dutton, J. S. Leigh and A. Scarpa (eds.), Frontiers of Biological Energetics, Vol. 2.

26. **Goulbourne, E. A., Jr. and E. P. Greenberg.** 1981. Chemotaxis of *Spirochaetia aurantia*: involvement of membrane potential in chemosensory signal transduction. J. Bacteriol. **148:** 837-844.

27. **Goulbourne, E. A., Jr. and E. P. Greenberg.** 1983. A voltage clamp inhibits chemotaxis of *Spirochaetia aurantia*. J. Bacteriol. **153:** 916-920.

28. **Goy, M. F., M. S. Springer and J. Adler.** 1978. Failure of sensory adaptation in bacterial mutants that are defective in a protein methylation reaction. Cell **15:** 1231-1240.

29. **Greenwood, D. and F. O'Grady.** 1973. Comparison of the responses of *Escherichia coli* and *Proteus mirabilis* to seven β-lactam antibiotics. J. Infect. Dis. **128:** 211-222.

30. **Hazelbauer, G. L. and S. Harayama.** 1983. Sensory transduction in bacterial chemotaxis. Int. Rev. Cyt. **81:** 33-70.

31. **Hodgkin, A. L. and R. D. Keynes.** 1957. Movements of labelled calcium in squid giant axons. J. Physiol. **138:** 253-281.

32. **Imae, Y., T. Mizuno and K. Maeda.** 1984. Chemosensory excitation and thermosensory excitation in adaptation-deficient mutants of *Escherichia coli*. J. Bacteriol. **159:** 368-374.

33. **Ishihara, A., J. E. Segall, S. M. Block and H. C. Berg.** 1983. Coordination of flagella on filamentous cells of *Escherichia coli*. J. Bacteriol. **155:** 228-237.

34. **Keith, A. D. and W. Snipes.** 1974. Viscosity of cellular protoplasm. Science **183:** 666-668.

35. **Khan, S. and R. M. Macnab.** 1980. The steady-state counterclockwise/clockwise ratio of bacterial flagellar motors is regulated by protonmotive force. J. Mol. Biol. **138:** 563-597.

36. **Krieg, N. R., J. P. Tomelty and J. S. Wells, Jr.** 1967. Inhibition of flagellar coordination in *Spirillum volutans*. J. Bacteriol. **94:** 1431-1436.

37. **Kosower, E. M.** 1983. Selection of ion channel elements in the serine and asparate methyl-accepting chemotaxis proteins of bacteria. Bioch. Bioph. Res. Comm. **115:** 648-652.

38. **Larsen, S. H., R. W. Reader, E. N. Kort, W. Tso and J. Adler.** 1974. Change in direction of flagellar rotation is the basis of the chemotactic response in *Escherichia coli*. Nature (London) **249:** 74-77.

39. **Macnab, R. M. and D. E. Koshland, Jr.** 1972. The gradient-sensing mechanism in bacterial chemotaxis. Proc. Nat. Acad. Sci. U.S.A. **69:** 2509-2512.

40. **Macnab, R. M. and M. K. Ornston.** 1977. Normal-to-curly flagellar transitions and their role in bacterial tumbling. Stabilization of an alternative quaternary structure by mechanical force. J. Mol. Biol. **112:** 1-30.

41. **Mathews, J. and R. L. Walker.** 1970. Mathematical methods of physics. 2nd ed., pp. 270-271. Benjamin, Menlo Park.

42. **McCloskey, M. and M.-M. Poo.** 1984. Protein diffusion in cell membranes: some biological implications. Int. Rev. Cyt. **87:** 19-81.

43. **Mesibov, R. and J. Adler.** 1972. Chemotaxis toward amino acids in *Escherichia coli*. J. Bacteriol. **112:** 315-326.

44. **Miller, J. B. and D. E. Koshland, Jr.** 1977. Sensory electrophysiology of bacteria: relationship of the membrane potential to motility and chemotaxis in *Bacillus subtilis*. Proc. Nat. Acad. Sci. U.S.A. **74:** 4752-4756.

45. **Ordal, G. W.** 1977. Calcium ion regulates chemotactic behaviour in bacteria. Nature (London) **270:** 66-67.

46. **Parkinson, J. S.** 1977. Behavioral genetics of bacteria. Ann. Rev. Genet. **11:** 397-414.

47. **Parkinson, J. S.** 1978. Complementation analysis and deletion mapping of *Escherichia coli* mutants defective in chemotaxis. J. Bacteriol. **135:** 45-53.

48. **Parkinson, J. S.** 1981. Genetics of bacterial chemotaxis. Symp. Soc. Gen. Microbiol. **31:** 265-290.

49. **Parkinson, J. S. and G. L. Hazelbauer.** 1983. Bacterial chemotaxis: molecular genetics of sensory transduction and chemotactic gene expression. *In* Gene Function in Prokaryotes, pp. 293-318. Cold Spring Harbor Laboratory, Cold Spring Harbor.

50. **Parkinson, J. S. and S. E. Houts.** 1982. Isolation and behavior of *Escherichia coli* deletion mutants lacking chemotaxis functions. J. Bacteriol. **151:** 106-113.

51. **Parkinson, J. S. and P. T. Revello.** 1978. Sensory adaptation mutants of *Escherichia coli*. Cell **15:** 1221-1230.

52. **Parkinson, J. S., S. R. Parker, P. B. Talbert and S. E. Houts.** 1983. Interactions between chemotaxis genes and flagellar genes in *Escherichia coli*. J. Bacteriol. **155:** 265-274.

53. **Reader, R. W., W. Tso, M. S. Springer, M. F. Goy and J. Adler.** 1979. Pleiotropic aspartate taxis and serine taxis mutants of *Escherichia coli*. J. Gen. Microbiol. **111:** 363-374.

54. **Reilley, C. N. and A. Vavoulis.** 1959. Tetraethylenepentamine, a selective titrant for metal ions. Anal. Chem. **31:** 243-248.

55. **Robinson, G. N.** 1980. Effect of β-lactam antibiotics on bacterial cell growth rate. J. Gen. Microbiol. **120:** 317-323.

56. **Russo, A. F. and D. E. Koshland, Jr.** 1983. Separation of signal transduction and adaptation functions of the aspartate receptor in bacterial sensing. Science **220:** 1016-1020.

57. **Segall, J. E., M. D. Manson and H. C. Berg.** 1982. Signal processing times in bacterial chemotaxis. Nature (London) **296:** 855-857.

58. **Silverman, M. and M. Simon.** 1972. Flagellar assembly mutants in *Escherichia coli*. J. Bacteriol. **112:** 986-993.

59. **Silverman, M. and M. Simon.** 1974. Flagellar rotation and the mechanism of bacterial motility. Nature (London) **249:** 73-74.

60. **Snyder, M. A., J. B. Stock and D. E. Koshland, Jr.** 1981. Role of membrane potential and calcium in chemotactic sensing by bacteria. J. Mol. Biol. **149:** 241-257.

61. **Springer, M. S., M. F. Goy and J. Adler.** 1979. Methylation in behavioral control mechanisms and in signal transduction. Nature (London) **280:** 279-284.

62. **Spudich, J. L. and D. E. Koshland, Jr.** 1975. Quantitation of the sensory response in bacterial chemotaxis. Proc. Nat. Acad. Sci. U.S.A. **72:** 710-713.

63. **Szmelcman, S. and J. Adler.** 1976. Change in membrane potential during bacterial chemotaxis. Proc. Nat. Acad. Sci. U.S.A. **73:** 4387-4391.

64. **Tanner, J. E.** 1983. Intracellular diffusion of water. Arch. Biochem. Biophys. **224:** 416-428.

65. **Tsang, N., R. Macnab and D. E. Koshland, Jr.** 1973. Common mechanism for repellents and attractants in bacterial chemotaxis. Science **181:** 60-63.

66. **Yonekawa, H., H. Hayashi and J. S. Parkinson.** 1983. Requirement of the *che*B function for sensory adaptation in *Escherichia coli*. J. Bacteriol. **156:** 1228-1235.

A comment concerning the nature of the signal. My personal preference at this time is that the signal is a protein or a group of proteins. This preference is inspired by the embarassing wealth of *che* gene products with unknown functions. The choice of *che*Y as the "strongest candidate" was intended to be provocative. The type of reversible modifications that a protein signal could undergo might range from phosphorylation to exchange of GDP for GTP, with subsequent hydrolysis of the GTP (Stiles et al., 1984).

Chapter VI

SUMMARY AND SPECULATIONS

Summary. In this thesis I have described my studies of bacterial chemotactic responses using iontophoretic stimulation. The first chapter discussed initial measurements of the maximal rates of bacterial responses. The second and third chapters described more sophisticated measurements using impulse and step stimuli. The fourth and fifth chapters presented the studies of the responses of filamentous cells and included was a rough model of how some of the *che* gene products might be involved in the generation of chemotactic responses.

Production of the impulse response. A more speculative analysis of the kinetics of the impulse response might shed some light on the nature of the system generating the impulse response. The fourier transform of the attractant impulse response (Text-figure 6B) has a broad peak centered at about 0.28 Hz, with a slope of +1 (units $\log_{10}$(response)/$\log_{10}$(frequency)) at low frequencies and a slope of about -2.5 at high frequencies. These slopes can be interpreted in terms of linear filters, with positive slopes corresponding to high pass filters (differentiators) and negative slopes corresponding to low pass filters (integrators). The fourier transform in Text-figure 6B could then be interpreted as a single high pass filter in series with 3.5 low pass filters (3.5 because one of the high pass filters is canceled by the low pass filter).

Contributing to the low pass filters in the impulse response is the switching speed of the flagellar motor. The exponential distributions of CW and CCW interval lengths suggest that the motor can be represented as a two-state system (Text-figure 2; Block et al., 1983); the motor can either be in a CW or CCW state, and the rates of switching between these two states are determined by first order rate constants (the mean interval lengths are the inverse of these rate constants).

$$CW \underset{k_{ccw}}{\overset{k_{cw}}{\rightleftharpoons}} CCW$$

The rate at which the CCW bias of the motor can change is limited by the values of these rate constants. For example, suppose that the rate constants are both equal to 1 per sec. At steady-state, the bias of the motor is 0.5. However, if the value of k_{CW} is changed to 9 per second, then the bias of the motor changes to the new steady-state value (0.9) with a rate constant of $(k_{CW} + k_{CCW}) = 10$ per second. It does not instantaneously switch to the new steady state bias value. As a result, high frequency changes in these rate constants are filtered by the rate at which the motor changes its bias (which in turn depends on the values of the rate constants). This complex situation can be simplified by studying the "instantaneous" bias of the motor; the value that the bias would have if the system were allowed to go to steady-state with no further change in the values of the rate constants - bias = $k_{CW}/(k_{CW} + k_{CCW})$. The rate constants can be estimated from the impulse response data, as described in Text-figure 14, which allows one to calculate the "bias signal" that the motor is receiving as a function of time. Text-figure 14B shows the bias signal that the motor is receiving during the attractant impulse response. This signal has faster kinetics than the impulse response, since it is now not filtered by the motor. However, it is also saturated, going to 1.0 (the maximum possible value) during the early portions of the impulse response, and dropping to 0.0 at later times. The points at 0.0 are probably not significant - very few reversals occurred at these times, resulting in very large uncertainties in the estimates of the bias. This is again a reflection of the response being saturated - most of the cells were rotating in the CCW direction, so that if one or two reversals occurred, they were likely to be changes in direction from CCW to CW. The fourier transform of the fit to the

Text-figure 14. Bias signal of wild type attractant impulse response

A. Wild type attractant impulse response. The thick line is the portion of the wild type attractant impulse shown in Text-figure 4 that occurs in the time interval from 5 to 12 seconds. The thin line is the fit in Text-figure 4.

B. Bias signal of A. The dots represent the bias signal calculated from the data in A and the smooth line is the fit of a sum of six exponentials plus a constant to the data occurring after 5.06 seconds. The rate constants k_{CW} and k_{CCW} were calculated from the data represented in A, by counting the number of CW-to-CCW transitions (for k_{CW}) and CCW-to-CW transitions (for k_{CCW}) in a 0.05 second interval and dividing by the average fraction of cells rotating CW (for k_{CW}) or CCW (for k_{CCW}). These ratios were then divided by the bin size. The bias signal was then calculated as $k_{CW}/(k_{CW} + k_{CCW})$ and plotted every 0.02 seconds. The fit to the data weighted each point equally (ignoring 0.0 values). One of the amplitude terms was constrained so that the value of the sum of the exponentials at 5.06 seconds (the start of the pulse) was equal to 0.0. A second amplitude term was constrained so that the areas of the curves above and below the baseline were equal. The amplitudes and rate constants (units of per second) for four exponentials were 76.9, 3.56; -89.0, 4.86; -28.7, 2.91; 36.2, 5.7. The rate constant for the amplitude that constrained the value at 5.06 to be equal to the baseline was 4.38. The value of the rate constant for the amplitude that constrained the areas to be equal was 3.18. The baseline value was 0.625.

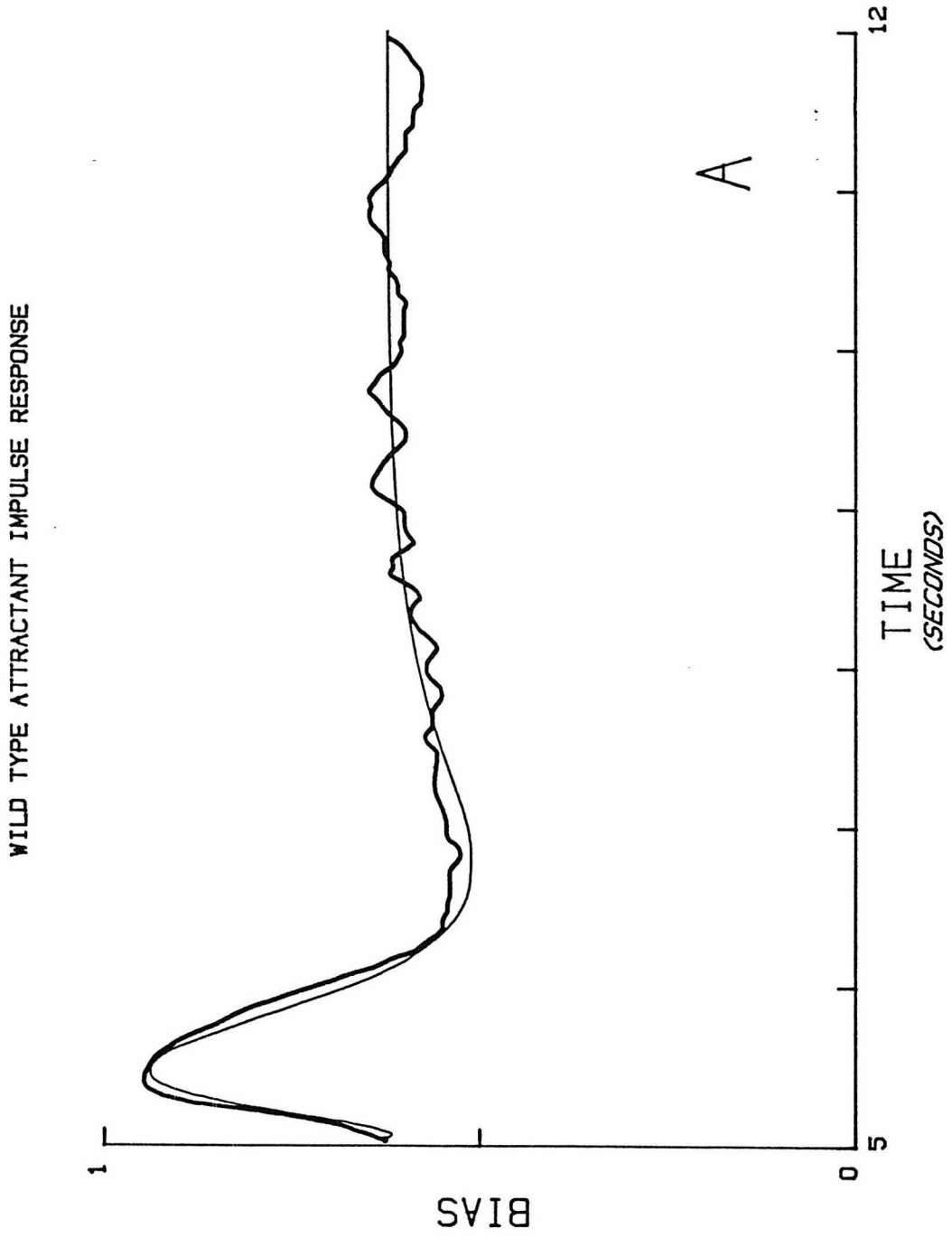
WILD TYPE ATTRACTANT IMPULSE RESPONSE
BIAS
1
0
5
12
TIME
(SECONDS)
A

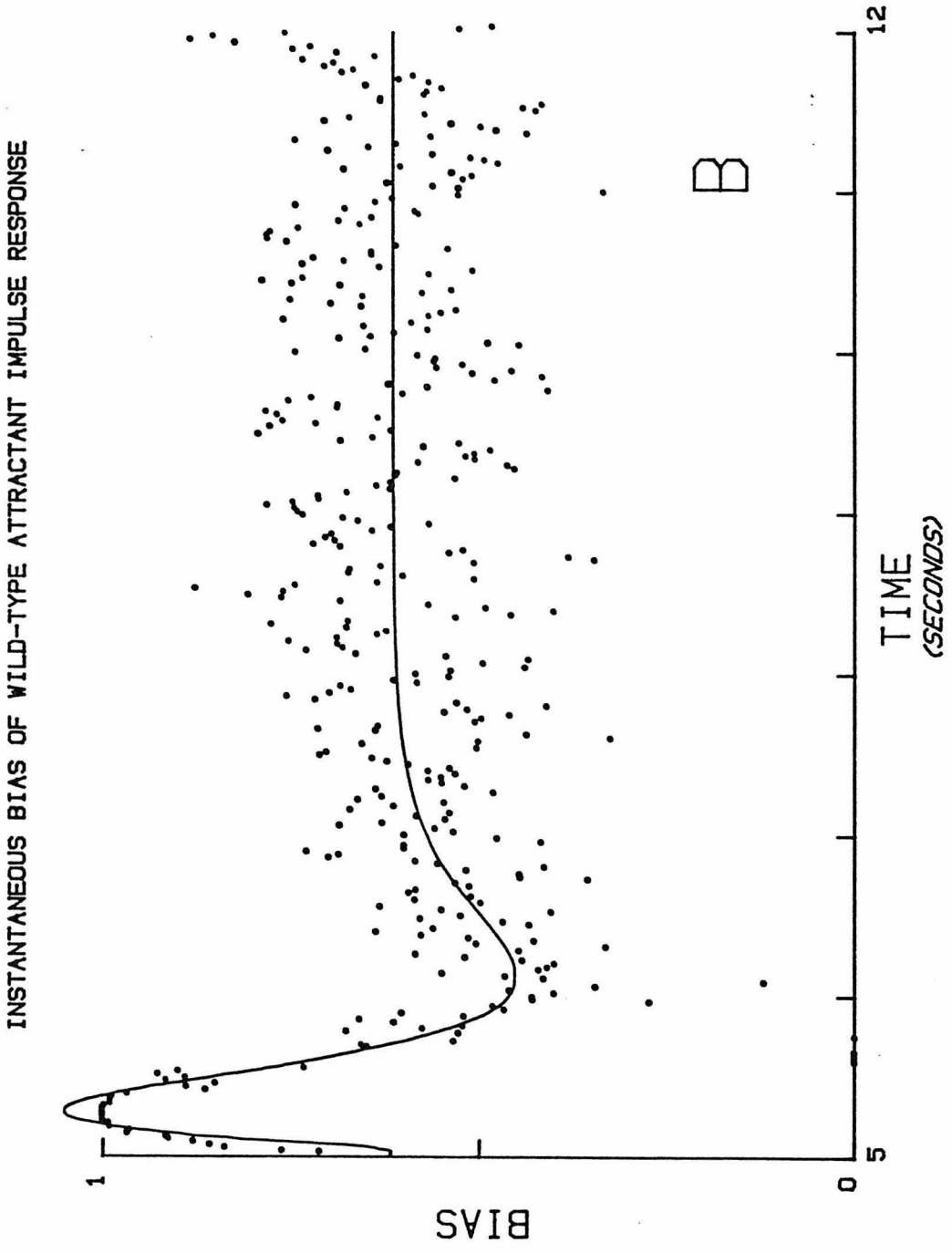
INSTANTANEOUS BIAS OF WILD-TYPE ATTRACTANT IMPULSE RESPONSE
B
BIAS
1
0
5
12
TIME
(SECONDS)

bias signal in Text-figure 14B has a slope of -2.0 (not shown), showing that part of the original impulse response kinetics is due to the switching kinetics of the motor (as is evident in Text-figure 14).

The rest of the kinetics of the impulse response (those shown in the bias signal) must be due to the biochemical mechanisms that produce the signal, and possibly due to other delays in the motor response about which we know nothing. Again the fourier transform provides a clue concerning these mechanisms. The limiting slopes of the fourier transform of the bias signal suggest that the transfer function for the signal-generating mechanism is of the form

$$G(s) = \frac{s}{s^3 + as^2 + bs + c}$$

where s is the Laplace transform variable, and a, b, and c are constants (Cannon, 1967). This transfer function suggests, in turn, that the time evolution of the bias signal can be described by a third order differential equation:

$$d^3B/dt^3 + \alpha d^2B/dt^2 + \beta\, dB/dt + \gamma\, B = \delta$$

where B(t) is the value of the bias as a function of time, and α, β, γ, and δ are constants. Such a differential equation could describe the behavior of a system which involves three biochemical reactions. Each individual reaction can be approximated by a first order linear differential equation, if the enzyme catalyzing the reaction is unsaturated and if each term in the equation is linear. For example, the model described in the appendix of Chapter 5 proposes that a signal is generated by the MCP's and destroyed by the *cheZ* gene product. The differential equation describing this process was

$$dS/dt = k_m - k_z S$$

where S is the signal, k_m is the rate of production of S (decreased by binding of attractant), and k_z the rate of inactivation. A second equation that is important for the chemotaxis system is the equation describing how methylation increases the rate of production of S (increases if S is a CW signal). For example, this process could be modeled by

$$dk_m/dt = - k_r * (S - S_o)$$

where k_r is a rate constant determining the rate of methylation or demethylation of the MCP's, depending on how far S is from some steady state value (S_o). Together, these two equations would give rise to a second order linear differential equation. Including a third process, possibly another intermediate which is generated by S and which then affects the bias of the motor, should then be sufficient to model the impulse response of the system to the level of accuracy demonstrated by the fits in Text-figure 14.

It is possible that the third low pass process is an artifact, due to the size of the pulses used to stimulate the cell. Although pulse lengths were generally short, the decay of concentration after the end of the pulse follows the kinetics of the diffusion equation. From a rough calibration of all the pulses used to generate the attractant impulse response (based on the calibration described in Chapter III), I estimate that .4 % of the receptors are still occupied about 0.3 seconds after the start of the pulse. To rule out this possibility, one should repeat the measurement of the impulse response without using saturating stimuli, so that the peak bias value is never 1, unlike the plot in

Text-figure 14B. The impulse response when α-methylaspartate was added to the bath appeared to be more rapid, although still saturated. I would recommend using those conditions and lower concentrations of α-methylaspartate in the pipette. An argument against this possibility can be made using the bias signal of the repellent impulse response (Text-figure 15). Although the kinetics are slightly faster than those of the attractant signal, and although the response is not saturated, the fourier transform still suggests that there are 3 low pass filters (slope at high frequencies about -1.9, data not shown).

Other possible explanations for the third process include the following. First, although it is obvious that the two processes described above--generation of the signal and adaptation through methylation--must be involved in the kinetics of the impulse response, the equations used above could easily be wrong. It is possible that a nonlinear version of the equations could fit the data. Alternatively, the kinetics of the binding and unbinding of the signal to the motor might be slow enough to be responsible. This is especially likely if the signal is a protein, with a concentration in the micromolar range. It is possible that the latencies to large attractant and repellent stimuli described in Chapter I (0.2 and 0.1 seconds) reflect the rates of unbinding and binding of a CW signal molecule combined with the rate of turnover of that molecule.

Interaction of the Signal with the Motor. It is important to keep in mind that the bias signal or bias need not be linearly related to the concentration of some intracellular signal. This will be true especially at high or low values of the bias. Since it is likely that binding of the signal to the motor produces a change in bias, saturation of binding at high concentrations of the signal will distort any estimates of concentration made from studying the bias.

Text-figure 15. Bias signal of wild type repellent impulse response

A. The portion of the wild type repellent impulse response shown in Text-figure 7 that occurs between 5 and 12 seconds.

B. The bias signal (dots) calculated as described in the legend to Text-figure 14. The smooth curve was a sum of six exponentials plus a constant fit to the data as described in Text-figure 14. The fit values of the amplitudes and rate constants for 4 exponentials were -1.32, 2.03; -52.0, 6.60; 351.1, 6.75; 1.19, 1.41. The rate constant for the exponential whose amplitude was constrained so that the sum of the exponentials was equal to 0.0 at 5.06 seconds was 6.72. The rate constant for the exponential whose amplitude was constrained so that the areas were equal was 2.02. The baseline value was 0.617.

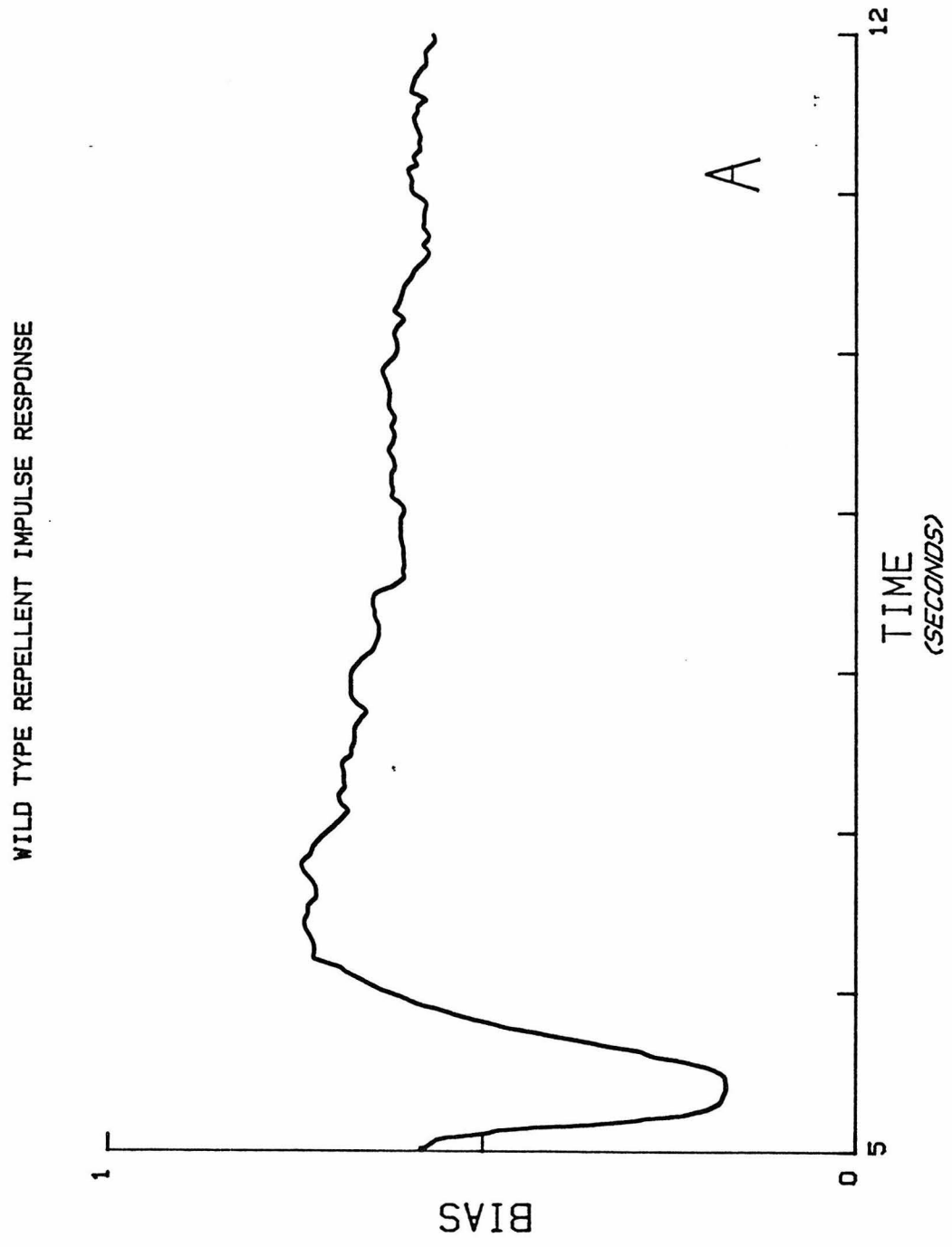
WILD TYPE REPELLENT IMPULSE RESPONSE
BIAS
1
0
5
12
TIME
(SECONDS)
A

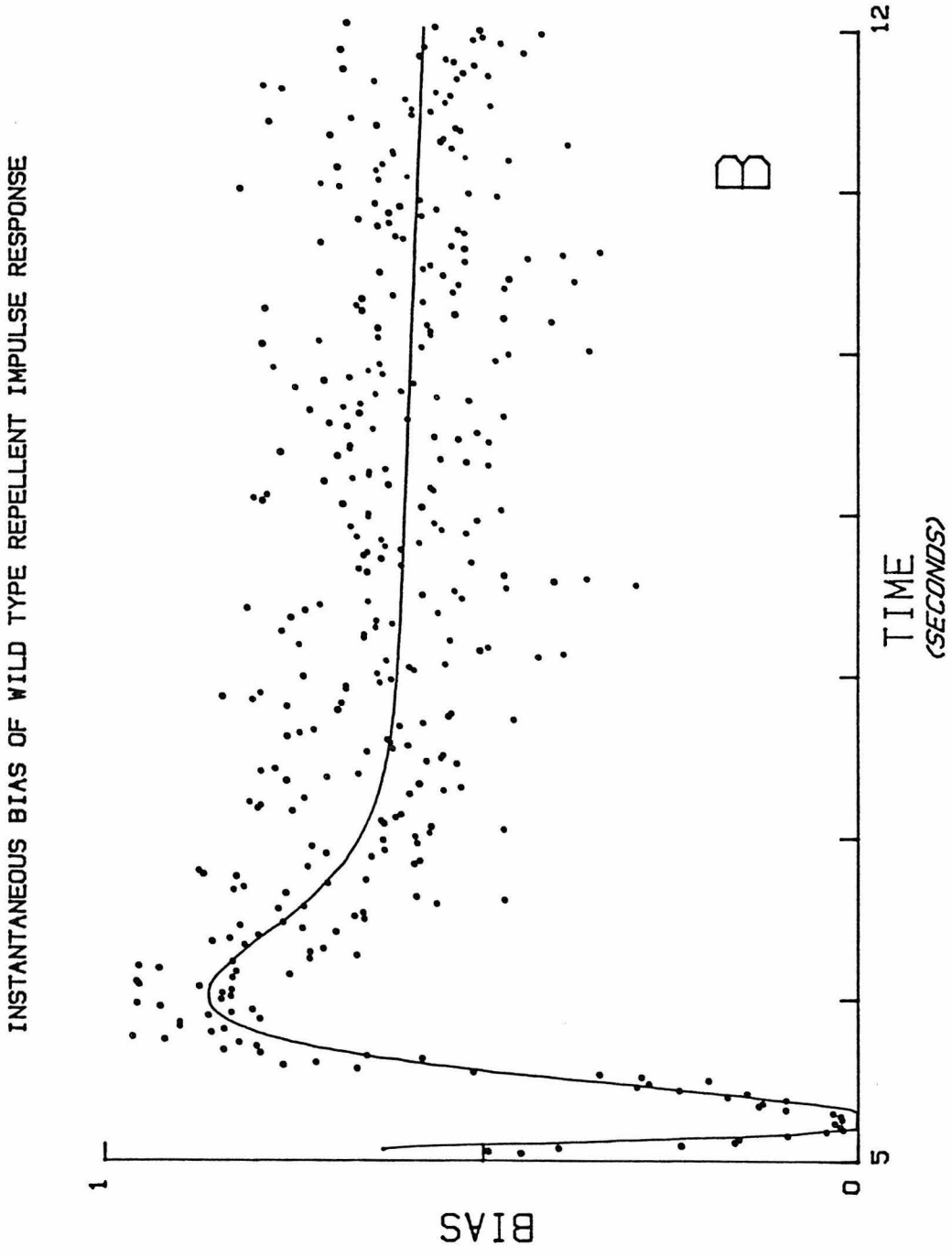
INSTANTANEOUS BIAS OF WILD TYPE REPELLENT IMPULSE RESPONSE
BIAS
1
0
5
12
TIME
(SECONDS)
B

A simple model (based on one described by Hanke and Miller, 1983), describing how the bias might depend on signal concentration is outlined below.

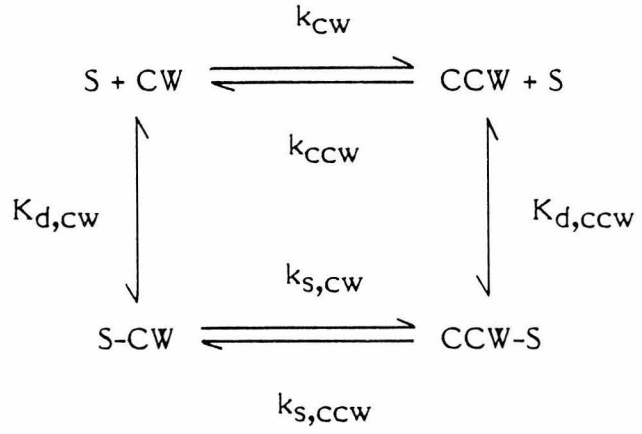

The signal, S, can bind to the motor when the motor is rotating either CW or CCW. Binding of the signal alters the rates of switching both from CCW to CW and vice versa. This is true because both CCW and CW rates vary during the impulse response (Block et al., 1982) and because the latencies to attractant and repellent stimuli are shorter than the unstimulated CW and CCW interval lengths. The exponential distributions of CCW and CW interval lengths (Block et al., 1983) implies that the binding and unbinding of the signal is fast compared to the switching rates, although paucities of events less than 0.1 seconds might reflect such kinetics. Therefore the mean rate of switching from, say, CCW to CW is the weighted average of the rates for switching with and without signal bound, weighting by the fraction of time that signal is bound. Conservation of energy around the cycle, and the fact that a motor has to be in either a CCW or CW state in the system can be used to eliminate some of the free parameters. I have attempted to fit the dependence of the mean CW and CCW lengths on bias, using data of unstimulated cells from Berg and Tedesco, 1975; Segall et al., 1982; and Block et al., 1983. Although the results are preliminary, it appears that the simple model described above does not adequately fit the data, unless energy is

put into the system. This suggests that switching the direction of rotation of the motor might require energy. It is interesting that ATP or a related metabolite is required for CW rotation of the motor (Kondoh, 1980; Arai, 1981; Shioi et al., 1982). This requirement appears to be in the generation of the signal reaching the motor, since ATP is not required for CW rotation of tethered *che*V envelopes (Ravid and Eisenbach, 1984).

More complex models involving cooperative binding of several molecules of S could also be modeled. My initial model as to how the binding of S would affect motor switching rates was inspired by the thought that binding and unbinding of S might be extremely fast relative to rates of switching of the motor. My thought was that perhaps this has an averaged effect on the motor such that the free energy of the motor is intermediate between the value when the concentration of S is 0, and when the concentration is extremely high. The free energy would be the weighted average of the energies of the motor without any S bound, and with S always bound. The net effect is to alter the way the rate constants vary with the concentration of S, compared to the model described in detail above. However, at this time there are so many free parameters that either this model or the one described earlier can fit the data. Much more data concerning the range of mean CCW and CW interval lengths will be easily acquired when the computerized data acquisition system now being developed in the lab is operational.

The mechanism of transmembrane signalling. I wish to discuss briefly possible mechanisms by which MCP's transmit a signal across the cell membrane. As described in the Introduction, the initial stage of signal generation involves, for example, with tar, aspartate binding to tar on the outside of the cytplasmic membrane, and then tar presumably generating a signal inside the cell. How

does the inside portion of the tar molecule realize that attractant has bound to the outside portion? This question is relevant to membrane receptors in all organisms.

Two possible mechanisms for transmembrane signalling come to mind (see Lauffenburger and DeLisi, 1983 for a recent review). One possibility is that receptors that bind attractant then aggregate, in pairs or greater numbers. This aggregation juxtaposes the interior portions of the molecules, allowing them to generate a signal (Boyd et al., 1982). Such mechanisms may occur in lymphocytes, where capping of receptors has been noted. I favor a model in which aggregation of receptors is not necessary. This model was inspired by the amino acid sequences of the MCP's (Boyd et al., 1983; Krikos et al., 1983). Except for the signal sequence, there is only one putative membrane spanning region in the MCP molecules. Mechanisms involving relative movements of several membrane spanning regions that generate conformational changes in the cytoplasmic portion of the molecule are ruled out. This leaves the pleasingly simple possibility that the periplasmic portion of the molecule signals the interior portion of the molecule by pushing or pulling on the transmembrane region. This shift of the transmembrane region could distort the cytoplasmic portion of the molecule, resulting in a conformation change that generates the signal (or, equivalently, shuts it off).

There is indirect evidence that in the bacterial chemotaxis system aggregation of receptors is not required. This evidence all relies on measurements of transition times--the amount of time required for the cell to adapt to a step increase in attractant concentration. The dependence of transition time on change in concentration of α-methylaspartate (Berg and Tedesco, 1975) implies that the transition time is linearly proportional to the fraction of receptors occupied. This could occur if such large numbers of MCP's

are activated that the methylating enzyme is saturated. The time required to adapt would then be the time required for the enzyme to methylate enough MCP's to offset the signal produced by attractant binding. Aggregation mechanisms should have adaptation times proportion to a power of the fraction of receptor occupied, with the power equal to the number of bound receptors that must aggregate to send a signal across the membrane. I have used iontophoresis to deliver small step changes in concentration below the dissociation constant of the tar molecule, conditions under which the fraction of receptor bound should be linearly related to the size of the current. I find that transition times to small steps vary linearly with the current size of the pulse. Aggregation mechanisms would again go as a power of the current size. Finally, in a strain that overproduced the tar MCP by a factor of 10 or more provided by M. Simon's group, I was able to study the responses to concentration changes produced by flow in the same range as was used in the iontophoresis study. This was possible because the transition times were abnormally longer, due presumably to the large increase in the number of receptors that had to be methylated for the cell to adapt. I found again that transition times varied linearly with concentration.

These results suggest that aggregation is not involved in transmembrane signalling, but they are indirect and rely upon measurements of transition times. A more direct experiment is possible because the genes have been cloned. Lengthening or shortening of the transmembrane region of the molecule should mimic pushing or pulling by the exterior portion when attractant is bound or released. This effect should trigger signalling just as attractant binding does, and in addition, methylation or demethylation of the MCP should occur in the absence of attractant or repellent. Thus the ideal test of this model is to lengthen and shorten the transmembrane region and determine whether, in the

absence of any other stimuli, the methylation level is altered. The only uncertainty is how great the shortening or lengthening of this region should be. An estimate can be made by estimating the difference in length between the region that is hydrophobic and the width of the cytoplasmic membrane, and altering the length of the region so that the alteration is a significant fraction of the difference.

I am particularly interested in this model because of some similarities between this system and the β-adrenergic receptor system. The molecular weight of the β-adrenergic receptor is about 58,000 to 64,000 in several systems (for a review see Stiles et al, 1984). It has recently been purified, and the data published, although preliminary, are consistent with a unimolecular transmembrane signalling mechanism (Cerione et al., 1983). Finally, the link between the receptor and the cyclase is a set of proteins, and it is possible that the link between MCP's and the flagellum is also a set of proteins, as discussed in Chapter V. Although they are by no means compelling, I think that the similarities are intriguing.

A last look at the impulse response. I wish to conclude by considering an intuitive (to me) interpretation of the shape of the impulse response. The convolution integral predicts the response of the system at time t, given the impulse response and the past history of stimulation:

$$y(t) = \int_0^\infty h(\tau)x(t-\tau)d\tau$$

where $y(t)$ is the response of the system at time t, $h(\tau)$ is the impulse response, and $x(\tau)$ is the stimulus history. A simple interpretation of this integral is that the response of the system at time t is a weighted average of its stimulus

history, with the weighting determined by the impulse response. Recent events are weighted by the early part of the impulse response and stimuli occurring further in the past are weighted by the later parts of the impulse response. Recent events are given a positive weighting by the positive lobe, and earlier events are given a negative weighting by the negative lobe. The combination of the two represents, then, a comparison of recent and past events. The widths of the lobes correspond to the times required to make accurate estimates of recent and past stimuli. The width of the positive lobe is roughly equal to the mean run length, so that that near the end of a typical run the cell behavior is determined by a comparison of events during the run with events occurring before it. The negative lobe decays exponentially, with a time constant (1.5 seconds) roughly equal to the time constant for the correlation between the present direction and the direction of movement of the cell in the past (1.3 seconds, using the data of Berg and Brown, 1972; Dahlquist et al., 1976; Macnab and Koshland, 1973). Thus the estimate of the earlier events is optimized for the statistical nature of *E. coli* swimming behavior. The impulse response appears to be ideally suited for the task that the cell must perform.

Conclusion. This thesis is a tribute to the quality of Howard's original idea--to test whether long range signalling exists in *E. coli*. Developing the techniques for doing the experiment opened up the possibility for a variety of experiments as are described in the first four chapters. In the fifth chapter, it could be argued, more was learned about the nature of the signal by proving that there was no long range coupling! To be able to plan experiments that produce such a rich variety of information, even when the original hypothesis is proven wrong, is a gift of great value. I can only hope that I, too, will be fortunate enough to have such ideas in the years to come.

REFERENCES

Adams, P. R. (1981). Acetylcholine receptor kinetics. J. Membrane Biol. **58,** 161-174.

Adler, J. (1966). Chemotaxis in Bacteria. Science **153,** 708-716.

Adler, J. (1969). Chemoreceptors in bacteria. Science **166,** 1588-1597.

Adler, J. (1973). A method for measuring chemotaxis and use of the method to determine optimum conditions for chemotaxis by *Escherichia coli*. J. Gen. Microbiol. **74,** 77-91.

Adler, J. and Epstein, W. (1974). Phosphotransferase-system enzymes as chemoreceptors for certain sugars in *Escherichia coli* chemotaxis. PNAS **71,** 2895-2899.

Adler, J., Hazelbauer, G. L. and Dahl, M. M. (1973). Chemotaxis toward sugars in *Escherichia coli*. J. Bacteriol. **115,** 824-827.

Adler,J. and Tso, W. (1974). "Decision"-making in bacteria; chemotactic responses of *Escherichia coli* to conflicting stimuli. Science **184,** 1292-1294.

Anderson, R. A. (1975). Formation of the bacterial flagellar bundle. **In:** Swimming and Flying in Nature, Vol. 1 (Plenum Publishing, N. Y.), Wu, T. Y.-T., Brokaw, C. J., Brennen, C. (eds.), 45-56.

Arai, T. (1981). Effect of arsenate on chemotactic behavior of *Escherichia coli*. J. Bacteriol. **145,** 803-807.

Armstrong, J. B. (1972). An S-adenosylmethionine requirement for chemotaxis in *Escherichia coli*. Can. J. Microbiol. **18,** 1695-1701.

Armstrong, J. B. and Adler, J. (1969). Complementation of nonchemotactic mutants in *E. coli*. Genetics **61,** 61-66.

Aswad, D. W. and Koshland, D., Jr. (1975). Evidence for an S-adenosylmethionine requirement n the chemotactic behavior of Salmonella typhimurium. J. Mol. Biol. **97**, 207-223.

Bardell, D. (1982). The roles of the sense of taste and clean teeth in the discovery of bacteria by Antoni van Leeuwenhoek. Microbiol. Rev. **47**, 121-126.

Berg, H. C. (1975). Chemotaxis in bacteria. Ann. Rev. Biophys. Bioengin. **4**, 119-136.

Berg, H. C. (1976). Does the flagellar rotary motor step? **In :** Swimming and Flying in Nature, Vol. **1** (Plenum Publishing, N. Y.), Wu, T. Y.-T., Brokaw, C. J., Brennen, C. (eds), 47-56.

Berg, H. C. and Anderson, R. (1973). Bacteria swim by rotating their flagellar filaments. Nature **245**, 380-382.

Berg, H. C. and Block, S. M. A miniature flow cell designed for rapid exchange of media under high-power microscope objectives. J. Gen. Microbiol. (in press).

Berg, H. C. and Brown, D. A. (1972). Chemotaxis in *Escherichia coli* analysed by three-dimensional tracking. Nature **239**, 500-504.

Berg, H. C. and Brown, D. A. (1972). Chemotaxis in *Escherichia coli* analysed by three-dimensional tracking. Nature **239**, 500-504. Reprinted with an addendum, 1974, p. 55-78. **In:** Antibiotics and chemotherapy, Vol. 19, Chemotaxis: its biology and biochemistry (S. Karger, Basel), Sorkin, E. (ed).

Berg, H. C. and Purcell, E. M. (1977). Physics of chemoreception. Biophys. J. **20**, 193-219.

Berg, H. C. and Tedesco, P. M. (1975). Transient response to chemotactic stimuli in *Escherichia coli*. PNAS **72**, 3235-3239.

Berg, H. C., Manson, M. D. and Conley, M. P. (1982). Dynamics and evergetics of flagellar rotation in bacteria. **In:** Prokaryotic and Eukaryotic Flagella; Society for Experimental Biology Sumposium Number XXXV (Cambridge Univ. Press; London) Amos, W. B. and Duckett, J. G. (eds), 1-31.

Black, R. A., Hobson, A. C. and Adler, J. (1980). Involvement of cGMP in intracellular signalling in the chemotactic response of *Escherichia coli.* PNAS **77**, 3879-3883.

Black, R. A., Hobson, A. C. and Adler, J. (1983). Adenylate cyclase is required for chemotaxis to phosphotransferase system sugars by *Escherichia coli.* J. Bacteriol. **153**, 1187-1195.

Block, S. M., Segall, J. E. and Berg, H. C. (1982). Impulse responses in bacterial chemotaxis. Cell **31**, 215-226.

Block, S. M., Segall, J. E. and Berg, H. C. (1983). Adaptation kinetics in bacterial chemotaxis. J. Bacteriol. **154**, 312-323.

Bogolmoni, R. A. and Spudich, J. L. (1982). Identification of a third rhodopsin-like pigment in *Halobacterium halobium* cells. PNAS. **79**, 6250-6254.

Boyd, A. and Simon, M. I. (1980). Multiple electrophoretic forms of methyl-accepting chemotaxis proteins generated by stimulus-elicited methylation in *Escherichia coli.* J Bacteriol. **143**, 809-815.

Boyd, A. and Simon, M. (1982). Bacterial chemotaxis. Ann. Rev. Physiol. **44**, 501-517.

Boyd, A., Krikos, A. and Simon, M. (1981). Sensory transducers of *Escherichia coli* are encoded by homologous genes. Cell **26**, 333-343.

Boyd, A., Kendall, K. and Simon, M. I. (1983). Structure of the serine chemoreceptor of *Escherichia coli.* Nature **301**, 623-626.

Boyd, A., Krikos, A., Mutoh, N. and Simon, M. (1982). A Family of homologous genes encoding sensory transducers in *Escherichia coli*. **In:** Mobility and Recognition in Cell Biology(Walter de Gruyter, Berlin H. and Veeger, C. (eds.), 551-562.

Brown, D. A. and Berg, H. C. (1974). Temporal stimulation of chemotaxis in *Escherichia coli*. PNAS **71**, 1388-1392.

Cannon, R. H., Jr. (1967). Dynamics of Physical Systems. McGraw-Hill Book Company, New York.

Cerione, R. A., Strulovici, B., Benovic, J. L., Lefkowitz, R. J., and Caron, M. G. (1983). Pure β-adrenergic receptor: the single polypeptide confers catecholamine responsiveness to adenylate cyclase. Nature **306**, 562 -566.

Chelsky, D. and Dahlquist, F. W. (1980a). Chemotaxis in *E. coli*: associations of protein components. Biochemistry **19**, 4633,4639.

Chelsky, D. and Dahlquist, F. W. (1980b). Structural studies of methyl-accepting chemotaxis proteins of *Escherichia coli*: evidence for multiple methylation sites. PNAS **77**, 2434-2438.

Chelsky, D. and Dahlquist, F. W. (1981). Methyl-accepting chemotaxis proteins of *Escherichia coli*: methylated at three sites in a single tryptic fragment. Biochemistry **20**, 977-982.

Chet, I. and Mitchell, R. (1976). Ecological aspects of microbial behavior. Ann. Rev. Microbiol. **30**, 2219-2239.

Clarke, S. and Koshland, D. E., Jr. (1979). Membrane receptors for aspartate and serine in bacterial chemotaxis. J. Biol. Chem. **254**, 9695-9702.

Dahlquist, F. W., Elwell, R. A. and Lovely, P. S. (1976). Studies of bacterial chemotaxis in defined concentration gradients. A model for chemotaxis toward L-serine. J. Supramol. Str. **4**, 329-342.

DeFranco, A. L. and Koshland, D. E., Jr. (1980). Multiple methylation in processing of sensory signals during bacterial chemotaxis. PNAS **77**, 2429-2433.

DeFranco, A., Parkinson, J. S. and Koshland, D. E., Jr. (1979). Functional homology of chemotaxis genes in *E. coli* and *S. typhi*. J. Bacteriol. **147**, 390-400.

Diehn, B., Feinleib, M., Haupt, W., Hildebrand, E., Lenci, F. and Nultsch, W. (1977). Terminology of behavioral responses of motile organisms. Photochem. and Photobiol. **26**, 559-560.

Doetsch, R. W. and Sjoblad, R. D. (1980). Flagellar structure and function in eubacteria. Ann. Rev. Microbiol. **34**, 69-108.

Dreyer, F. and Peper, K. (1974). Iontophoretic application of acetylcholine: advantages of high resistance micropipettes in connection with an electronic current pump. Pflugers Arch. **348**, 263-272.

Dreyer, F., Peper, K., and Sterz, R. (1978). Determination of dose-response curves by quantitative ionophoresis at the frog neuromuscular junction. J. Physiol. **281**, 395-410.

Eisenbach, M., Margolin, Y., Ciobotario, A. and Rottenberg, H. (1983). Distinction between changes in membrane potential and surface charge upon chemotactic stimulation of *Escherichia coli*. Biophys. J. **45**, 463-467.

Engstrom, P. and Hazelbauer, G. L. (1980). Multiple methylation of methyl-accepting chemotaxis proteins during adaptation of *Escherichia coli* to chemical stimuli. Cell **20**, 165-171.

Freter, R. and O'Brien, P. C. M. (1981). Role of chemotaxis in the association of motile bacteria with intestinal mucosa: fitness and virulence of nonchemotactic *Vibrio cholerae* mutants in infant mice. Infection and Immunology **34**, 215-221.

Goulbourne, E. A., Jr. and Greenberg, E. P. (1981). Chemotaxis of *Spirochaetia aurantia*: involvement of membrane potential in chemosensory signal transduction. J. Bacteriol. **148**, 837-844.

Goulbourne, E. A., Jr. and Greenberg, E. P. (1983). A voltage clamp inhibits chemotaxis of *Spirochaetia aurantia*. J. Bacteriol. **153**, 916-920.

Goy, M. F., Springer, M. S. and Adler, J. (1977). Sensory transduction in *Escherichia coli*: role of a protein methylation reaction in sensory adaptation. PNAS **74**, 4964-4968.

Goy, M. F., Springer, M. S. and Adler, J. (1978). Failure of sensory adaptation in bacterial mutants that are defective in a protein methylation reaction. Cell **15**, 1231-1240.

Hanke, W. and Miller, C. (1983). Single chloride channels from *Torpedo* electroplax. J. Gen. Physiol. **82**, 25-45.

Hayashi, H, Minoshima, S. and Ohba, M. (1982). Autonomous control of the level of methylation of methyl-accepting chemotaxis pr. J. Biochem. (Tokyo) **92**, 391-397.

Hazelbauer, G. L. and Adler, J. (1971). Role of the galactose binding protein in chemotaxis of *Escherichia coli* toward galactose. Nature New Biol. **230**, 101-104.

Hazelbauer, G. L. and Engstrom, P. (1981). Multiple forms of methyl-accepting chemotaxis proteins distinguished by a factor in addition to multiple methylation. J. Bacteriol. **145**, 35-42.

Hazelbauer, G. L. and Harayama, S. (1983). Sensory transduction in bacterial chemotaxis. Int. Rev. Cyt. **81**, 33-70.

Hazelbauer, G. L., Mesibov, R. E. and Adler, J. (1969). *Escherichia coli* mutants defective in chemotaxis toward specific chemicals. PNAS **64**, 1300-1307.

Herrmann, B. and Burman, L. G. (1983). Chemoattracting effect of human urine on motile *Escherichia coli*. FEMS Microbiol. **20**, 411-415.

Iino, T. (1977). Genetics of structure and function of bacterial flagella. Ann. Rev. Genet. **11**, 161-182.

Kehry, M. R. and Dahlquist, F. W. (1982a). The methyl-accepting chemotaxis proteins of *Escherichia coli*: identification of the multiple methylation sites of methyl-accepting chemotaxis protein I. J. Biol. Chem. **257**, 10378-10386.

Kehry, M. R. and Dahlquist, F. W. (1982b). Adaptation in bacterial chemotaxis: *che*B-dependent modification permits additional methylations of sensory transducer proteins. Cell **29**, 761-772.

Kehry, M. R., Bond, M. W., Hunkapillar, M. W. and Dahlquist, F. W. (1983). Enzymatic deamidation of methyl-accepting chemotaxis proteins in *Escherichia coli* catalyzed by the *che*B gene product. PNAS **80**, 3599-3603.

Khan, S. and Macnab, R. M. (1980). The steady-state CCW/CW ratio of bacterial flagellar motors is regulated by protonmotive force. J. Mol. Biol. **138**, 563-597.

Kihara, M. and Macnab, R. M. (1981). Cytoplasmic pH mediates pH taxis and weak-acid repellent taxis of bacteria. J. Bacteriol. **145**, 1209-1221.

Kleene, S. J., Hobson, A. C. and Adler, J. (1979). Attractants and repellents influence methylation and demethylation of methyl-accepting chemotaxis proteins in an extract of *Escherichia coli*. PNAS **76**, 6309-6313.

Kleene, S. J., Toews, M. L., and Adler, J. (1977). Isolation of glutamic acid methyl ester from an *Escherichia coli* membrane protein involved in chemotaxis. J. Biol. Chem. **252**, 3214-3218.

Kobayasi, S., Maeda, K. and Imae, Y. (1977). Apparatus for detecting rate and direction of rotation of tethered cells. Rev. of Sci. Inst. **48**, 407-410.

Koch, A. L. (1971). The adaptive responses of *Escherichia coli* to a feast and famine existence. Adv. Microb. Physiol. **6**, 147-217.

Kondoh, H. (1980). Tumbling chemotaxis mutants of *Escherichia coli*: possible gene-dependent effect of methionine starvation. J. Bacteriol. **142**, 527-534.

Kondoh, H., Ball, C. B. and Adler, J. (1979). Identification of a methyl-accepting chemotaxis protein for the ribose and galactose chemoreceptors of *Escherichia coli*. PNAS **76**, 260-264.

Kort, E. N., Goy, M. F., Larsen, S. H. and Adler, J. (1975). Methylation of a membrane protein involved in bacterial chemotaxis. PNAS **72**, 3939-3943.

Kosower, E. M. (1983). Selection of ion channel elements in the serine and aspartate 's of bacteria. Bioch. Bioph. Res. Comm. **115**, 648-652.

Krieg, N. T., Tomelty, J. P., and Wells, J. S., Jr. (1967). Inhibition of flgellar coordination in *Spirillum volutans*. J. Bacteriol. **94**, 1431-1436.

Krikos, A., Mutoh, N., Boyd, A. and Simon, M. I. (1983). Sensory transducers of *Escherichia coli* are composed of discrete structural and functional domains. Cell **33**, 615-622.

Lanni, F., Taylor, D. L., and Ware, B. R. (1981). Fluorescence photobleaching recovery in solutions of labeled actin. Biophys. J. **35**, 351-364.

Larsen, S. H., Adler, J., Gargus, J. J. and Hogg, R. W. (1974a). Chemomechanical coupling without ATP: the source of energy for motility and chemotaxis in baceteria. PNAS **71**, 1239-1243.

Larsen, S. H., Reader, R. W., Kort, E. N. and Adler, J. (1974b). Change in direction of flagellar rotation is the basis of the chemotactic response in *Escherichia coli*. Nature **249**, 74-77.

Lauffenburger, D., and DeLisi, C. (1983). Cell surface receptors: physical chemistry and cellular regulation. Int. Rev. Cyt. **84**, 269-302.

Lauffenburger, D., Aris, R. and Keller, K. H. (1982). Effects of cell motility and chemotaxis on microbial population growth. Biophys. J. **40**, 209-219.

Laszlo, D. J. and Taylor, B. L. (1981). Aerotaxis in *S. typhi*: role of electron transport. J. Bacteriol. **145**, 990-1001.

Lowy, J. and Hanson, J. (1965). Electron microscope studies of bacterial flagella. J. Mol. Biol. **11**, 293-313.

Macnab, R. M. (1977). Bacterial flagella rotating in bundles: a study in helical geometry. PNAS **74**, 221-225.

Macnab, R. M. and Koshland, D. E., Jr. (1972). The gradient-sensing mechanism in bacterial chemotaxis. PNAS **69**, 2509-2512.

Macnab, R. and Koshland, D. E., Jr. (1973). Persistence as a concept in the motility of chemotactic bacteria. J. Mechanochem. Cell Mot. **2**, 141-148.

Macnab, R. and Koshland, D. E., Jr. (1974). Bacterial motility and chemotaxis: light-induced tumbling response and visulaization of individual flagella. J. Mol. Biol. **84**, 399-406.

Macnab, R. M. and Ornston, M. K. (1977). Normal-to-curly flagellar transitions and their role in bacterial tumbling. Stabiliaztion of an alternative quaternary structure by mechanical force. J. Mol. Biol. **112**, 1-30.

Maeda, K. and Imae, Y. (1977). Thermosensory transduction in *Escherichia coli*: inhibition of the thermoresponse by L-serine. PNAS **76**, 91-95.

Manson, M. D., Tedesco, P., Berg, H. C., Harold, F. M. and van der Drift, C. (1977). A protonmotive force drives bacterial flagella. PNAS **74**, 3060-3064.

Margolin, Y. and Eisenbach, M. (1984). Voltage-clamp effects on bacterial chemotaxis. Submitted.

Mesibov, R., Ordal, G. and Adler, J. (1973). The range of attractant concentrations for bacterial chemotaxis of and the threshold and size of the response over this range. J. Gen. Physiol. **62**, 203-223.

Miller, J. B. and Koshland, D. E., Jr. (1977). Sensory electrophysiology of bacteria: relationship of the membrane potential to motility and chemotaxis in *B. sub*. PNAS **74**, 4752-4756.

Mizuno, T. and Imae, Y. (1984). Conditional inversion of the thermoresponse in *Escherichia coli*. J. Bacteriol. **159**, 360-367.

Niwano, M. and Taylor, B. L. (1982). Novel sensory adaptation mechanism in bacterial chemotaxis to oxygen and phosphotransferase substrates. PNAS **79**, 11-15.

Old, D. C. and Duguid, J. P. (1970). Selective outgrowth of fimbriate bacteria in static liquid medium. J. Bacteriol. **103**, 447.

Oosawa, K. and Imae, Y. (1983). Glycerol and ethylene glycol: members of a new class of repellents of *Escherichia coli* chemotaxis. J. Bacteriol. **154**, 104-112.

Ordal, G. W. (1977). Calcium ion regulates chemotactic behavior in bacteria. Nature (London) **270**, 66-67.

Ordal, G. W. and Adler, J. (1974). Isolation and complememntation of mutants in galactose taxis and transport. J. Bacteriol. **117**, 509-516.

Parkinson, J. S. (1975). Genetics of chemotactic behavior in bacteria. Cell **4**, 183-188.

Parkinson, J. S. (1978). Complementation analysis and deletion mapping of *E. coli* mutants defective in chemotaxis. J. Bacteriol. **135**, 45-53.

Parkinson, J. S. (1981). Genetics of bacterial chemotaxis. Symp. Soc. Gen. Microbiol. **31**, 265-290.

Parkinson, J. S. and Parker, S. R. (1979). Interaction of the *che*C and *che*Z gene products is required for chemotactic behavior in *E. coli*. PNAS **76**, 2390-2394.

Parkinson, J. S. and Revello, P. T. (1978). Sensory adaptation mutants of *Escherichia coli*. Cell **15**, 1221-1230.

Parkinson, J. S., Parker, S. R., Talbert, P. L. and Houts, S. E. (1983). Interactions between chemotaxis genes and flagellar genes in *E. coli*. J. Bacteriol. **155**, 265-274.

Pecher, A., Renner, I. and Lengeler, J. W. (1982). The phosphoenolpyruvate-dependent carbohydrate: phosphotransferase system enzymes II, a new class of chemoreceptors in bacterial chemotaxis. **In:** Mobility and Recognition in Cell Biology (Walter de Gruyter, Berlin), Sund, H. and Veeger, C. (eds.), 517-529.

Purves, R. (1980). Ionophoresis - progress and pitfalls. Trends Neuro. Sci

Reader, R. W., Tso, W., Springer, M. S., Goy, M. F. and Adler, J. (1979). Pleotropic aspartate taxis and serine taxis mutants of *Escherichia coli*. J. Gen. Microbiol. **111**, 363-374.

Ravid, S. and Eisenbach, M. (1984). Direction of flagellar rotation in bacterial cell envelopes. J. Bacteriol. **158**, 222-230.

Reader, R. W., Tso, W., Springer, M. S., Goy, M. F. and Adler, J. (1979). Pleiotropic aspartate taxis and serine taxis mutants of *Escherichia coli*. J. Gen. Microbiol. **111**, 363-374.

Reilley, C. N. and Vavoulis, A. (1959). Tetraethylenepentamine, a selective titrant for metal ions. Anal. Chem. **31**, 243-248.

Repaske, D. R. and Adler, J. (1981). Change in intracellular pH of *Escherichia coli* mediates the chemotactic response to certain attractants and repellents. J. Bacteriol.**145**, 1196-1208.

Ridgway, H. F., Silverman, M. and Simon, M. I. (1977). Localization of proteins controlling motility and chemotaxis in *E. coli*. J. Bacteriol. **132**, 657-665.

Rollins, C. M. and Dahlquist, F. W. (1980). Methylation of chemotaxis-specidfic proteins in *Escherichia coli* cells permeable to S-adenosylmethionine. Biochemistry **19**, 4627-4632.

Rollins, C. and Dahlquist, F. W. (1981). The methyl-accepting chemotaxis proteins of *Escherichia coli*: a repellent-stimulated covalent modification, distinct from methylation. Cell **23**, 333-340.

Russo, A. F. and Koshland, D. E., Jr. (1983). Separation of signal transduction and adaptation functions of the aspartate receptor in bacterial sensing. Science **220**, 1016-1020.

Savageau, M. A. (1983). *Escherichia coli* habitats, cell types, and molecular mechanisms of gene control. Am. Natur. **122**, 732-744.

Schanne, O. F., Lavallee, M., Laprade, R., and Gagne, S. (1968). Electrical properties of glass microelectrodes. Proc. I. E. E. E. **56**, 1072-1082.

Schellenberg, G. D. and Furlong, C. E. (1977). Resolution of the multiplicity of the glutamate and aspartate transport systems of *Escherichia coli*. J. Biol. Chem. **252**, 9055-9064.

Segall, J. E., Manson, M. D., and Berg, H. C. (1982). Signal processing times in bacterial chemotaxis. Nature **296**, 855-857.

Seymour, F. W. K. and Doetsch, R. N. (1973). Chemotactic responses by motile bacteria. J. Gen. Microbiol. **78**, 287-296.

Sherris, D. and Parkinson, J. S. (1981). Postranslational processing of methyl-accepting chemotaxis proteins in *Escherichia coli*. PNAS **78**, 6051-6055.

Shioi, J., Galloway, R. J., Niwano, M., Chinnock, R. E. and Taylor, B. L. (1982). Requirement of ATP in Bacterial chemotaxis. J. Biol. Chem. **257**, 7969-7975.

Silverman, M. (1980). Building bacterial flagella. Quart. Rev. Biol. **55**, 395-408.

Silverman, M. and Simon, M. (1974). Flagellar rotation and the mechanism of bacterial motility. Nature **249**, 73-74.

Silverman, M. and Simon, M. (1977). Chemotaxis in *Escherichia coli*: methylation of *che* gene products. PNAS **74**, 3317-3321.

Slonczewski, J. L., Macnab, R. M., Alger, J. R. and Castle, A. M. (1982). Effects of pH and repellent tactic stimuli on protein methylation levels in *Escherichia coli*. J. Bacteriol. **152**, 384-399.

Smith, J. L. and Doetsch, R. N. (1969). Studies on negative chemotaxis and the survival value of motility in *Pseudomonas fluorescens*. J. Gen. Microbiol. **55**, 379-391.

Smith, R. A. and Parkinson, J. S. (1980). Overlapping genes at the *che*A locus of *E. coli*. **77**, 5370-5374.

Snyder, M. A. and Koshland, D. E., Jr. (1981). Identification of the esterase peptide and its interaction with the *che*Z peptide in bacterial sensing. Biochimie **63**, 113-117.

Snyder, M. A., Stock, J. B. and Koshland, D. E., Jr. (1981). Role of membrane potential and calcium in chemotactic sensing by bacteria. J. Mol. Biol. **149**, 241-257.

Soby, S. and Bergman, K. (1983). Motility and chemotaxis of *Rhizobium meliloti* in soil. Appl. and Env. Microbiol. **46**. 995-998.

Springer, M. S., Goy, M. F. and Adler, J. (1977). Sensory transduction in *E. coli*: two complementary pathways of information processing that involve methylated proteins. PNAS **74**, 3312-3316.

Springer, M. S., Goy, M. F. and Adler, J. (1979). Methylation in behavioral control mechanisms and in signal transduction. Nature **280**, 279-284.

Springer, M. S., Zanolari, B., and Pierzchala, P. A. (1982). Ordered methylation of the methyl-accepting chemotaxis proteins of *Escherichia coli*. J. Biol. Chem. **257**, 6861-6866.

Springer, W. R. and Koshland, D. E., Jr. (1977). Identification of a protein methyltransferase as the cheR gene product in the bacterial sensing system. PNAS **74**, 533-537.

Spudich, J. L. and Koshland, D. E., Jr. (1975). Quantitation of the sensory response in bacterial chemotaxis. PNAS **72**, 710-713.

Stock, J. B. and Koshland, D. E., Jr. (1978). A protein methylestrase involved in bacterial sensing. PNAS **75**, 3659-3663.

Stock, J. B. and Koshland, D. E., Jr. (1981). Changing reactivity of receptor carboxyl groups during bacterial sensing. J. Biol. Chem. **256**, 10826-10833.

Stock, J. B., Maderis, A. M. and Koshland, D. E., Jr. (1981). Bacterial chemotaxis in the absence of receptor carboxymethylation. Cell **27**, 37-44.

Stiles, G. L., Caron, M. G., and Lefkowitz, R. J. (1984). β-adrenergic receptors: biochemical mechanisms of physiological regulation. Physiol. Rev. **64**, 661-743.

Szmelcman, S. and Adler, J. (1976). Change in membrane potential during bacterial chemotaxis. PNAS **73**, 4387-4391.

Taylor, B. L. (1983). Role of protonmotive force in sensory transduction in bacteria. Ann. Rev. Microbiol. **37**, 551-573.

Toews, M. L. and Adler, J. (1979). Methanol formation *in vivo* from methyl-accepting chemotaxis proteins in *Escherichia coli*. J. Biol. Chem. **254**, 1761-1764.

Toews, M. L., Goy, M. F., Springer, M. S. and Adler, J. (1979). Attractants and repellents control demethylation of methylated chemotaxis proteins in *Escherichia coli*. PNAS **76**, 5544-5548.

Trueba, F. J. and Woldringh, C. L. (1980). Changes in cell diameter during the division cycle of *Escherichia coli*. J. Bacteriol. **142**, 869-878.

Tsang, N., Macnab, R. M. and Koshland, D. E., Jr. (1973). Common mechanism for repellents and attractants in bacterial chemotaxis. Science **181**, 60-63.

Wang, E. A. and Koshland, D. E., Jr. (1980). Receptor structure in the bacterial sensing system. PNAS **77**, 7157-7161.

Wang, E. A., Mowry, K. L., Clegg, D. O. and Koshland, D. E., Jr. (1982). Tandem duplication and multiple functions of a receptor gene in bacterial chemotaxis. J. Biol. Chem. **257**, 4673-4676.

Weibull, C. (1960). Movement. **In:** The Bacteria, Vol **1** (Academic Press, N. Y.), Gunsalus, C. and Stanier, R. Y. (eds), 153-205.

van der Werf, P. and Koshland, D. E., Jr. (1977). Identification of a γ-glutamyl methyl ester in a bacterial membrane protein involved in chemotaxis. J. Biol. Chem. **252**, 2793-2795.

Yonekawa, H., Hayashi, H. and Parkinson, J. S. (1983). Requirement of the cheB function for sensory adaptation in *Escherichia coli*. J. Bacteriol. **156**, 1228-1235.